EVALUATING SURFACE INDUCED PLATELET ADHESION AND ACTIVATION WITH SURFACE PATTERNING AND PROTEIN IMMOBILIZATION TECHNIQUES

by

Lindsey Elizabeth Corum

A dissertation submitted to the faculty of
The University of Utah
in partial fulfillment of the requirements for the degree of

Doctor of Philosophy

Department of Bioengineering

University of Utah

August 2011

Copyright © Lindsey Elizabeth Corum 2011

All Rights Reserved

The University of Utah Graduate School

STATEMENT OF DISSERTATION APPROVAL

The dissertation of **Lindsey Elizabeth Corum**

has been approved by the following supervisory committee members:

Vladimir Hlady	, Chair	**5/17/2011** Date Approved
Yan-Ting Shiu	, Member	**6/10/2011** Date Approved
David Grainger	, Member	**6/7/2011** Date Approved
Patrick Kiser	, Member	**5/25/2011** Date Approved
Andrew Weyrich	, Member	**6/9/2011** Date Approved

and by **Patrick Tresco**, Chair of the Department of **Bioengineering**

and by Charles A. Wight, Dean of The Graduate School.

ABSTRACT

Platelet surface interactions play a critical role in the hemocompatibility of blood contacting biomaterials. When blood leaves the natural vessel and contacts a synthetic material, the body senses this change. Immediately, a host of responses occur at the blood material interface including plasma protein adsorption and platelet adhesion and activation. Platelet activation stimulates local coagulation factors eventually leading to the formation of a blood clot. Clot formation on vascular implants can have many adverse effects and ultimately lead to the failure of these devices.

To date, an extensive amount of research has been focused on controlling surface induced platelet adhesion and activation. Although a number of studies have shown promising in vitro results, the translation to successful hemocompatible biomaterials has been somewhat limited. This is largely due to the complexity behind the mechanisms driving the platelet response.

In this dissertation, well defined microenvironments, as a function of both surface chemistry and protein immobilization, were used to characterize and understand the molecular mechanisms of surface induced platelet responses. Specifically, molecular gradients were investigated as a high throughput technique in which the platelet response could be rapidly screened over a variety of surface chemistries. Here, it was discovered that the upstream environment

affected the downstream platelet response and that upstream surface interactions may actually prime platelets for downstream adhesion and activation. This phenomenon was further explored using microcontact printing to prepare test samples with covalently immobilized fibrinogen “priming” regions. The downstream platelet response was characterized and found to be dependent on the presence of an upstream priming region. The use of microcontact printing was also investigated as a tool to control platelet adhesion and morphological characteristics using random micropatterns of fibrinogen at varying relative coverage areas. The experiments described in this dissertation provided well controlled environments in which specific surface-induced platelet adhesion and activation mechanisms were examined and will serve as a foundation for future fundamental studies.

TABLE OF CONTENTS

LIST OF FIGURES

LIST OF ABBREVIATIONS

Defining Term	Abbreviation
3-mercaptopropyltrimethoxysilane	MTS
4-(2-hydroxyethyl)-1-piperazineethanesulfonic acid	HEPES
Adenosine diphosphate	ADP
Albumin	Alb
Anticoagulant citrate dextrose	ACD
Arginine-glycine-aspartic acid binding epitope	RGD
Atomic force microscopy	AFM
Cardiovascular Disease	CVD
Circularity	C
Concentration	c
Differential interference contrast	DIC
Electron spectroscopy for chemical analysis	ESCA
Electron volt	eV
Endothelial cell	EC
Extracellular matrix	ECM
Fibrinogen	Fbg
Fused silica	FS
Glycoprotein Ib-IX-V	GPIb-IX-V

Lateral force microscopy ..... LFM

Microcontact printing ..... µCP

N-hydroxysuccinimide ..... NHS

Nitric Oxide ..... NO

Phosphate buffered saline ..... PBS

Platelet poor plasma ..... PPP

Platelet rich plasma ..... PRP

Polydimethylsiloxane ..... PDMS

Polyethylene glycol ..... PEG

Prostaglandin E_1 ..... PGE1

Scanning electron microscopy ..... SEM

Sulfosuccinimidyl-4-(N-maleimidomethyl)cyclohexane-1-carboxylate ..sulfo-SMCC

Ultraviolet ..... UV

von Willebrand factor ..... vWf

X-ray photoelectron spectroscopy ..... XPS

ACKNOWLEDGMENTS

I would first like to express my sincerest gratitude to my advisor, Dr. Vladimir Hlady, for providing numerous hours of guidance over the past four years. As a mentor, you continuously challenged and motivated me to put forth my best effort. I would also like to thank my committee, Drs. Yan-Ting Shiu, David Grainger, Patrick Kiser, and Andy Weyrich, for providing feedback and support while I was pursuing my research endeavors. I also wish to acknowledge the members of the Protein and Polymers at Interfaces Research Group: Katie Job, Tony Hsiao, Collin Eichinger, and Vimal Swarup for providing much appreciated support and input on a daily basis. I am also grateful for the undergraduate research assistants, Lydia Potekhina, Ashley Cook, Krystin Meidell, and Caleb Campbell for assisting with experiments and data analysis. Outside of the lab I would like to thank the members of the Weyrich/Zimmerman research group for generously providing human blood for these studies. I would also like to thank Adrianna Broxado for her assistance with flow cytometry experiments. Finally, I would like to thank my friends and family, especially my mother Barbara and my sister Alison. You have been the source of immense support and encouragement over the years.

CHAPTER 1

INTRODUCTION

Cardiovascular disease (CVD) is the number one killer in America. With increasing life expectancy, a growing incidence of type II diabetes, and the epidemic proportion of obese individuals, health care professionals expect to see the incidence of CVD continue to rise. According to the American Heart Association, approximately 40% of American's will have some form of CVD by 2030 [1]. Many of these conditions cannot be effectively treated pharmacologically. As a result, therapeutic cardiovascular devices such as heart valves, vascular grafts, and stents are often implanted as the last opportunity for the patient. Regrettably, in spite of years of intensive research, the response of blood to these devices still presents many challenges [2,3]. Specifically, patients who receive cardiovascular implants are plagued with an increased risk of infection and surface induced thrombus formation which can ultimately lead to the failure of the device [4,5]. This requires that device implantation is coupled with the use of systematic anticoagulant and antithrombotic therapies that often result in adverse side effects for the patient [6,7].

When blood contacts the surface of a synthetic vascular prosthetic the body senses this change and host of responses occur at the blood-material

interface. Immediately, plasma proteins adsorb to the surface of the device [8,9]. This adsorbed protein layer serves as a bioactive coating capable of initiating both immunological and thrombogenic responses including, platelet adhesion/activation, coagulation, complement activation and inflammation (6, Figure 1.1). The activation mechanisms of these systems are highly interwoven. For example, the biomaterial surface can directly stimulate complement activation and coagulation through the intrinsic pathway and extrinsic pathways respectively. Biomaterials also support platelet adhesion and activation. Activated platelets are capable of up-regulating and mediating coagulation reactions as well as thrombus formation. Leukocytes are activated by both direct interactions with the implant surface or through interactions with activated platelets mounting an inflammatory response [6,10]. Platelet activation, specifically, has been a key focus of biomaterials research due to its central role in coagulation and its role in mediating inflammatory responses. An adverse platelet response to vascular implants can lead to many complications including occlusion, neointimal hyperplasia, and embolism.

This introduction provides an overview of the events that occur when a synthetic material contacts the bloodstream with a focus on platelet adhesion and activation. Recent advancements in improving material hemocompatibility as well as using surface patterning tools to better understand protein-platelet interactions are also reviewed. Finally, a brief synopsis of each research project described in the subsequent chapters of this dissertation is provided.

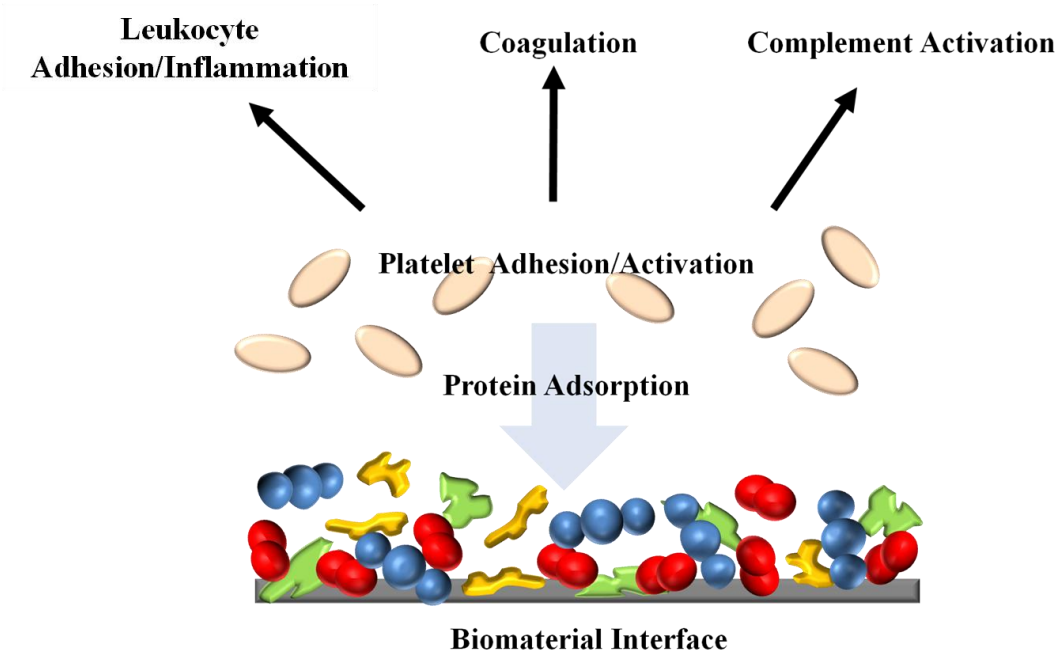

Figure 1.1 Events that occur after a biomaterial contacts the bloodstream.

1. 1 Plasma Protein Adsorption on Biomaterials

Over 150 plasma proteins make up approximately 7% of the total volume of blood and serve a variety of important functions, including maintaining osmotic pressure, facilitating immune responses, and mediating the coagulation response. However, for cardiovascular implants, the protein response can ultimately lead to device failure. Within seconds after an artificial material is placed into contact with the bloodstream, these proteins adsorb to the surface [8,9]. This adsorbed layer serves as a substrate for cell and platelet adhesion via specific interactions between the proteins and membrane receptors on the cell surface. Adsorbed proteins can activate a multitude of intracellular responses and trigger adverse effects such as thrombus formation, inflammation and complement activation [6]. Given that the adsorbed protein layer serves as the primary mediator for cell-surface interactions, the nature of this layer ultimately dictates the host response to the implant [11]. While in some biomedical applications protein adsorption can be a desired result [12-14], for blood-contacting materials, it is almost entirely detrimental. Consequently, an extensive amount of effort has been devoted to understanding and controlling protein adsorption to vascular biomaterials [15-17].

1.1.1 Surface Considerations in Protein Adsorption

The ability of a surface to minimize protein adsorption is believed to be linked to improved blood compatibility; consequently, quantifying protein adsorption is a popular tool for material evaluation [15,18,19]. Properties such as surface, topography, chemistry, hydrophobicity, and charge are all critical in

determining protein response at the blood-material interface and subsequently, the host response to the device. Increased protein adsorption has been observed on surfaces with more topographical features than smooth surfaces [20]. This is believed to be due to the increased surface area available for protein adsorption on rough surfaces. Surface chemistry is also critical in determining the protein response. The surface chemical makeup dictates the type of chemical bonds the protein may make with the surface. Stronger chemical bonds between the protein and the interface will increase its affinity for the surface [11,20]. Chemistry also dictates factors such as hydrophobicity and charge. Hydrophobic surfaces have been shown to adsorb proteins more readily than hydrophilic surfaces [21,22] due to hydrophobic interactions between the protein and the interface. Plasma proteins have also been shown to adsorb less readily to negatively charged surfaces [23,24]. This is likely due to the fact that plasma proteins carry an overall net negative charge. However, negatively charged surfaces alone do not completely inhibit adsorption. Plasma proteins may also contain positively charged regions on their surface due to the presence of amino acids that carry a positive charge (histidine, lysine, arginine) and therefore are capable of interactions with negative surfaces.

1.1.2 Why are Proteins So Sticky? Properties Affecting Adsorption

Proteins are large amphiphilic molecules and very surface active. All proteins are polymeric chains built from 20 amino acids called polypeptides. These amino acids can be neutral or charged, hydrophobic or hydrophilic and ultimately determine both its structure and function. Noncovalent interactions

such as hydrogen bonding, van der Waals forces and ionic/hydrophobic interactions drive the formation of spatial structures such as helicies, sheets, and turns within the polypeptide chain. These secondary structures fold upon themselves forming a globular 3-dimensional structure. Folding is initially driven by non specific hydrophobic interactions but maintained by specific interactions such as hydrogen bonding, the formation of salt bridges, and disulfide bonds [25,26]. The heterogeneity of protein composition makes preventing adsorption an extremely difficult task. Hydrophobic amino acids, generally found in the inner core of a soluble protein, will interact with hydrophobic surface regions driving both adsorption and unfolding [11,20,2]. Charged amino acids, generally more hydrophilic and commonly found on the protein surface, will interact with oppositely charged surface regions also driving adsorption [20,23,28].

Adsorption is also affected by structural properties such as size and stability of the protein. As proteins increase in size, their affinity for the surface also increases. This is because larger molecules are capable of making more contacts with the surface and subsequently more stable once adsorbed [20]. Protein unfolding is a critical factor in biomaterial-induced protein adsorption since this frequently results in the exposure of cryptic binding epitopes capable of cell and platelet activation. Unfolding is dependent on the structural and thermodynamic stability of the protein. Interactions within the protein molecule such as disulfide and hydrogen bonds increase stability. The more bonds present within the protein, the less likely it is to unfold after adsorption. The thermodynamic stability or, in other words, the free energy change between the

folded and unfolded state also drives this process. The free energy change can be calculated by subtracting entropy from the binding energy of the protein. Dispersion forces, electrostatic interactions, van der Waals potential and hydrogen bonding all contribute to the binding energy while hydrophobic interactions are described by the entropy term. As the binding energy increases or the entropy difference between the two states decreases, the folded protein is more stable [27]. It is believed that the hydrophobic effect or the change in entropy between the two states is the predominant stabilizing effect [25,27].

1.1.3 Protein Transport From the Bulk to the Biomaterial Interface

In order for adsorption to occur, the protein must be transported from the bulk to the interface; thus, both diffusion and convection also play a role in adsorption. Since smaller molecules have higher diffusion coefficients, smaller plasma proteins are generally the first to arrive and adsorb to interface [29]. Also, proteins at a higher bulk concentration generally are quick to populate the surface [20,29]. Over time, molecules with higher overall affinity for the surface, but slower diffusion rates (due to their larger size and/or lower solution concentration) will approach the surface and compete for binding sites. Although, generally, simple desorption of proteins does not occur, it is possible for proteins with a higher surface affinity to compete and exchange with proteins already present on the surface. This process is called the Vroman effect [30].

With over 150 proteins in plasma, adsorption kinetics are complex but also critical in determining the nature of the protein layer. The rate at which a protein adsorbs to a surface can affect both its conformation and orientation on the

surface. At high concentrations, adsorption is fast, making it likely that after initial adsorption, the binding site next to it will also be populated before the protein has a chance to unfold. The faster the protein arrives the smaller the footprint [22,31]. The conformation of the adsorbed protein is important in determining its bioactivity. For example, enzymes often require a certain structure to maintain their activity. If they unfold following adsorption this activity may be lost [32]. Conversely, unfolding may expose cell binding epitopes that were originally buried within the protein when it was in its natured state [33-35]. In the case of blood compatibility, there is growing evidence that conformation is more important in determining the host response than the type or amount of protein adsorbed [34,36].

1.1.4 Plasma Proteins Relevant to Platelet-Biomaterial Interactions

Human plasma contains numerous proteins with a variety of important physiological roles. In the case of biomaterial-platelet interactions, plasma proteins such as albumin, fibrinogen, fibronectin, vitronectin, and von Willebrand factor (vWf) have all been studied in great detail. Albumin makes up the largest percentage of blood proteins (~60%) [29]. Due to its high concentration in blood and relatively small size it is the first plasma protein to adsorb to a biomaterial after implantation. However, over time, it is replaced with proteins with higher surface affinities such as fibrinogen [29]. For many years albumin has been believed to be relatively inert to platelet adhesion. Thus attempts have been made to design surfaces that either promote albumin adsorption [37,38] or are directly coated with albumin [39]. However, more recently, albumin has been

shown to support platelet adhesion and thus may not be completely inert [35]. It has been postulated that this may be due to the conformational exposure of binding epitopes for platelets. Fibrinogen (c_{plasma} = 3 mg/ml) has been extensively studied by blood compatibility researchers and is required for both platelet adhesion and aggregation. Platelet adhesion to biomaterials has been shown to be drastically reduced when fibrinogen is removed from plasma [40,41]. Due to its central role in adhesion, preventing fibrinogen adsorption has been one approach used to develop more compatible biomaterials. However, it is interesting to note that in its native state, fibrinogen is relatively inert to quiescent platelets; it is only when it is adsorbed and unfolds that adhesion is supported [42]. Once platelets are activated, fibrinogen is then able to support further adhesion and aggregation. Although fibrinogen is the key protein that mediates platelet adhesion to biomaterials, vWf (c_{plasma} = 10 µg/ml), has been shown to be critical in supporting platelet adhesion under flow conditions [43-46]. Vitronectin and fibronectin have also been shown to support platelet adhesion but are not believed to be as critical as fibrinogen in the case of biomaterials [47,48].

1.2 Platelets

Platelets are anuclear cell fragments derived from megakaryocytes in the bone marrow and play a crucial role in hemostasis ($c \approx 2 \cdot 10^8$ platelets/ml). After vessel damage occurs, the coagulation cascade is initiated when tissue factor is released from the site of vascular endothelial injury [49]. Tissue factor initiates a series of enzymatic reactions that ultimately lead to the formation of thrombin [50]. Thrombin recruits and activates platelets which are involved in local

amplification of the coagulation cascade and clot formation. Unfortunately, platelets also adhere and are activated by the adsorbed protein layer on biomaterials. Thrombus formation on the surface of vascular implants can lead to occlusion of the device lumen, embolism, and inflammatory responses. To avoid these potentially life threatening complications, the ability to eliminate surface induced platelet activation has been a central goal of material hemocompatibility.

1.2.1 Platelet Membrane Receptors

The platelet membrane is rich in glycoprotein receptors embedded in the phospholipid bilayer which include tyrosine kinase receptors, integrins, leucine rich receptors, protein G coupled transmembrane receptors, selectins and immunoglobulin domain receptors. These proteins are critical in transducing external signals into intracellular signaling events that mediate both cell-platelet and platelet-substrate interactions and are involved in haemostatic functions, inflammation, tumor growth and immunologic reactions. This section will review the two most abundant receptors on the platelet membrane, integrin $\alpha_{IIb}\beta_3$, and glycoprotein Ib-IX-V (GPIb-IX-V), which control platelet adhesion and activation processes.

The most abundant receptor on the platelet membrane is the $\alpha_{IIb}\beta_3$ integrin receptor. This receptor, unique to platelets, is a key mediator of adhesive and aggregation interactions [51]. The main ligand for $\alpha_{IIb}\beta_3$ is fibrinogen, [52,53] a dimeric protein with each monomer consisting of an α, β and γ-chain. Three binding epitopes for $\alpha_{IIb}\beta_3$ exist in fibrinogen, two RGD motifs in the α-chains and

one dodecapeptide sequence in the γ-chain [54,55]. The importance of the RGD binding motifs in adhesion and aggregation has received some speculation [56,57] and may even be inhibitory, while the dodecapeptide γ sequence is believed to be critical [58]. Also, the possibility for other binding motifs to exist cannot be ruled out [51]. In quiescent platelets, $\alpha_{IIb}\beta_3$ exists in an inactive form and must be activated to bind soluble fibrinogen [59]. However, when fibrinogen is adsorbed, $\alpha_{IIb}\beta_3$ is capable of binding even in the absence of activation [60]. Besides fibrinogen, vWF, fibronectin, thrombospondin and vitronectin can all bind to the $\alpha_{IIb}\beta_3$ complex [61,62]. Other integrins expressed on the platelet membrane include $\alpha_{II}\beta_1$, $\alpha_V\beta_1$, and $\alpha_{VI}\beta_1$ that support platelet-vessel wall adhesive interactions to the ECM proteins collagen, fibronectin, and laminin, respectively [63-65]. However, detailed descriptions of these mechanisms are beyond the scope of this dissertation and can be reviewed elsewhere [61].

GPIb-IX-V is a leucine rich transmembrane receptor formed by a multiprotein complex of four different glycoproteins. This is the second most abundant receptor on the platelet membrane and is involved in the initial attachment of platelets to the vessel wall or a biomaterial under high shear conditions via the ligand vWf [43,66]. The interaction between vWf and GPIb-IX-V is not as strong as the interaction between $\alpha_{IIb}\beta_3$ and fibrinogen; therefore, it is not believed to be sufficient in supporting irreversible adhesion [43]. Binding of vWf to GPIb–IX–V is also involved in transmitting intracellular activation signals, triggering degranulation, elevation of cytosolic Ca^{2+}, cytoskeletal actin rearrangements, and “inside-out” activation of $\alpha_{IIb}\beta_3$ that binds vWf or fibrinogen

and mediates platelet aggregation [67,68]. Aside from platelet adhesion and activation, GPIb-IX-V can also bind both P-selectin expressed on endothelial cells and the integrin Mac-1 (integrin $\alpha_M\beta_2$) on leukocytes and consequentially may be involved in inflammatory interactions [69,70].

1.2.2 Mechanism of Platelet Adhesion

Platelet adhesion is supported by specific interactions between membrane receptors and adsorbed plasma proteins. The receptors GPIb-IX-V and integrin $\alpha_{IIb}\beta_3$ discussed in the previous section are the key adhesion receptors and interact with both vWf and fibrinogen respectively [53,66] Specifically, the GPIb-IX-V complex transiently binds to surface immobilized vWf to promote stable platelet adhesion. This process referred to as “platelet tethering” acts to slow down platelets in flowing conditions. The bonds between vWf and GPIb-IX-V are relatively weak and reversible, but nonetheless facilitate stable $\alpha_{IIb}\beta_3$-fibrinogen binding which is a slower bond to form (Figure 1.2). Thus fibrinogen and vWf work synergistically to promote stable platelet adhesion on both a damaged vessel and biomaterials [43,71]. It is commonly cited that the amount of adsorbed fibrinogen is an important determinant in the hemocompatibility of a biomaterial. This is likely due to fibrinogen’s ability to support irreversible adhesion. Fibrinogen has also been shown to convert platelets to a procoagulant state [40] in which many activation events occur including the up regulation of $\alpha_{IIb}\beta_3$ receptor expression on the platelet membrane. Other plasma proteins such as collagen, fibronectin, and vitronectin have also been shown to support platelet adhesion specifically on an exposed subendothelium. However, their

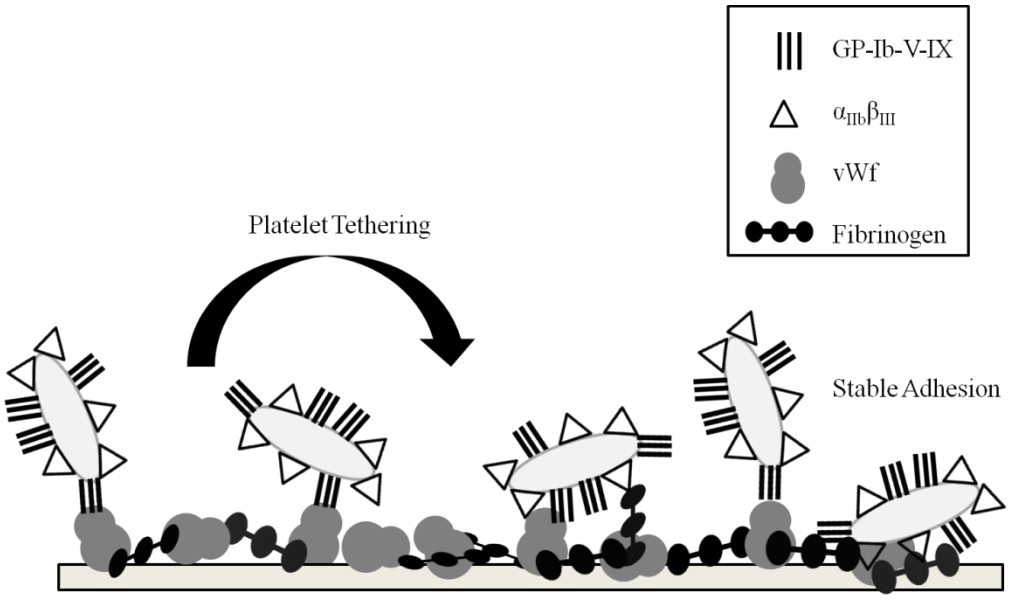

Figure 1.2 The mechanism of platelet adhesion: stable adhesion involves synergistic interactions between immobilized vWf and fibrinogen. vWf is involved in the initial arrest of flowing platelets. This interaction is weak and reversible but facilitates stable fibrinogen adhesive contacts.

involvement in biomaterial-induced platelet adhesion has been shown to be less critical [40,72].

1.2.3 Platelet Activation

A variety of stimuli are capable of activating platelets. Platelets become activated when they interact with matrix proteins, such as collagen, at the site of vascular injury. Platelets are also activated by adsorbed proteins on synthetic materials and are the first cells to adhere to the biomaterial surface [73]. Platelets also become activated by agonists such as ADP released by platelets themselves, thromboxane A_2 from inflammatory cells and thrombin generated by the coagulation response [74].

Platelet activation is a crucial step in thrombus formation and is characterized by a series of overlapping events which include morphological changes, membrane receptor expression/activation, release of procoagulant factors, and the translocation of negatively charged phospholipids from the inner to the outer face of the lipid bilayer [75]. In their quiescent state, the $\alpha_{IIb}\beta_3$ integrin is unable to bind soluble ligands [59]. However, it is capable of interacting with immobilized fibrinogen and vWf present on the surface of implanted biomaterials [60]. Binding to these ligands triggers an outside-in signaling cascade that converts $\alpha_{IIb}\beta_3$ to its active conformation and initiates spreading [76,77]. When platelets initially adhere to a surface they convert from a discoid to a spherical morphology. Interactions between $\alpha_{IIb}\beta_3$ and GPIb-V-IX with adsorbed adhesion proteins initiate phosphorylation dependent cytoskeletal rearrangements characterized by the extension of filopods from the adhered

platelet. These filopods become more extensive as more specific adhesive contacts with the substrate are established. This is followed by spreading which occurs by the growth of lamellipods that coalesce to form circular lamellae (Figure 1.3). These conformational changes also lead to an inside-out conformational change in integrin $\alpha_{IIb}\beta_3$ that facilitates platelet aggregate formation.

Platelets contain secretory organelles called α-granules, dense granules, and lysosomes that undergo release reactions called “degranulation” when platelets are activated. In this process of exocytosis, many coagulation factors including adhesive proteins, growth factors, hydrolytic enzymes, and other coagulation stimuli are released [78]. The morphological changes described previously allow for the centralization of granules that subsequently secrete procoagulant factors and stimulate further activation and thrombus formation [79]. It has been observed that secretion events occur more frequently when platelets are in their fully spread state [80]. Also, during this process, $\alpha_{IIb}\beta_3$ integrins and P-selectin are translocated from the α-granule membrane to the platelet membrane [81,75] where they are capable of supporting homotypic and heterotypic cell aggregation. These receptors also act as a catalytic surface for coagulation and inflammatory reactions.

1.2.4 Hemodynamic Considerations

The rheological environment of the vasculature is an important modulator of thrombosis. Specifically, shear forces have been shown to induce platelet

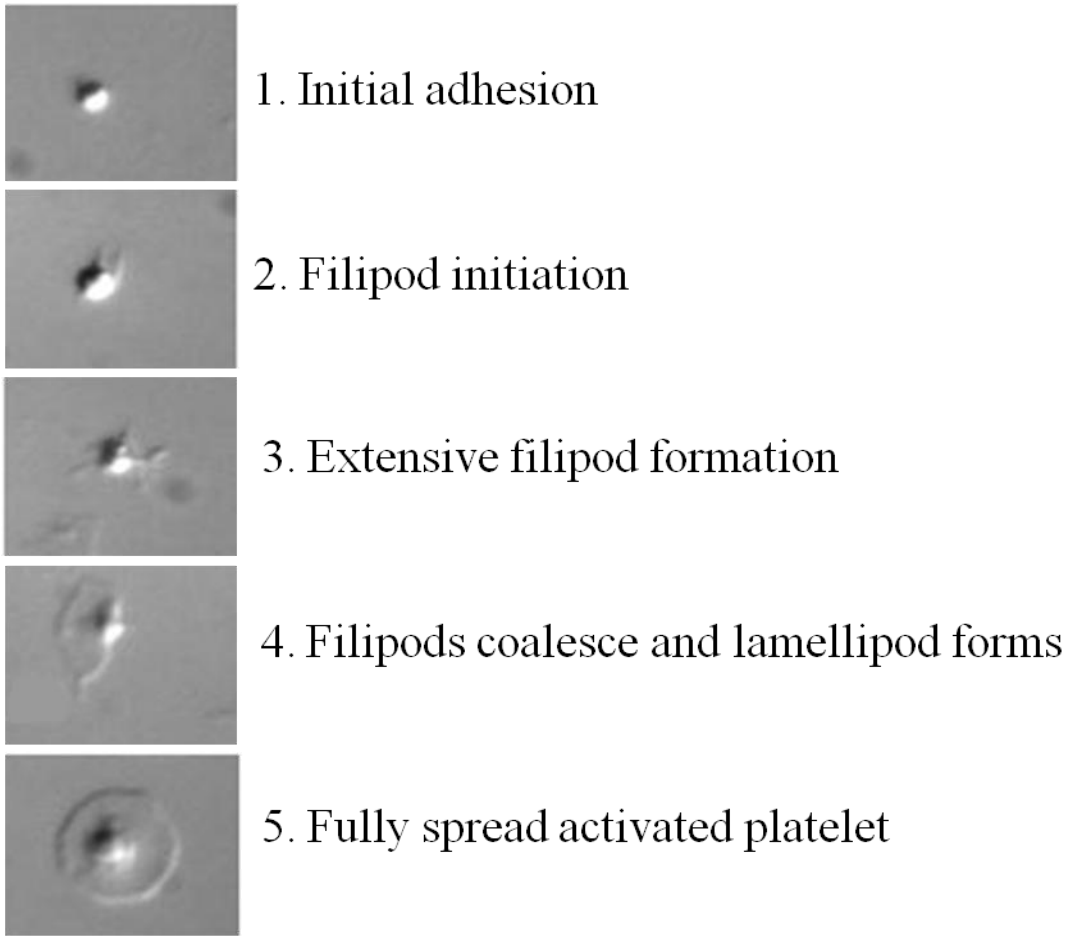

Figure 1.3 Differential interference contrast images of the spreading platelet.

activation and aggregation. However, as the velocity increases, the time membrane receptors have to contact immobilized ligands decreases thus lowering the efficiency of platelet recruitment to the substrate. Only the interaction between platelets and vWf is fast enough to initiate adhesion in high shear conditions [43]. Thus, elevated shear forces promote the initial binding of vWf by activating the GPIb-IX-V receptor [44]. This interaction induces intracellular signaling cascades characterized by Ca^{2+} mobilization [82,45], cytoskeletal rearrangements [83], protein kinase expression [84], and integrin $\alpha_{IIb}\beta_3$ expression/activation [67,82]. This is coupled with the release of soluble vWf from the platelet α-granules. Fibrinogen along with vWf then work synergistically to form stable adhesive contacts [43,68,71].

In the vasculature, cells are exposed to hydrodynamic induced pressure, strain and shear forces. Shear stress results in a force per unit area on the cell which can damage platelets at high flows [85]. Platelet lysis results in the release of procoagulant factors and subsequent activation of surrounding platelets. The extent of mechanical damage to platelets is related to both the magnitude and the duration of exposure [85,86].

1.2.5 Platelet-Material Interactions: A Central Issue in Hemocompatibility Research

Due to the central role of platelets in thrombus formation and coagulation, platelet adhesion often serves as a key criterion in material hemocompatibility testing. Many approaches in designing platelet-inert materials have been explored. Efforts to reduce platelet adhesion and activation commonly follow one

of three approaches: 1) endothelialization, 2) surface modification, and 3) bioactive coatings.

The only truly blood compatible surface, known to prevent platelet activation, is an intact and functional endothelial cell (EC) monolayer. ECs make up the innermost lining of blood vessels and possess many anti thrombotic properties. Naturally, researchers have sought to improve vascular device compatibility by seeding viable ECs on the device surface prior to implantation [87-89]. The process to achieve successful endothelialization is complex and currently there exists no method that can be used in a clinical setting. This process requires an autologous source of cells that must be isolated and expanded prior to seeding. Issues with contamination and dedifferentiation are also problematic [89]. Furthermore, after seeding, the confluent EC monolayer must be preconditioned under a dynamic flow environment that mimics the natural vasculature. Often, in transition from *in vitro* to *in vivo* conditions, ECs are lost due to handling and reperfusion injury. However, when done successfully, this modification has resulted in lower overall platelet adhesion *in vitro* as well as some animal studies. Unfortunately, this technique is expensive and slow, not allowing for its use in emergency situations [90]. As an alternative, researchers have sought to promote EC proliferation on implants post implantation by precoating the surface with extracellular matrix proteins that promote EC adhesion and migration. However, these proteins (i.e., fibronectin and collagen) are also thrombogenic and increase complications such as embolism [91]. For

these reasons, it is unlikely endothelialization will see any practical applications in the near future despite promising *in vitro* results.

To try and mimic the natural vessel, bio-inspired surface modifications have been explored. ECs continuously produce and release nitric oxide (NO) from the vessel wall and NO is known to inhibit platelet adhesion and activation [92]. As a result, polymers doped or grafted with NO donors been explored to reduce platelet adhesion and activation to biomaterials [93,94]. However the development of polymers capable of long term consistent NO release has been challenging [95]. The geometry of the EC monolayer has also been hypothesized to play a role in its anti-coagulant properties. Fan *et al*. demonstrated that platelet adhesion could be reduced on surfaces that were fabricated to be geometrically similar to the lining of vessels which may be a result of low collision frequencies on such geometries [96]. Unfortunately, some adhesion/activation still occurred suggesting that thrombus formation is still possible in time. Also, there is no information on complement, immune, and coagulation responses to these surfaces. Biomembrane mimetic vascular biomaterials have been prepared by surface immobilization of phosphorylcholine chemical groups and other phospholipids [97-99]. Both techniques have been shown to minimize protein adsorption and platelet adhesion. It is hypothesized that this phenomenon may be due to the zwitterionic nature of these surfaces and their ability to maintain a stable hydration layer. Again, however, *in vivo* studies have produced conflicting results on the efficacy of these materials in reducing thrombosis [98,99].

Given that cell and platelet adhesion is mediated by plasma proteins, surface modification techniques aimed at minimizing protein adsorption have also been explored. Both natural and synthetic molecules have been investigated as potential protein resistant coatings. Carbon coatings including pyrolytic carbon and diamond-like carbon have raised much interest as potential wear resistant coatings for biomedical applications due to their attractive properties such as high hardness, high chemical inertness, and low friction coefficient [100-102]. However, the ability of these coatings to improve the blood response to synthetic vascular devices is still inconsistent. In fact, a recent study explored the thrombogenicity of carbon coated grafts compared to controls and showed no significant difference in long term compatibility [103].

As discussed in section 1.1.4, the plasma protein albumin is believed to be relatively inert to platelets [38]. Subsequently, researchers have sought to passivate biomaterials either by precoating them with albumin or by tailoring the surface to favor albumin adsorption [37,38,104]. Although albumin coated surfaces demonstrate improved biocompatibility, improvements in long term patency have been limited when compared to controls [105]. This may be due to the eventual denaturation or displacement of albumin by plasma proteins with a higher surface affinity *in vivo*.

Polyethylene glycol (PEG) has been immobilized to various biopolymers and been shown to be very effective in minimizing protein adsorption and platelet adhesion [106,100,107,108]. This is hypothesized to be due, in part, to its low interfacial free energy and solubility of these polymer chains in water [107]. Also

PEG chains may have a steric stabilization effect in which protein adsorption results in a loss of configurational entropy. Regrettably, developing strategies to firmly attach PEG to biomaterials has been troublesome and coatings still do not possess long term stability in biological fluids [109]. Also, only a few *in vivo* studies have been conducted and long term results are inconsistent [99,110].

Another approach involves using bioactive coatings that function to inhibit thrombin generation [111]. Specifically, compounds such as heparin [112-114] and thrombomodulin [115] have been grafted to biomaterials and have been demonstrated to reduce platelet adhesion *in vitro*. Commercially available heparinized devices, including the PROPATEN vascular graft (W.L. Gore & Associates, Inc. Flagstaff, Arizona), have also demonstrated promising *in vivo* results [113]. However, their success in long term applications such as vascular access for hemodialysis patients has been limited [114]. It is important to note that immobilization of these compounds may result in an overall loss of activity. Also, once implanted, their preservation on the surface is limited due to the harsh physiological environment.

Despite extensive efforts to minimize platelet adhesion and activation the development of a truly biocompatible material has yet to be realized. As discussed above, numerous studies have demonstrated materials capable of reducing platelet adhesion and activation; however, translation of these materials to clinical practice is almost completely stagnant. This is likely due to the fact that the mechanisms of blood activation are tremendously complex, and these strategies alone still cannot completely eliminate an adverse response. Our

understanding of the mechanisms behind these processes is still incomplete, making in depth fundamental studies of platelet adhesion/activation a critical precursor to the development of hemocompatible materials.

1.3 Surface Patterning and Biological Applications

The fate of a synthetic biomaterial after implantation is largely determined by the properties of its surface. As discussed in previous sections, the surface characteristics determine the nature of the adsorbed protein layer which subsequently directs the cellular response. Consequently, a significant amount of work has been devoted to studying cause effect-relationships between cells and their substrate. Surface patterning is one tool that allows for the precise geometric control of both the physical and physiochemical composition of the substrate. Novel patterning techniques have been implemented to design surfaces with variations in properties, such as topography, charge, hydrophobicity, and the spatial orientation of ligands, such as proteins and synthetic peptides [108,117-122]. The patterning of chemical gradients has been used as a high throughput method to rapidly screen protein and cell surface interactions over a variety of conditions [24,123-131]. If a particular surface property is found to have a desired response, it can be exploited for the given application. Patterned substrates have also been developed to contain spatially defined domains presenting biomolecules surrounded by an inert background. These surfaces have been extremely valuable in the development of protein/oligonucleotide arrays, biosensors, and cell-based arrays [132]. They have also been useful for fundamental studies of cellular processes including

adhesion, migration, proliferation and apoptosis [120, 133-136]. Even surfaces patterned with specific mixed hydrophilic/hydrophobic chemistries resist the attachment of marine organisms and have been explored as a potential solution for biofouling of ships and other marine structures [137]. Hence, surface patterning techniques have proven to be a valuable tool used for a wide variety of applications.

This section will review two types of surface patterning techniques: photolithography and soft lithography, and their applications in studying platelet-substrate interactions.

1.3.1 Photolithography

Photolithography has been used widely for surface patterning applications in the biomedical field. Generally, this technique first involves the deposition of a photosensitive polymer onto a surface. The sample is then selectively exposed to ultraviolet light through a mask possessing the desired surface pattern. Only the exposed areas polymerize. Nonpolymerized regions can be washed away with a solvent leaving only the desired pattern (Figure 1.4).

Photolithography can be used to pattern well defined microfluidic networks that allow for a high throughput experimental design while minimizing the required sample size, a particularly valuable asset in biological studies [138]. Using a similar concept, thermo responsive polymers, such as poly(N-isopropylacrylamide), can be removed by selective UV light exposure. Photoablation of this polymer has been used to control patterns of cell growth [139] and detachment [140]. Compounds such as azidoaniline, which are

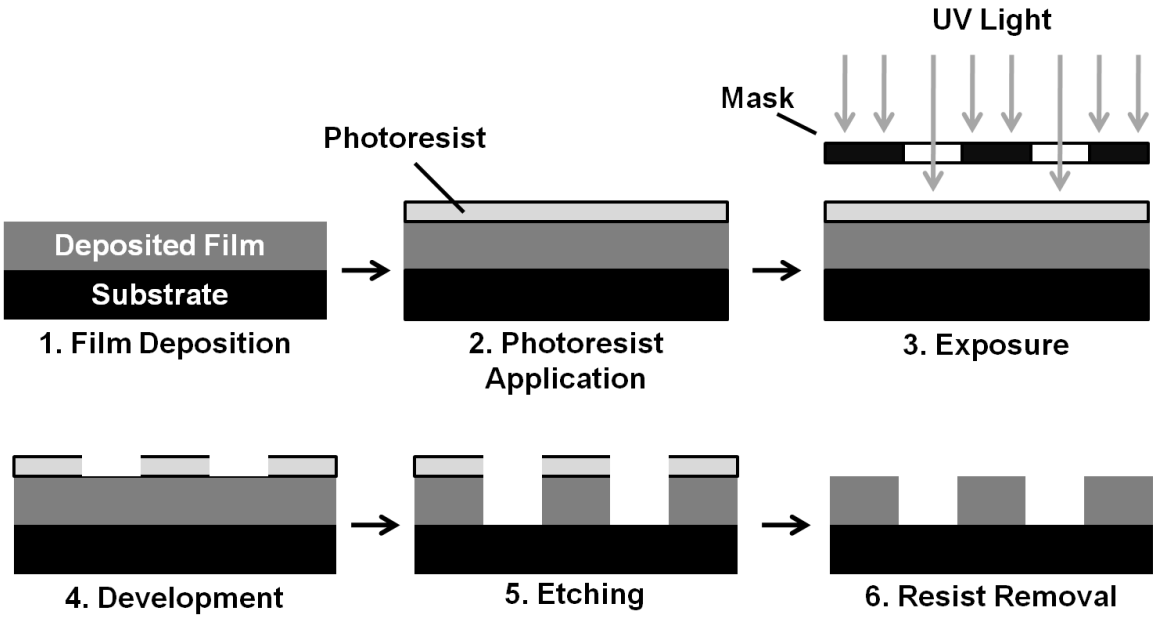

Figure 1.4 Schematic representation of the photolithography process.

sensitive to photolysis, have been coupled to polysaccharides and used to pattern molecules such as hylauronic acid [141] and heparin [123] on surfaces.

Photolithography can also be applied to generate patterns of different surface chemistries [142]. For example, Bhatia *et al.* designed surfaces by selectively exposing thiol monolayers to UV light. Exposed regions oxidized to sulfonate groups and demonstrated good resistance to protein adsorption. Proteins were covalently immobilized to the unoxidized thiol regions allowing for well defined protein surface

patterns to be designed [122,143]. Photolithography continues to be a popular tool due to its ability to provide excellent control and reproducibility over the surface patterns. However, it is not compatible with compounds that are sensitive to UV light energy or etchants, such as certain biological agents. Also, this technique is dependent solely on UV light exposure and can only be used to fabricate binary surface patterns; thus, a more robust patterning technique is needed.

1.3.2 Soft Lithography

Soft lithography is a technique in which flexible elastomeric stamps are used to fabricate surface structures or patterns and possesses many advantages over standard photolithography techniques. Soft lithography is less expensive [144], more robust, does not require the use of photosensitive substrates, and can be applied to the patterning of nonpolar surfaces, all important features for many biological applications [145]. First, the elastomer stamp is prepared by cast molding in a mask or template. Masks are prepared by a variety of

techniques including photolithography, micromachining and e-beam writing. Polydimethylsiloxane (PDMS) is often used for stamp fabrication due to its low interfacial energy, dimensional shape fidelity and thermal stability. However, other polymers such as polyurethanes and polyimides have also been explored [145]. After the elastomer is poured over the mask, the polymer is cured and carefully peeled off the template. These stamps can be used to pattern surfaces in a variety of ways, including microcontact printing, microtransfer molding, replica molding, soft embossing, and micromolding in capillaries. Schematics of these processes are presented in Figure 1.5 and can be reviewed elsewhere [145-148]. Here, the review will focus on microcontact printing since it is the primary patterning technique used for the studies in this dissertation.

Microcontact printing (μCP) is a soft lithography technique in which a patterned elastomeric stamp is used to directly transfer an 'inked' material onto a substrate (Figure 1.5a) and allows for the precise deposition of inked surface ligands (i.e., proteins/peptides) with excellent control over amount, size and position. Micro contact printing has proven to be a useful technique for surface functionalization and has been particularly valuable in the patterning of biological materials [135]. Originally, μCP was used as a method to pattern gold [149]; however, its value in patterning surfaces for other applications quickly became obvious [119,150]. Microcontact printing has been used to study many different cellular phenomena including adhesion, migration, and apoptosis [118,120,133]. This technique has even been used to engineer the surface of human tissue [151]. Lee *et al.* patterned the surface of human eye lens capsules with inhibitory

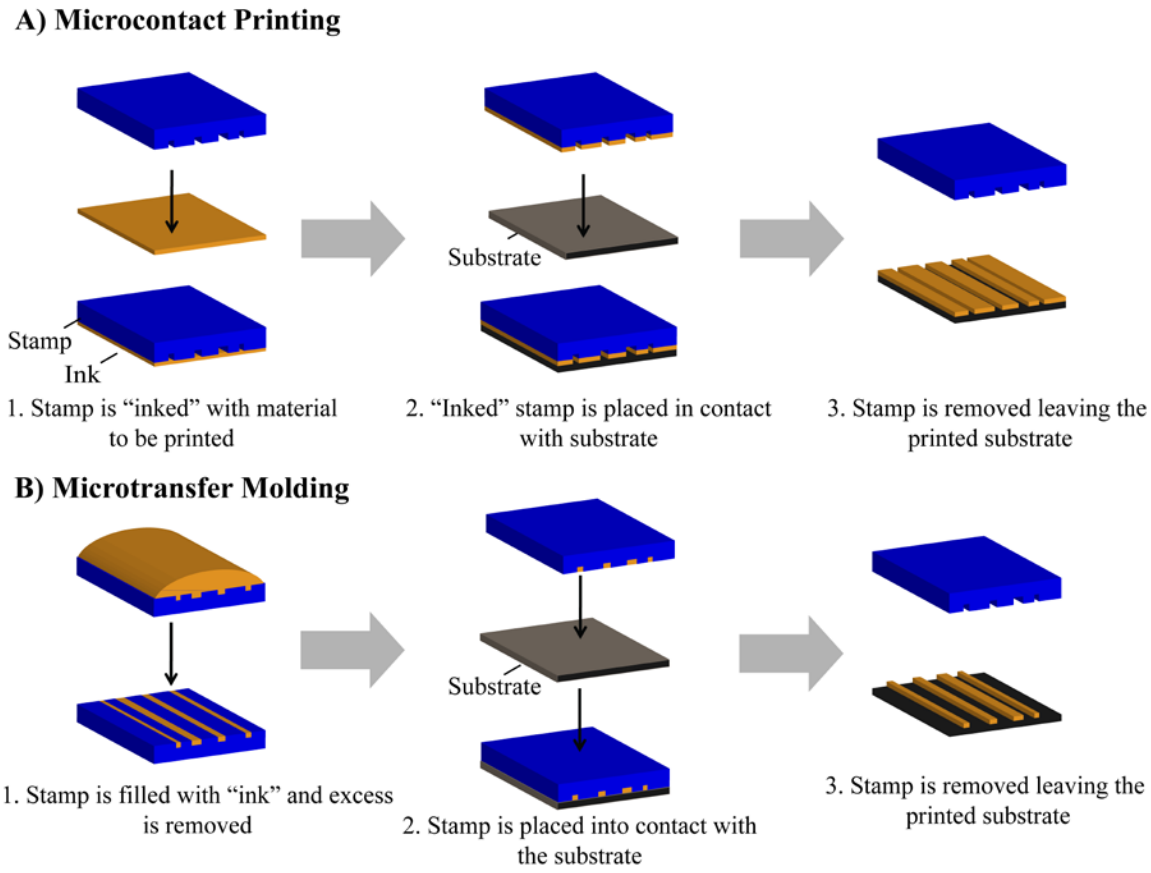

Figure 1.5 Schematic representations of soft lithography techniques: (A) microcontact printing, (B) microtransfer molding, (C) soft embossing, and (D) micromolding in capillaries.

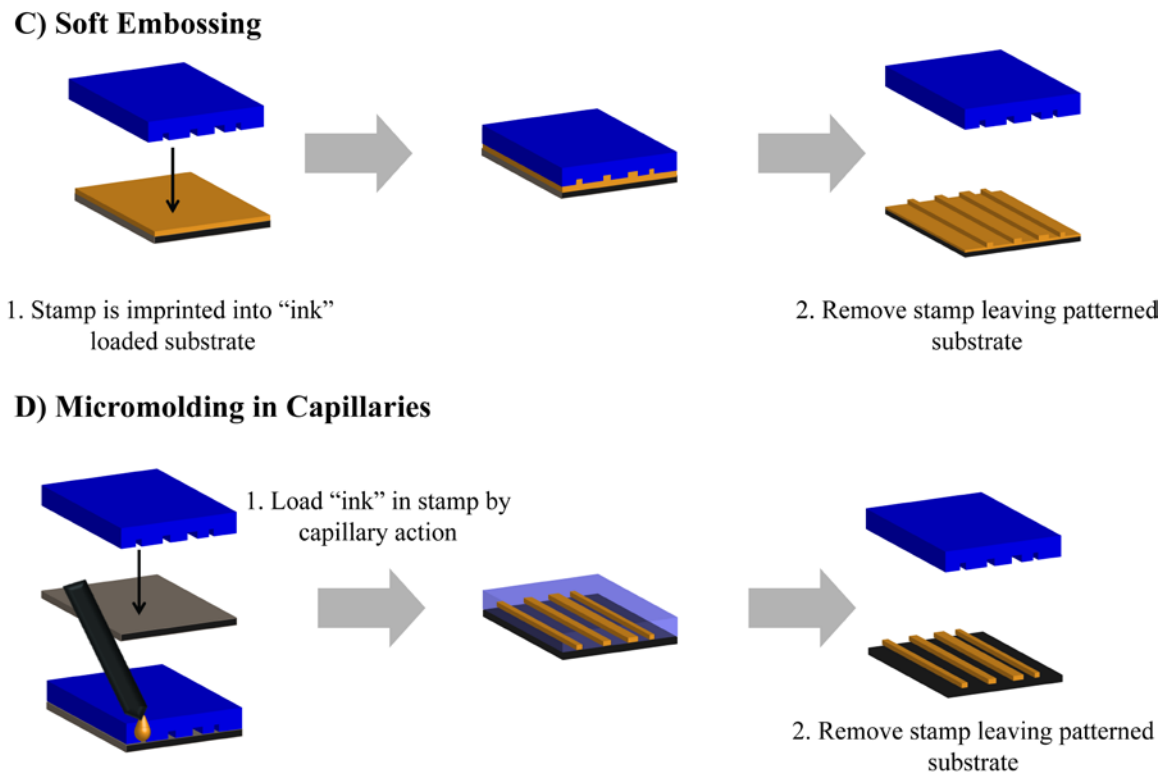

Figure 1.5 continued

molecules to control the growth pattern of epithelial cells on the substrate [151].

1.3.3 Surface Patterning and Applications in Platelet-Material Studies

The platelet membrane is covered with membrane receptors. Interactions between platelet receptors and immobilized ligands are central to adhesion, activation and aggregation mechanisms. Also, platelet morphology plays a critical role in activation processes. Thus there is inherent value in the use of surface patterning techniques to study both fundamental platelet adhesion mechanisms as well as biomaterial-induced platelet responses.

The preparation of surface chemistry gradients is one patterning technique widely used to study both protein adsorption and platelet adhesion phenomena. Chemical gradients have been prepared using photolithographic techniques and provide a combinatorial advantage over homogeneous test samples. Lee *et al*. first used surface gradients in platelet adhesion assays. Samples were prepared by treating polystyrene surfaces with varying levels of corona discharge resulting in a gradient of reactive functional groups on the substrate [124]. PEG molecules of varying chain lengths were immobilized to these substrates and used to quantify protein adsorption and platelet adhesion [108]. Gradients prepared to have varying wettabilities and charges have also been used in platelet adhesion studies [121,125].

Applications of μCP for platelet adhesion assays have also been explored. Basabe-Desmonts *et al.* used this technique to immobilize fibrinogen, vWf and CD42b antibodies to glass substrates and then subsequently capture platelets from whole blood. This technique allows for quantification of adhesion,

morphology changes, and platelet receptor expression potentially improving platelet adhesion and functionality studies [152].

Ekblad *et al*. recently patterned protein resistant PEG based hydrogels onto polystyrene surfaces using standard photolithography techniques to graft the polymer to the surface. After incubation with fibrinogen, excellent control over platelet adhesion was observed. Furthermore, the hydrogel was functionalized with reactive NHS ester groups for protein covalent immobilization. The surface was then selectively incubated with both anti-GPIb and fibrinogen using microfluidic patterning techniques. Platelet adhesion was observed on both protein substrates suggesting that protein covalent immobilization to the hydrogel results in platelet reactive subsrates [153]. Microfluidic patterning of proteins has also been used by Kastrup *et al*. to study coagulation. Specifically, they patterned surfaces with different sized dots of the coagulation stimuli, tissue factor. They were able to show that the initiation of clot formation depends on a threshold size as well as spacing between the dots suggesting roles for both amount and diffusion in initiating a clotting response [154].

Surface patterning techniques provide researchers simplified physical or chemical model systems. These are attractive for understanding biological complexity because these models can be made simple to probe, analyze, and understand specific variables in a well controlled environment. Well-defined surface patterns have been applied to many studies of basic cellular processes such as geometrically controlled apoptosis [134] and cell adhesion/migration [118,120,133,155]. However, the application of surface patterning to studying

fundamental platelet phenomena is still relatively new. In this dissertation, photolithography prepared chemical gradients and μCP patterning techniques were used to explore both fundamental and biomaterial-induced platelet adhesion and activation mechanisms.

1.4 Dissertation Overview

The central goal of the work described in this dissertation was to develop well defined microenvironments to uncover fundamental cause/effect relationships related to surface induced platelet responses. Specifically, molecular patterning techniques were used to control both the chemistry and immobilized protein content of the surface. In Chapter 1, molecular charge gradients were used to screen the platelet response over a variety of chemistries with varying preadsorbed protein layers. In this study, it was observed that upstream platelet interactions with the surface may affect downstream adhesion. The potential ability of platelets to be “primed” for downstream adhesion and activation was further characterized in Chapter 2. In this study, the position of fibrinogen “priming” regions was controlled using μCP. The platelet response in downstream “capture” regions (also prepared using μCP) was evaluated and compared with samples that do not contain a “priming” region. In Chapter 3, the use of μCP was explored further as a means to directly control platelet adhesion and morphology. The ability to control the adhesive and morphological platelet response will be valuable in designing future studies aimed to directly link these variables to physiological processes.

1.4.1 Screening Platelet-Surface Interactions Using Negative Surface Charge Density Gradients

The selection of biomaterials for vascular devices requires consideration of both their bulk and surface properties. Polymeric and metallic materials such as polyurethane, polytetrafluoroethylene, and stainless steel are often chosen for their favorable mechanical and processing properties. Unfortunately, the surfaces of these materials are often thrombogenic, leading to platelet activation and thrombus formation. As discussed in section 1.2.5, surface modification is a popular method used to improve the platelet response to biomaterials without altering its bulk properties. Many surface modification techniques have been attempted with some success [100,156-161]. However, a truly blood compatible interface has yet to be realized. This is primarily due to the complexity behind surface-induced protein and platelet interactions and the virtually infinite number of surface modification techniques that can be considered.

Molecular gradients provide a combinatorial advantage to screen surface induced protein and platelet interactions over a variety of chemistries [125,126,162]. This tool is also capable of providing insight on potential synergistic phenomena that may occur in regions of mixed properties. In Chapter 2 of this dissertation a versatile negative charge density gradient based on selective oxidation of a thiol monolayer was developed. Gradients were preadsorbed with three protein solutions (human fibrinogen, albumin, or plasma) and platelets were perfused over the sample in a parallel plate flow chamber. Adhesion patterns were found to be affected by the type and concentration of the preadsorbed plasma as well as the negative charge density. Interestingly,

adhesion patterns were also affected by the orientation of the gradient samples suggesting that the history of transient upstream platelet-surface interactions can affect downstream results.

Traditionally, blood compatibility studies focus on establishing the local platelet response to the biomaterial. However, since platelet adhesion and activation is often transient, these studies are not sufficient to understand the whole story [163] and have serious implications for the design of *in vitro* studies using molecular gradients. Also, characterizing the effect of upstream platelet-agonist interactions on the downstream response is crucial in understanding biomaterial-induced platelet adhesion, activation and aggregation.

1.4.2 Effect of Upstream Platelet-Agonist Interactions on Downstream Adhesion and Activation

The region where a vascular device joins native vessel, known as the anastomosis, is characterized by high rates of stenosis (narrowing) and subsequently, higher fluid shear rates [100]. The anastomosis is also characterized by adsorption of fibrinogen and the exposure of collagen due damage of the vessel endothelium at this location [107]. This presents an ideal environment for platelet activation to occur and may have serious consequences for the blood compatibility of the downstream biomaterial. Also, in vitro studies only focused on local platelet-material interactions do not account for activation that does not result in an adhesion event. For example, upstream platelet activation on devices such as prosthetic heart valves and stents, may cause downstream thromboembolic complications [5,86]. Also, the most common cause

of arteriovenous graft failure in hemodyalisis patients is neointimal hyperplasia at the graft-venous anastomoses [164,165]. The exact mechanism is not yet understood, however, it has been suggested that the physiology of the venous endothelial layer may play a role [165]. It is possible however, that the upstream artery-graft anastomoses may be preactivating platelets for downstream adhesion since this region is characterized by both high shear forces as well as a damaged endothelial layer. To better understand the role of platelet activation in device failure we must take into account the transient nature of adhesion and activation.

In Chapter 3 of this dissertation, the effect of upstream platelet-fibrinogen interactions on downstream adhesion, activation and aggregation was characterized. Test samples were prepared by covalently immobilizing an upstream platelet “priming” region and a downstream capture region using microcontact printing of fibrinogen. The activation state of platelets that did not adhere was also considered by quantifying expression levels of P-selectin, and the active form of integrin $\alpha_{IIb}\beta_3$ using flow cytometry. It was discovered that the presence of surface-immobilized upstream fibrinogen did in fact result in an increase in downstream adhesion, activation and aggregation when compared with controls. This effect was attenuated when the upstream priming region was blocked with a polyclonal antibody for fibrinogen further confirming its role in “priming” platelets for downstream activation.

1.4.3 Well-Defined Protein Micropatterns for Platelet Adhesion and Activation Studies Using Microcontact Protein Printing

As discussed in section 1.3, protein patterning has been widely applied to *in vitro* studies of cellular mechanisms. However its use in fundamental platelet adhesion and activation studies is relatively unexplored. In Chapter 4, well characterized random fibrinogen micropatterns with 20%, 50% and 85% surface coverage areas were prepared using microcontact printing. It was discovered that both platelet adhesion and activation could be titrated by varying the relative surface coverage of fibrinogen. Varying the surface ligand coverage also resulted in different feature shapes and sizes which were capable of controlling platelet morphological characteristics. The ability to precisely control the amount and distribution of immobilized platelet ligands will be valuable in establishing direct cause-effect relationships between platelet-surface interactions and adhesion and activation mechanisms.

CHAPTER 2

SCREENING PLATELET-SURFACE INTERACTIONS USING NEGATIVE SURFACE CHARGE DENSITY GRADIENTS

2.1 Introduction

When a vascular device is implanted a host of responses occur at the blood-material interface including protein adsorption and platelet activation. Surface properties such as charge, roughness, and hydrophobicity all play critical roles in determining both the protein and platelet response and subsequently, the material's blood-compatibility. A popular approach to the development of hemocompatible materials is to try and tailor the properties of the surface such that it is inert to platelet activation [106,156,157]. However, surface properties can be varied in an unlimited number of ways and the plasma protein and platelet responses can be complex and difficult to elucidate. Surface chemistry gradients provide a more rapid approach to screen blood-material interactions over a variety of surface properties. They are also valuable in providing insight on potential synergistic phenomena that may occur in regions of mixed properties [126]. Molecular gradients have been used to study many different types of biological phenomena including both protein adsorption [127,128,169] and cell and platelet adhesion [129, 170]. Specifically, gradients have been used to study the effects of variables such as wettabillity, charge, and polymer chain length on

platelet adhesion [121,125,162,130]. The inherent value of using surface gradients lies in the ability to identify local effects over a variety of chemistries in a single experiment. However, the reproducibility of local effects once the homogeneous surface is prepared as well as the effect of gradient orientation have not been well documented.

The work included in this chapter describes a versatile method to produce one-dimensional negative surface charge density gradients. The design was based on the selective oxidation of a uniform thiol monolayer to negatively charged sulfonate groups by UV irradiation [171]. Platelets were perfused over the samples and adhesion patterns on the gradient surfaces was measured and compared with uniform thiol monolayer control surfaces. Three protein solutions (platelet free plasma, fibrinogen and albumin) were preadsorbed onto the gradient and control samples to study the role of adsorbed proteins in platelet adhesion. Also the extent to which gradients provide information on local surface effects was studied by comparing the effect of gradient orientation on platelet adhesion patterns.

2.2 Methods

2.2.1 Preparation of Thiol Monolayers

Negative surface charge gradients were prepared by selective oxidation of thiol monolayers on 3” fused silica (FS) slides. Before surface modification, FS slides had to be rigorously cleaned using a four-step cleaning procedure. First the FS slides were cleaned in an oxidizing acid bath overnight. On the following

day, the samples were dried with N_2 gas and then placed in a 10 minute oxygen plasma treatment (Plasmod, Tegal Inc., 50W @ 200mTorr). The FS slides were then incubated in a 7:3 H_2SO_4-H_2O_2 ("piranha") solution for 1 hour. This was followed by a final 10 minute oxygen plasma treatment to activate the surface prior to the reaction. To prepare the thiol monolayer, clean FS slides were incubated in a 1% v/v solution of 3-mercaptopropyltrimethoxysilane (MTS, United Chemical Technologies) in toluene for 4 hours (Figure 2.1). FS slides were rinsed in sequence using solutions of increasing hydrophilicity (toluene, acetone, ethanol, and water) and dried with N_2 gas. The samples were stored under vacuum until use and were not kept for longer than one week.

2.2.2 Preparation of Negative Charge Density Gradients

A gradient of surface charge was achieved by selectively exposing thiol monolayers to UV light (ELC-4000, Electrolite Corp.) in a custom designed patterning chamber (Figure 2.2). The physical length of the gradient as well as the extent of the thiol to sulfonate conversion was controlled by linear translation of an edge mask over the center of the sample. For these studies, the translator moved the edge mask at a constant rate of 0.25 cm/min across center of the slide for four minutes, creating a 1 cm long oxidation gradient in the center of the slide. As a consequence of UV oxidation the surface thiol (-SH) group is oxidized into a sulfonate ($-SO_3^-$) group thus creating a 1-D variation of surface charge, from fully ionized sulfonate to weakly ionized thiol groups. Furthermore, the remaining reactive surface thiols on the sulfonate-to-thiol surface gradient can be

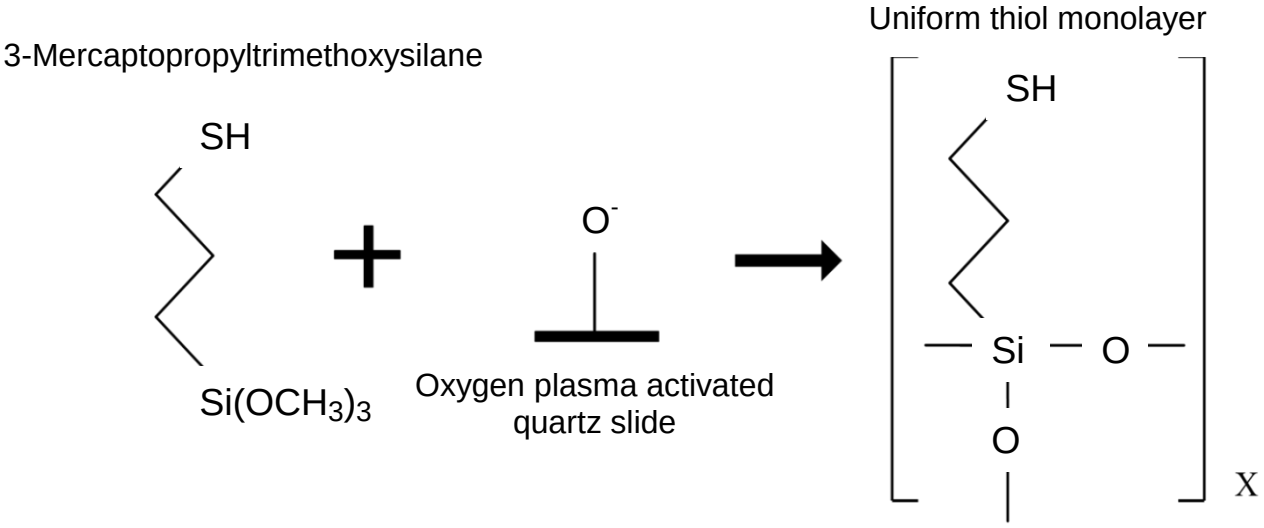

Figure 2.1 Fused silica silanization reaction scheme: thiol monolayers were prepared by reacting MTS (1% v/v in toluene) with an oxygen plasma activated quartz slide for 4 hours.

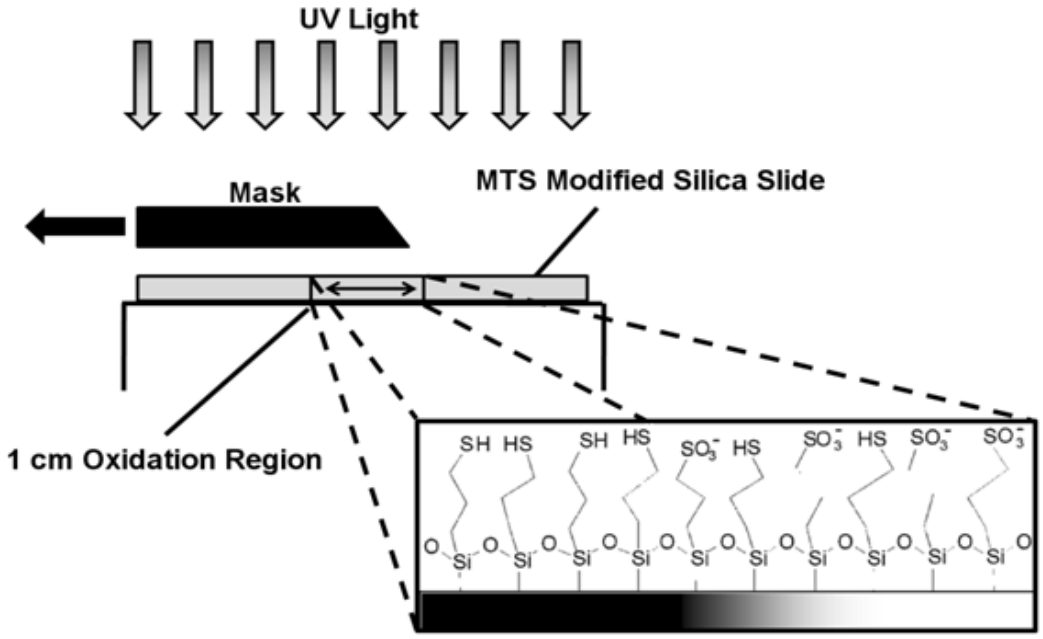

Figure 2.2 Preparation of the surface charge density gradient is accomplished by translating the edge mask at a constant rate over a 1 cm region of the uniformly modified MTS silica slide. On the UV exposed region the surface thiol group is oxidized into a negatively charged sulfonate group.

utilized for a second chemical reaction thus making the MTS + UV oxidation method a versatile basis for several different surface chemistry gradients [172].

2.2.3 Gradient Characterization

Water contact angle measurements are an easy way to detect the wettability changes of the thiol to sulfonate gradients. Prior to each experiment, receding water contact angles were measured by the sessile drop method using a contact angle instrument (CAM 100, KSV Instruments). Equal 5 µl purified water droplets were dispensed along the length of the sample and water contact angle was plotted as a function of position on the FS slide. The extent of the thiol to sulfonate conversion was also verified using high resolutions ESCA spectra of S2p peaks. The XPS spectra of MTS-modified silica and UV oxidized MTS modified silica was recorded with a XPS spectrometer (Axis-Ultra DLD, Kratos) at the University of Utah Nanofab Lab.

2.2.4 Protein Solution and Washed Platelet Preparation

Three different human protein solutions were prepared: platelet free plasma, fibrinogen (plasminogen free, Calbiochem) and albumin (Fraction V, Sigma) in phosphate buffered saline (PBS). Platelet free plasma was obtained by filtration of the platelet poor plasma (PPP) collected during the washed platelet preparation using 0.22 µm low protein binding filters (Millipore). For the studies involving testing the effect of PFP concentration on platelet adhesion the PFP concentration was adjusted using PBS (pH 7.4) to 1%, 10% or 50% of normal

physiological PFP concentration. Fibrinogen and albumin solutions were prepared in PBS at 10% of each protein's normal physiological concentration.

Washed platelets were prepared from whole blood from healthy human donors. Blood was collected in a 1:7 anticoagulant citrate dextrose (ACD) solution and centrifuged for 15 minutes at 1500 rpm to separate platelet rich plasma (PRP) from the red blood cells. The PRP supernatant was aspirated off using a transfer pipette. Prostaglandin E_1 (PGE1, 300 nM) was added to the PRP to inhibit aggregation during preparation [173]. PRP was centrifuged for 15 minutes at 2100 rpm for platelet isolation. The PPP supernatant was carefully transferred to a clean polypropylene test tube, not disturbing the platelet pellet. The platelet pellet was gently resuspended in prewarmed Tyrode's-HEPES buffer (37 ^{0}C, pH 7.4) [174] and 300 nM PGE_1. Platelets were counted using a hemocytometer and the concentration was adjusted to $1.5 \bullet 10^7$ platelets/ml.

2.2.5 Platelet Adhesion Studies

All protein and washed platelet solutions were maintained at 37^{0}C throughout the experiments. A syringe pump (Kent Scientific) was used to draw solutions through a parallel plate flow chamber (length 7 cm, width 0.5 cm, thickness 0.05 cm) at a constant flow rate (40 ml/hr) thus creating a shear rate of 92 s^{-1}. The flow cell was connected to the solutions using 15 cm long polyethylene tubing (shear rate of 24 s^{-1}) (Figure 2.3). A three step perfusion process was used to study platelet adhesion. First a protein solution was perfused through the flow cell for 15 minutes to allow for plasma protein adsorption to the gradient surface. The protein solution was followed by a 5-

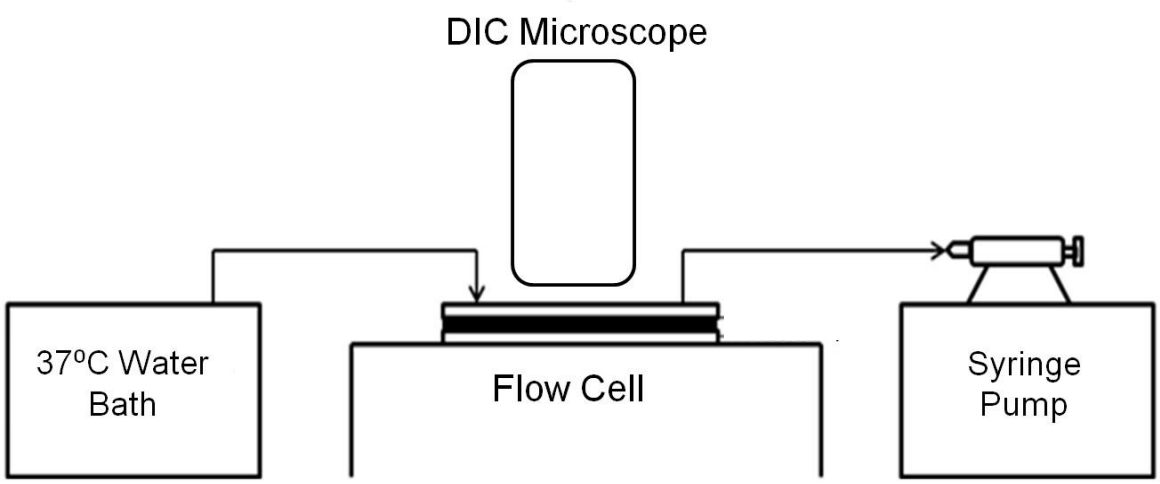

Figure 2.3 Flow system for platelet perfusion studies.

minute perfusion of a washed platelet suspension avoiding any surface-air contact. The washed platelet suspension was diluted to 10^7 platelets/ml and activated by adding Ca^{2+} (2 mM) and ADP (1 μM) to the solution prior to perfusion.

The platelet perfusion time of 5 minutes was selected to minimize the formation of platelet aggregates which may be more indicative of platelet-platelet interactions than of interactions with the protein covered gradient surface. In the final step a 1% glutaraldehyde solution was injected into the chamber for 15 minutes to fix the sample. All unbound platelets were washed from the sample with PBS prior to counting.

The platelets adhered to the surfaces were visualized using differential interference contrast microscopy (DIC, Diaphot 300, Nikon). Separate counts (n = 10) for 20 positions at 1 mm increments including the gradient region were taken and converted to the number of platelets per mm^2. To account for variable platelet activity over different donors, all data were normalized using a uniform thiol sample (i.e., MTS modified silica with no gradient) preadsorbed with 10% PFP as a baseline. Adhesion contrast on gradient samples was determined to be significant by performing an unpaired t-test comparing adhered platelets found in the sulfonate and the thiol regions (n = 20).

2.3 Results and Discussion

2.3.1 Surface Characterization

Receding water contact angles between 50^0-55^0 were measured in the thiol region of the sample and between 8^0-12^0 in the sulfonate region (Figure

2.4a). Water contact angles decreased through the region exposed to variable UV irradiation times indicating the presence of a gradient in the center of the sample. The XPS S2p spectra of the MTS-modified silica and 4 minutes UV oxidized MTS-modified silica are shown in Figure 2.4b. The elemental XPS analysis showed ~2 atomic % of sulfur, an expected value for an MTS monolayer [172]. For MTS-modified silica (dashed line, Figure 2.4b) a strong S2p peak at 163.5 eV confirmed the presence of surface thiols. After 4 minutes of UV irradiation (full line, Figure 2.4b), the 163.5 eV peak decreased in magnitude while the peak at 168 eV increased. The higher binding energy peak indicated that the sulfur atoms from the –SH groups has combined with oxygen, forming a sulfonate moiety [171]. The conversion of thiol to sulfonate was incomplete: the fraction of sulfur in the oxidized state was around 0.6. Also, a small fraction of oxidized thiols was present on the MTS-modified silica which was not irradiated by UV, possibly due to spontaneous oxidation of thiols in air.

2.3.2 Effect of PFP Concentration and Platelet Adhesion

Blood plasma concentration has been noted to influence the composition of the adsorbed protein layer as well as subsequent platelet-surface interactions [175,176]. In this study, sulfonate-to-thiol gradient surfaces were preadsorbed with three different PFP concentrations (1%, 10%, and 50% of physiological PFP concentration). Average platelet adhesion (n = 10) was quantified over a 20 mm region of the sample, including the gradient region, at 1 mm intervals with the gradient located between 5 mm and 15 mm (Figure 2.5a). The error bars represent the standard deviation of each sample. An increase in adhesion

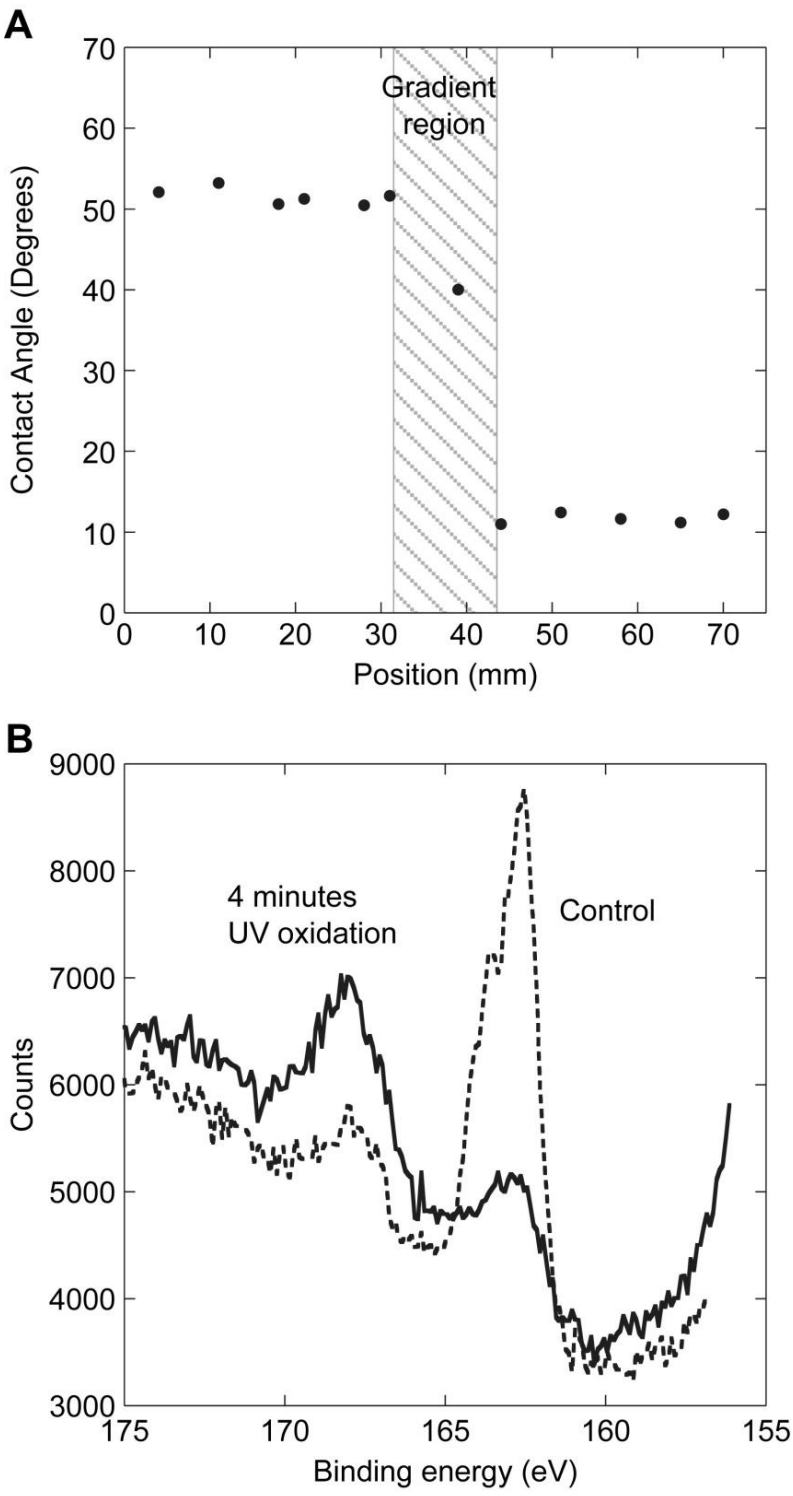

Figure 2.4 Characterization of negative charge density gradients: (A) Receding water contact angles plotted as a function of distance from the negatively charged sulfonate end of the gradient sample. (B) High resolution XPS S2p spectra of the MTS-modified silica control (dashed line) and 4 minutes UV oxidized MTS-modified silica (full line).

corresponding to a decrease in negative charge density was observed for all three PFP concentrations. An unpaired t-test comparing the sulfonate region with the thiol region was performed for all three concentrations and shown to be significantly different with a confidence interval of $p < 0.0001$, $n = 20$. Samples preadsorbed with 1% and 50% PFP showed less adhesion contrast across the gradient region compared to samples preadsorbed with 10% PFP. Brash *et al*. have reported that the amount of adsorbed fibrinogen on glass is dependent on plasma concentration while albumin is not [175]. Thus, one possible explanation for less adhesion contrast at 1% dilutions is that the ratio of adsorbed fibrinogen to adsorbed albumin is not enough to support extensive platelet adhesion. In other words, the overall fibrinogen concentration may not be sufficient to out compete albumin and override its inhibitory effect.

A higher number of platelet aggregates was observed on gradient samples preadsorbed with 50% PFP compared to 1% and 10% PFP (Figure 2.5b). The increase in aggregate formation may be more representative of platelet-platelet rather than platelet-surface interactions. Gradient surfaces preadsorbed with 10% PFP provided the best adhesion contrast and therefore this concentration was used for the remaining platelet adhesion experiments.

2.3.3 Platelet Adhesion on Gradient Surfaces

Platelet adhesion on sulfonate-to-thiol gradient surfaces preadsorbed with three different 10% protein solutions (PFP, fibrinogen, and albumin) is shown in Figure 2.6. The platelet suspension was perfused in the sulfonate to thiol direction across the gradient. Adhered platelets were counted over a central

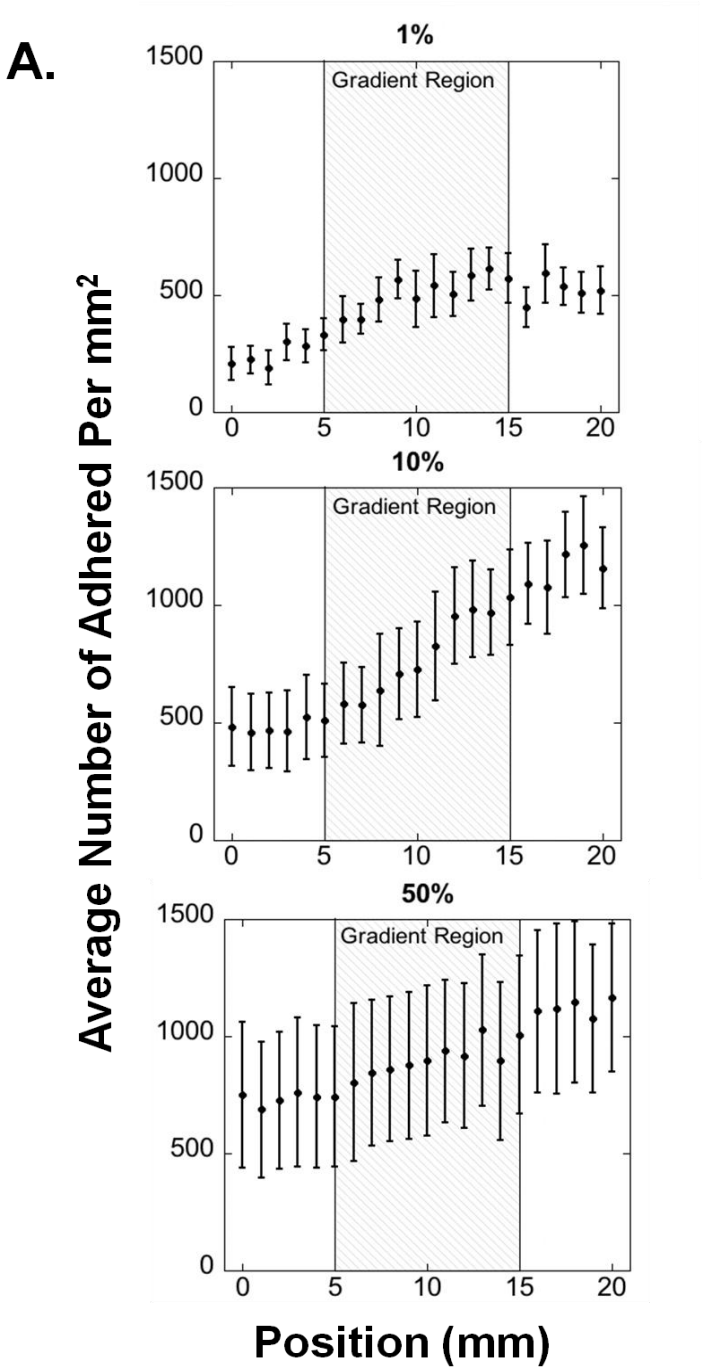

Figure 2.5 Effect of PFP concentration on platelet adhesion to gradient surfaces: (A) Average number of adhered platelets were measured. For every position the adhesion values represent a mean value where n = 20. Positions 0 – 5 mm represent the sulfonate region and 15 - 20 mm the thiol region with the gradient region between 5 mm – 15 mm. The platelet suspension was perfused in the direction from the sulfonate region, over the gradient, to the thiol region. (B) DIC images of platelet adhesion on sulfonate and thiol regions for 1%, 10%, and 50% preadsorbed PFP concentrations.

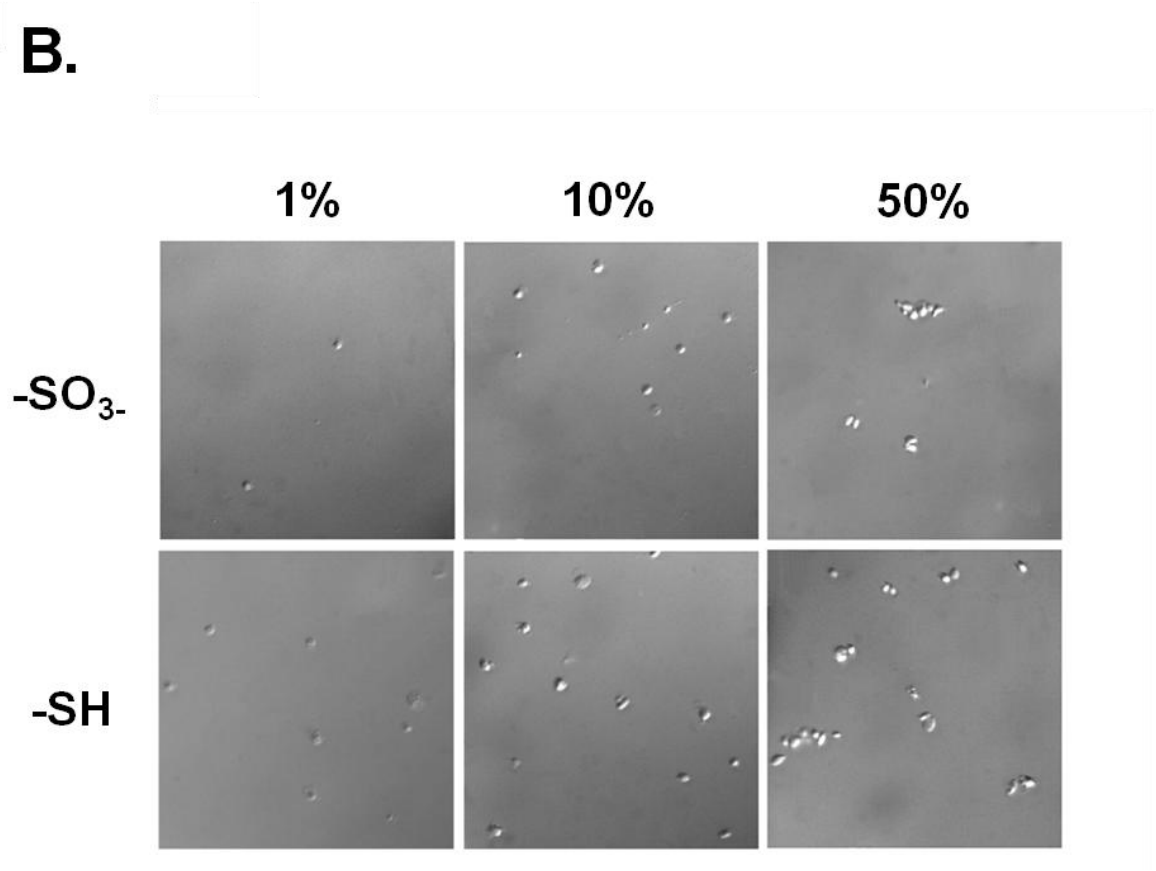

Figure 2.5 continued.

20 mm region covering approximately 5 mm on each side of the gradient at 1 mm intervals (n = 10) with the gradient located between 5 mm – 15 mm. The normalized platelet count for each position is plotted as a function of distance with the error bars representing the standard deviation of each sample. Uniform thiol surface (i.e., with no gradient) served as a control.

Surprisingly, nonoxidized control samples (uniform thiol monolayers) preadsorbed with 10% human fibrinogen and 10% PFP did see a significant increase in adhesion as a function of distance from the flow inlet ($n = 20$, $p < 0.001$) (Figure 2.6 b and d) despite lacking a charge density gradient. Uniform thiol monolayers preadsorbed with PFP displayed an adhesion increase in the 0 mm – 5 mm region, while the same surfaces preadsorbed with fibrinogen displayed a significant increase in adhesion over the length of the sample (Figures 2.6 b vs. 2.6 d). We infer that the increased downstream adhesion is likely due to upstream surface contact activation. Surface fibrinogen-platelet interactions convert platelets from a quiescent to a procoagulant state [177]. In addition, once platelets adhere to a substrate, they do not always remain there and contacts can be transient [173]. Taken together, a downstream increase in platelet adhesion may be the result of upstream preactivation. Control samples preadsorbed with 10% human albumin showed a minimal variation of platelet adhesion as a function of distance from the flow inlet (Figure 2.6f). Overall, the controls with 10 % PFP and 10 % fibrinogen resulted in similar levels of platelet adhesion while samples preincubated with albumin resulted in the lowest adhesion.

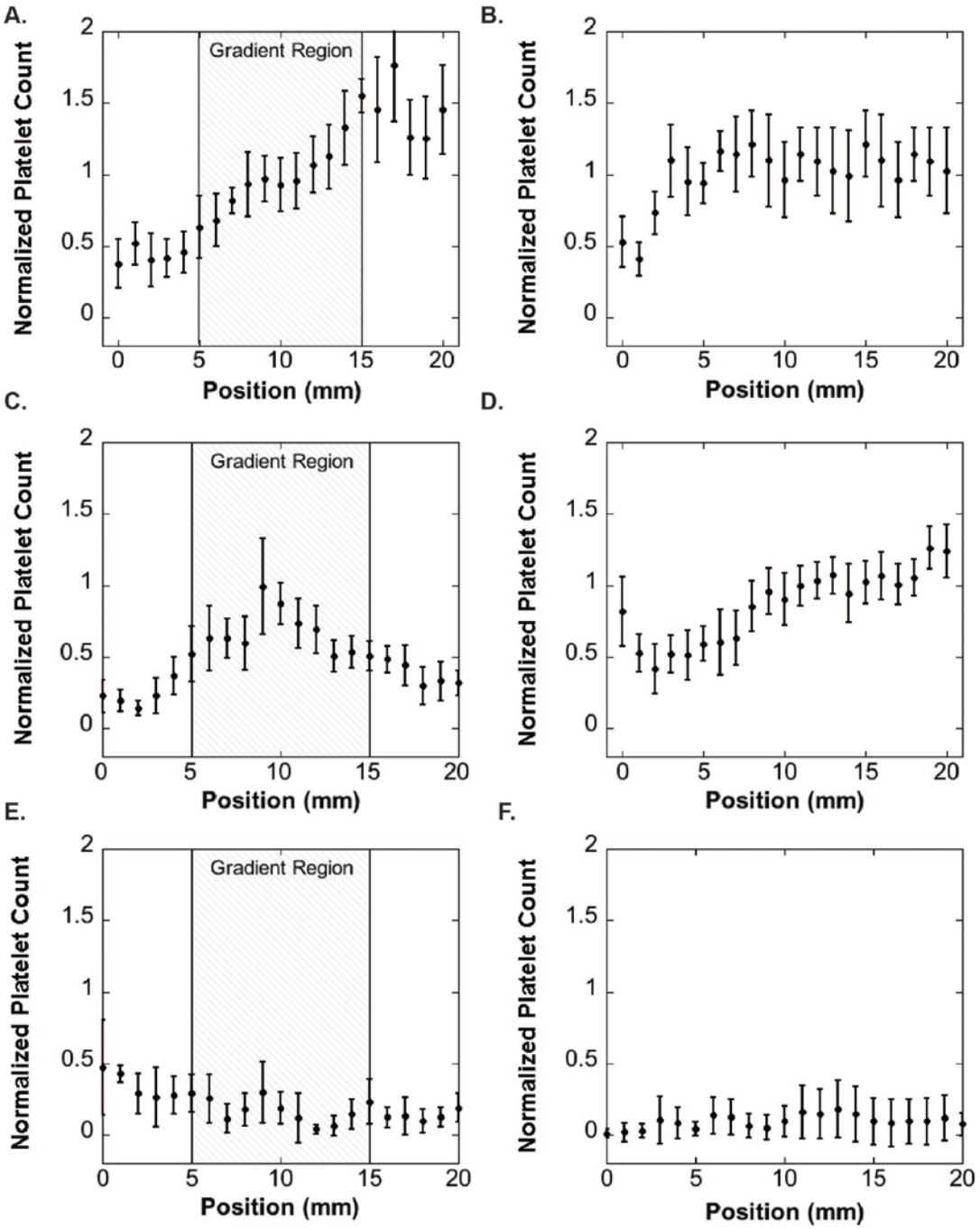

Figure 2.6 Effect of negative surface charge density gradients on platelet adhesion. Normalized platelet adhesion on sulfonate-to-thiol gradient samples and on non-gradient MTS controls preadsorbed with plasma (panels A,B), fibrinogen (panels C,D) and albumin (panels E,F). Adhesion values represent a mean ± standard deviation; n = 20. Platelet counts were normalized by dividing data from each sample by the average adhesion for a PFP control sample (panel B).

Sulfonate-to-thiol gradients preadsorbed with 10% human PFP displayed a gradient of platelet adhesion compared to the non-gradient control with a significant ($n = 20$, $p < 0.001$) difference between the negatively charged sulfonate region of the gradient and the thiol region of the sample (Figure 2.6a). Platelet adhesion increased with respect to the distance from the flow inlet which was also inversely related to the surface charge density. These results compare well with the previous studies that have shown platelet adhesion to increase with increasing hydrophobicity in the presence of plasma proteins [121,125]. The chemistry difference between thiol and sulfonate mattered as well: sulfonate groups have been incorporated into various biomaterials and shown to improve hemocompatibility [178,179].

The effect of the surface charge gradient on platelet adhesion and its relationship to the nature of the adsorbed protein layer was further investigated by preadsorbing a 10% fibrinogen solution prior to platelet perfusion. Interactions between fibrinogen and the $\alpha_{IIb}\beta_3$ integrin receptors on platelets are central in platelet adhesion and aggregation [46,180] thus making it a logical next choice for this study. Gradient samples preadsorbed with human fibrinogen displayed an adhesion maximum in the center of the gradient region, (Figure 2.6c) an effect not observed either on the nonoxidized thiol monolayer control sample (Figure 2.6d) or gradient preadsorbed with PFP (Figure 2.6 a). This platelet adhesion maximum on fibrinogen preadsorbed gradient sample is different than the additive effect seen on gradient samples preadsorbed with PFP, thus confirming

the importance of not only the surface properties but the nature of the adsorbed protein layer as well.

Gradients preadsorbed with 10% human albumin did not show any significant adhesion contrast (Figure 2.6e). Overall platelet adhesion, however, on the sulfonate region of the albumin coated gradient sample was somewhat higher than on the thiol region for both the uniform thiol control and sulfonate-to-thiol gradient samples. The lack of an upstream effect on downstream adhesion was initially interpreted as being the result of albumin inhibition on platelet adhesion [104]. However, contrary to the uniform thiol monolayer data, platelet adhesion in the sulfonate region of the gradient samples was somewhat higher than in the thiol region of the gradient as well as in thiol controls. In a separate study, we found that sulfonate and thiol regions adsorbed similar amounts of albumin, implying that the lack of inhibition was not due to the lower amount of adsorbed albumin [24]. Significant platelet attachment to albumin coated surfaces has been recently reported, presumably due to exposure of a hidden binding site for platelets on albumin upon surface adsorption [35]. A conjecture can be made that the inhibition of platelet adhesion by adsorbed albumin depends more on its conformation than on the variation of adsorbed amount. The results here may also indicate that low platelet adhesion to surfaces preadsorbed with PFP may not be due to increased albumin adsorption but perhaps to protein conformation or to some other variability in the composition of the protein surface layer.

2.3.4 Effect of Sample Orientation on Platelet Adhesion

To further investigate the effect of upstream conditions on downstream platelet adhesion, the orientation of the gradient sample preadsorbed with 10% PFP was reversed and compared. Platelets were perfused over samples with the sulfonate region in the upstream position of the flow cell (Figure 2.7a). These adhesion patterns were compared with samples with the thiol region in the upstream position (Figure 2.7b) before reaching the gradient. Platelet adhesion on gradient samples with the upstream sulfonate region displayed similar adhesion contrast seen in previous experiments (Figures 2.5a and 2.6a). When the orientation of the sample was reversed, adhesion contrast was lost and overall adhesion values on the thiol and sulfonate rich regions decreased and increased, respectively. The results support the conclusion that upstream platelet-surface interactions could exhibit enhanced downstream adhesion. In the surface gradient experiments the relationships between surface composition and correlated with the surface properties of that position alone. Thus, it turns out that the history of transient surface-platelet interactions must be considered as well. Discrepancies between results obtained on gradient vs. control samples were also reported by Zelzer *et al.* [129]. It is thus crucial we acknowledge these inconsistencies when using gradients as a tool to study various biological phenomena.

To reduce the complexity of blood-surface interactions and obtain direct insight on the cause-effect relationship between surface chemistry, adsorbed protein and platelet adhesion, we used washed platelets instead of whole blood

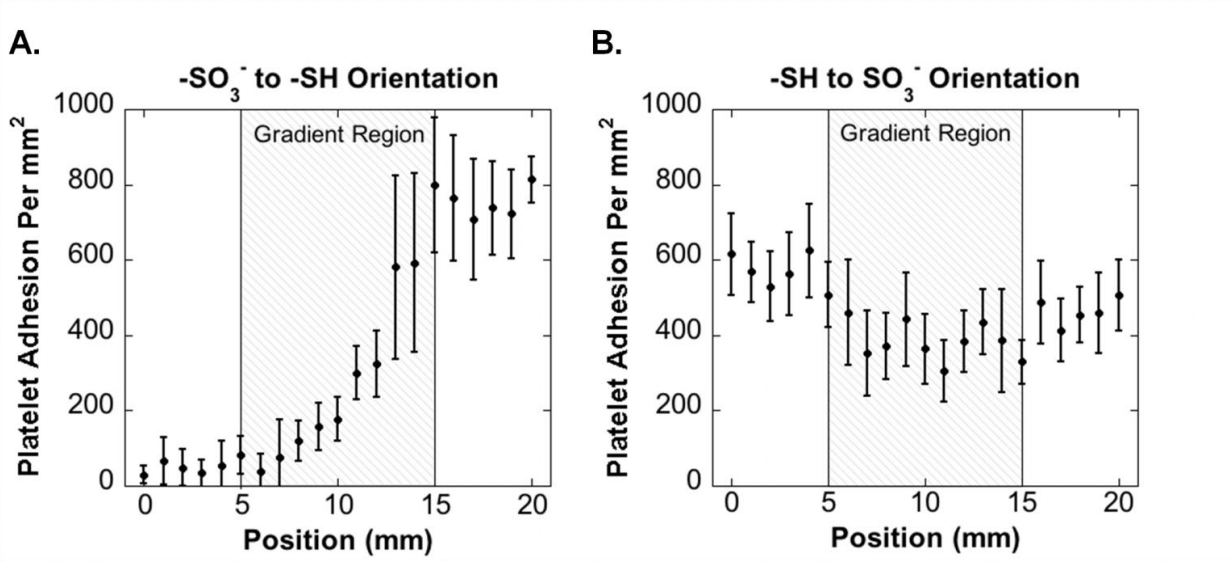

Figure 2.7 Effect of sample orientation on platelet adhesion to gradient surfaces. Platelet adhesion comparison on sulfonate-to-thiol gradient surfaces with (A) the sulfonate region in the upstream position and with (B) the thiol region in the upstream position of the flow cell. Samples were preadsorbed with 10% human PFP. Adhesion values represent a mean ± standard deviation; n = 20.

or PRP; however such an approach neglects the effect of red blood cells, which have been shown to increase platelet adhesion through a “mixing” effect [181]. Although the “mixing effect” could have influenced overall adhesion amounts in the experiments described here, it was not expected to significantly affect the adhesion contrast seen in these experiments since red blood cells do not actively interact with the surface.

Another concern might be due to the presence of albumin in the platelet wash buffer used to prevent premature platelet activation during handling. One may question its effect on the nature of the adsorbed protein layer during adhesion experiments. The presence of albumin in the wash buffer (3 mg/ml) is expected to have little effect on surfaces precoated with albumin since any exchange reactions would not change the nature of the protein layer. Surfaces preadsorbed with 10% fibrinogen may be affected by the presence of albumin in the platelet wash buffer due to the Vroman effect; however this may also be unlikely due to the fact that preadsorbed fibrinogen has a higher affinity for surfaces than albumin making this exchange energetically unfavorable [183].

2.4 Conclusions

In this work platelet adhesion on surfaces with varying negative charge densities was studied. Platelet adhesion was also related to the nature of the adsorbed protein layer (specifically: albumin and fibrinogen). Platelet adhesion onto gradients was affected by both the type and concentration of preadsorbed protein as well as related to the negative charge density. The high-throughput potential of surface gradients is a useful concept for testing platelet adhesion and

material hemocompatibility in general. However, it is important to consider that local surface effect may be affected by the upstream surface-platelet interactions. The orientation of gradient samples was shown to affect platelet adhesion patterns suggesting that the history of transient surface contacts must be considered.

The ability of platelets to be “preactivated” by the upstream environment has many implications for biomaterial hemocompatibility, specifically for of *in vitro* screening studies and in the design of blood-compatible biomaterials. In the next study, an *in vitro* system was developed to characterize the effect of “priming” platelets with upstream surface immobilized fibrinogen on downstream adhesion and activation.

CHAPTER 3

THE EFFECT OF UPSTREAM PLATELET-FIBRINOGEN INTERACTIONS ON DOWNSTREAM ADHESION AND ACTIVATION

3.1. Introduction

Surface induced platelet adhesion and activation is a dynamic process. Platelets attach/detach and roll [43,163,183], before ultimately forming stable adhesive interactions. In fact, most platelet-surface contacts are transient [163]. Even though transient interactions do not result in local platelet adhesion and aggregate formation it is unlikely that they leave the activation state of the platelet unaffected. With each surface contact, there is the opportunity to interact with plasma protein agonists such as fibrinogen and vWf, both known to activate platelets [40,84,184].

Traditionally, research has worked to establish local cause and effect relationships between surface properties and platelet adhesion and activation. Quantification of local platelet adhesion [15,106,157,185] and morphological changes [186-188] has been widely used to characterize the blood compatibility of biomaterials. In Chapter 2 an increase in platelet adhesion was observed on

homogeneous surfaces pre-adsorbed with fibrinogen as a function of distance from the flow inlet (2.3.3). Also, when the orientation of surfaces patterned with negative charge density gradients was reversed, adhesion patterns also changed. This led us to hypothesize that upstream-platelet surface interactions may affect the downstream platelet response. Specifically, upstream interactions with adsorbed protein agonists may “prime” platelets for downstream adhesion and activation.

In this study, we characterized effect of upstream platelet-fibrinogen interactions on downstream adhesion and activation. Micro contact protein printing (μCP) was used to covalently immobilize fibrinogen priming regions onto reactive substrates. The downstream platelet response was observed on two model surfaces; sulfo-SMCC modified thiol monolayers and commercially available Nexterion-H slides. Downstream adhesion, activation and aggregation were significantly higher on Nexterion-H samples containing a fibrinogen priming region than control samples. Also, the increase in downstream adhesion was attenuated when the priming region was blocked with a polyclonal antibody for fibrinogen suggesting fibrinogen is, in fact, capable of inducing a downstream response. Reactive substrates prepared by sulfo-SMCC modification of thiol monolayers [189, 190] did show an increase in adhesion downstream of the fibrinogen priming regions however high background platelet adhesion was also observed which made the results difficult to elucidate. The effect of transient platelet-surface contacts on bulk platelet activation was also assessed by quantifying P-selectin and active $\alpha_{IIb}\beta_3$ using flow cytometry. A slight increase in

bulk platelet activation was observed after perfusion over samples prepared with covalently immobilized fibrinogen versus albumin.

3.2 Methods

3.2.1 Preparation of Reactive Surfaces

Surfaces capable of protein covalent immobilization were prepared using protocols previously established in our lab in which RGD peptides were immobilized to thiol monolayers (Appendix A). Immobilization was achieved using a two-step process: preparation of a surface thiol monolayer followed by incubation with a heterobifunctional crosslinker, sulfosuccinimidyl-4-(N-maleimidomethyl)cyclohexane-1-carboxylate (sulfo-SMCC) [189, 190]. The sulfo-SMCC crosslinker contains an amine reactive N-hydroxysuccinimide (NHS) ester and a thiol reactive maleimide group making it an ideal agent for coupling proteins to silanized quartz slides. Covalent immobilization was achieved through formation of an amide bond between the amine reactive NHS ester group and a primary amine on lysine residues in the protein molecule (Figure 3.1). Reactive thiol monolayers were prepared following the protocol described in section 2.2.1. Silanized FS slides were incubated with sulfo-SMCC (Sigma) in 0.05M PBS (1 mg/ml, pH 8.5) for 30 minutes. After the reaction, FS slides were thoroughly rinsed in distilled water and dried with N_2 gas. All samples were stored under vacuum and used for experiments within 1 week.

A second set of reactive slides (Nexterion-H, Schott) purchased commercially were also used for this study. These slides contain a reactive coating in which a cross-linked poly(ethylene glycol) PEG layer is functionalized

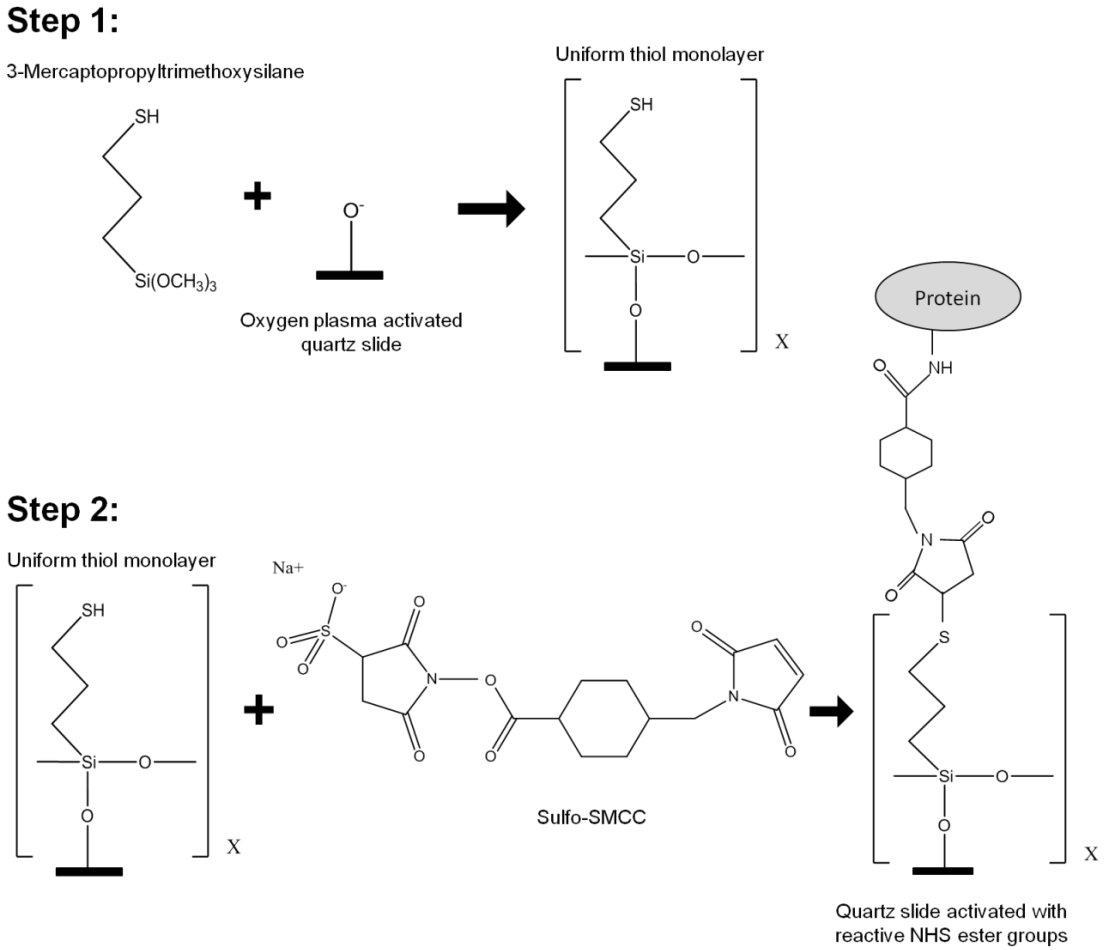

Figure 3.1 Chemistry of the sulfo-SMCC surface modification process. First, quartz slides are silanized with 3-mercaptopropyltrimethoxysilane resulting in a monolayer of reactive surface thiol groups. These groups are modified by incubation with the heterobifunctional crosslinker sulfo-SMCC. Sulfo-SMCC contains a maleimide on one end which is reactive to the thiol monolayer and a reactive NHS ester on the other end which is capable of covalent protein immobilization.

with NHS esters providing means for covalent protein immobilization through the terminal amine group [191]. These samples provided a comparable protein immobilization scheme to sulfo-SMCC modified quartz slides. However, the presence of the PEG hydrogel matrix minimized nonspecific protein and platelet interactions.

3.2.2 Preparation of Polydimethylsiloxane (PDMS) Stamps for μCP

PDMS stamps were prepared from masks with randomly distributed micrometer sized features that were defined to cover 85% of the stamp surface area. Mask patterns were developed by generating a 500 x 500 array of randomly distributed black and white pixels using Mathematica (Wolfram). Patterns were transferred to chromium coated silica wafers using conventional photolithography. First, the pattern was uploaded into a mask making software, L-Edit (Tanner), where each pixel was defined to be 25 μm x 25 μm. An Electromask MM250 (Interserv Technology) pattern generator was used to produce the first mask (A_{mask} = 1.25cm x 1.25cm and A_{pixel} = 25 μm x 25 μm). This was followed by two 5x image reductions and one repeat step to produce a final mask with a 20 x 20 pattern array of randomly distributed micron sized features (A_{mask} = 1cm x 1cm and A_{pixel} = 1 μm x 1 μm). Sylgard 184 silicone elastomer (Dow Corning) was mixed with curing agent in a 10:1 ratio and poured over the patterned mask. PDMS was degassed by placing the samples under vacuum for 30 minutes. The samples were cured for 30 minutes at 100°C and carefully peeled away from the mask to remove the patterned stamps. This was followed by an additional 60 minutes of curing at 60°C. After curing the stamps

were incubated overnight in hexane to remove any polymer that did not crosslink. To eliminate swelling that occurred after hexane incubation, stamps were rinsed for 30 minutes in a 95% ethanol solution, 30 minutes in Milli Q water, and dried for 30 minutes at 60°C.

3.2.3 Sample Preparation Using µCP

Printing on sulfo-SMCC Samples: PDMS stamps were "inked" with either fibrinogen or albumin in PBS (c = 1 mg/ml, pH 8.5) for 15 minutes, rinsed in Milli-Q water and dried with N_2 gas. The fibrinogen covered stamps were placed in contact with 490 Pa of pressure applied evenly using a 5g weight. PDMS stamps were positioned in the center of sulfo-SMCC reactive slides for 45 minutes allowing for protein covalent immobilization (Figure 3.2a). Following protein immobilization, samples were vigorously rinsed in a 1% Tween solution to remove any protein not covalently immobilized on the surface. Samples were then rinsed thoroughly with Milli-Q water, dried with N_2 gas and stored under vacuum until use.

Preparation of Nexterion H Samples: PDMS Stamps were "inked" with human fibrinogen in PBS (c = 1 mg/ml, pH 8.5) for 15 minutes, rinsed in Milli-Q water and dried with N_2 gas. The fibrinogen coated stamps were placed in contact with Nexterion-H (Schott) reactive slides under the same conditions as described for sulfo-SMCC reactive samples above. A fibrinogen "priming" region was printed in the upstream region on test samples and a platelet capture region was printed 10 mm downstream of the priming region (Figure 3.2a). After

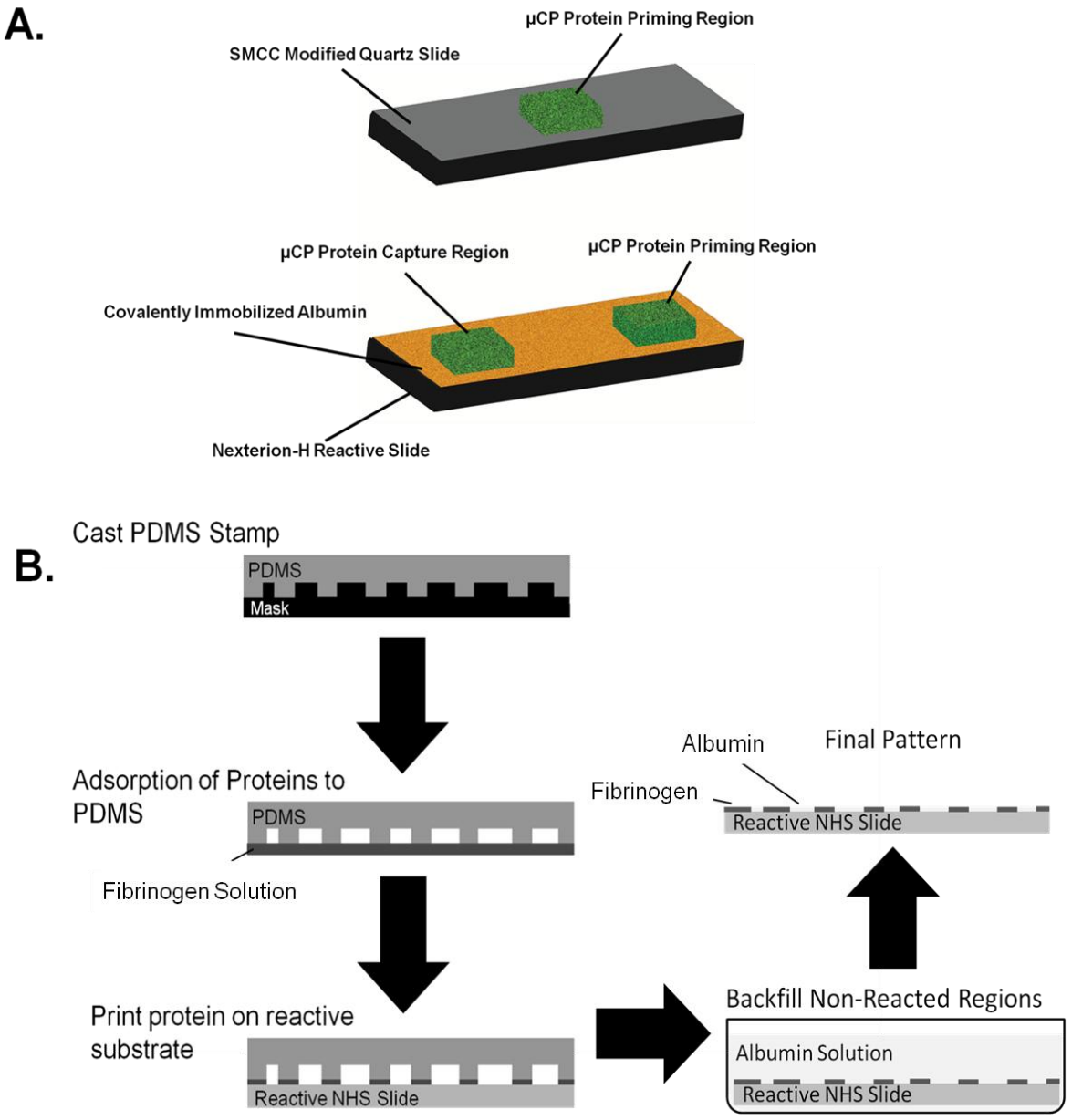

Figure 3.2 Sample preparation using μCP: (A) sulfo-SMCC and Nexterion-H test samples were prepared with covalently immobilized protein patterns using μCP. (B) A schematic representation of the μCP process. First PDMS stamps are cast and cured in patterned masks. The stamps are transferred to a protein solution where they are "inked" by allowing the protein to adsorb to the surface. The protein coated stamp is placed in contact with the reactive surface allowing the protein transfer to occur. On Nexterion-H substrates, the printed surface was incubated in an albumin solution to passivate the unpatterned regions.

fibrinogen was printed, the nonreacted regions were passivated by incubating the samples in an albumin solution in PBS(c = 1 mg/ml, pH 8.5) for 30 minutes (Figure 3.2b). Albumin was chosen over small molecules such as ethanolamine for background passivation because it demonstrated an improved ability to eliminate platelet adhesion (data not shown). Following protein immobilization, samples were vigorously rinsed in a 1% Tween solution to remove any protein not covalently immobilized on the surface. Samples were then rinsed thoroughly with Milli-Q water, dried with N_2 gas and stored under vacuum until use. A schematic of the μCP procedure is shown in Figure 3.2b.

3.2.4 Surface Characterization

Thiol monolayers were prepared and characterized as described in sections 2.2.1 and 2.3.1. The conjugation of sulfo-SMCC to surface thiols was confirmed water contact angle. Briefly, receding water contact angles were measured along the length of the sample using a contact angle instrument (CAM 100, KSV Instruments). The average contact angle for the surface was calculated before and after sulfo-SMCC incubation of the thiol monolayers. The conjugation protocol of sulfo-SMCC to an MTS thiol monolayer for RGD peptide immobilization has been characterized with ESCA and ToF SIMS analysis in our lab previously (Appendix A).

The integrity of the protein patterns and the protein transfer efficiency was characterized visually using fluorescence microscopy and by lateral force microscopy. LFM measurements were obtained in air on an Explorer AFM (TopoMetrix) with silicon cantilevers (Mikromasch) having a force constant of

0.03 N/m and a radius of curvature < 10nm. These measurements (n = 10) were used to compare the actual printed protein area with target values.

3.2.5 Fibrinogen Labeling

In order to visualize immobilized protein patterns, fibrinogen was labeled with Alexa Fluor 488 succinimidyl ester (Invitrogen). Human fibrinogen (c = 10 mg/ml, Calbiochem) in 0.1M sodium bicarbonate buffer (pH 8.5) was incubated for 2 hours with Alexa Fluor 488 (c = 0.25 mg/ml). After incubation, the protein solution was loaded into a PD-10 desalting column (GE Healthcare) which excludes molecules according to size and was used separate labeled fibrinogen from unlabeled fluorophores. Labeled protein was eluted with a protein printing buffer (Schott, pH 8.5). Protein aggregates were filtered out using 0.22 µm low protein binding PES syringe filters (Millipore) and the labeled protein was immediately frozen at -20 °C until use.

3.2.5 Blocking Immobilized Fibrinogen Priming Regions

Control samples were prepared by blocking the upstream fibrinogen region with a rabbit α-polyclonal antibody raised against human fibrinogen, (Calbiochem). Blocking was achieved by selectively incubating the priming region with 1:100 dilution of anti-fibrinogen in 0.1M PBS (ph 7.4) for 30 minutes. The samples were rinsed three times in Milli-Q water following blocking, and immediately used for experiments.

3.2.6 Platelet Adhesion Studies

Fresh whole blood was collected from healthy human donors in a 1:7 ACD solution. Washed platelets were prepared as described in section 2.24. Briefly, whole blood was centrifuged for 15 minutes at 1500 rpm to separate platelet rich plasma (PRP). The PRP supernatant was aspirated off using a transfer pipette. Prostaglandin E_1 (PGE1, 300 nM) was added to the PRP to inhibit aggregation during preparation [173]. PRP was then centrifuged for another 15 minutes at 2100 rpm to isolate the platelet pellet. The platelet poor plasma (PPP) supernatant was carefully discarded and the platelet pellet was gently re-suspended in prewarmed Tyrodes-HEPES buffer (37 ^{0}C, pH 7.4) [174]. Platelets were counted using a hemocytometer and the concentration was adjusted to 2.5 $\bullet 10^7$ platelets/ml.

Platelet perfusion studies were conducted in a parallel plate flow cell as described in section 2.2.5. Adhesion was quantified by averaging samples (n=30) downstream of the priming region. In studies where Nexterion-H reactive substrates were used, average platelet spreading area and the number of aggregates per sample was also calculated. Area values were obtained by taking the average area of 100 spreading platelets in the downstream region. Platelet aggregates were defined as a cluster of 3 or more platelets and the average number per sample was quantified (n = 30). Significance between data sets was established using unpaired t-tests.

3.2.7 Flow Cytometry

Flow cytometry was used to measure levels of expressed P-selectin and the active conformation of integrin $\alpha_{IIb}\beta_3$ on the membranes of platelets. Following platelet perfusion over samples printed with both albumin and fibrinogen, a 100 µl aliquot of the platelet supernatant was collected and incubated for 30 minutes with either anti-CD62P (BD Biosciences) or PAC-1 (BD Biosciences) to label P-selectin and active $\alpha_{IIb}\beta_3$, respectively (c = 1 µg/ml, BD Biosciences). Also, two 100 µl aliquots were obtained and labeled prior to perfusion. One sample was stimulated by addition of thrombin immediately prior to labeling (c = 0.1 units/ml) and the other was left un-stimulated to serve as positive and negative controls, respectively. In order to ensure platelets are properly identified, they were also labeled with CD41b (BD Biosciences) which binds to the α_{IIb} subunit of integrin $\alpha_{IIb}\beta_3$ regardless of the activation state of the receptor. Rat monoclonal anti-mouse IgG and IgM served as a negative control for P-selectin and PAC-1 test samples, respectively. Following labeling, platelets were fixed in 1% paraformaldehyde and stored at 4°C. Analysis of 10,000 events was conducted on a FACScan (BD Biosciences) analyzer.

3.3 Results and Discussion

3.3.1 Surface Characterization

The preparation of thiol monolayers was characterized previously (Section 2.3.1). The functionalization of surface thiol groups with reactive NHS ester groups was confirmed by measuring receding water contact angles along the

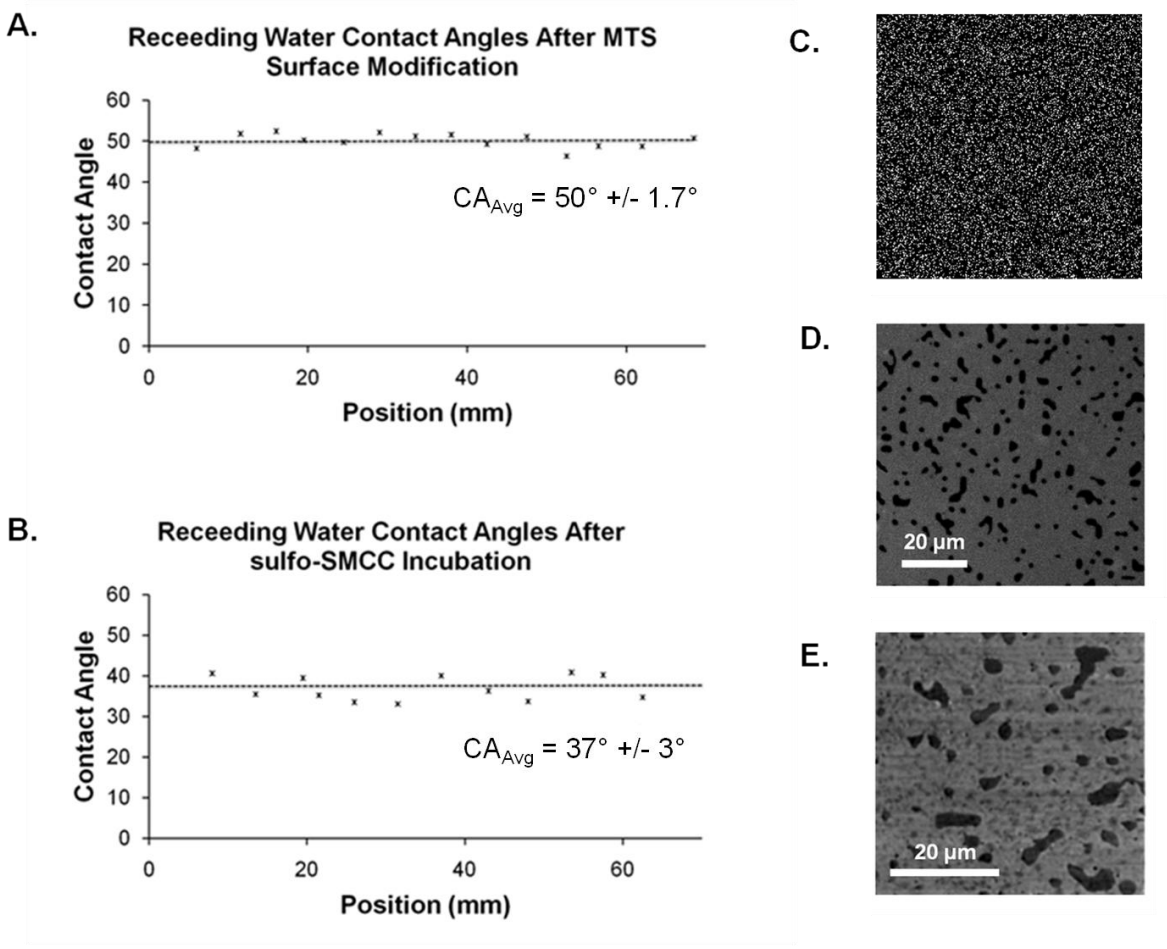

Figure 3.3 Characterization of sulfo-SMCC surface modification and printing protein micropatterns: (A) Receding water contact angles were measured to confirm the modification of the thiol monolayer contain a reactive NHS ester surface chemistry. Prior to sulfo-SMCC incubation the average contact angle was measured to be 50° +/- 1.7°. (B) After incubation the average contact angle reduced to 37° +/- 3° suggesting the surface was in fact modified. PDMS stamps for printing were prepared with a mask defined with an 85% feature coverage area (C). The integrity of the printed protein patterns after surfactant rinsing was confirmed by (D) fluorescence microscopy. LFM microscopy (E) was used to quantify the efficiency of protein transfer. Dark grey regions represent the printed fibrinogen regions.

length of the sample (Figures 3.3a and 3.3b) before and after sulfo-SMCC incubation. Thiol modified samples had an average receding water contact angle of 50° +/- 1.7°, an expected value for this surface modification scheme [192]. After sulfo-SMCC incubation, a reduction in the average receding water contact angle was observed to 37° +/- 3°, suggesting the surface was in fact modified. Furthermore, previous studies in our lab have shown an increase in the atomic percentage of elemental nitrogen and carbon following sulfo-SMCC incubation of a thiol monolayer (Appendix A).

Fluorescence images of 85% printed protein micropatterns (Figure 3.3c) were acquired to qualitatively assess the integrity of printed fibrinogen patterns and ensure no major defects were present. Figure 3.3d provides a representative image for fibrinogen printed surfaces. The same technique was also used for albumin printed surfaces (data not shown). These images were also acquired after samples were vigorously rinsed in a 1% Tween solution suggesting the protein present on the surface was, in fact, covalently immobilized.

In order to determine the efficiency of protein transfer, samples were scanned with LFM. This technique measures deflections of a cantilever tip that arise from variations in friction over heterogeneous surfaces providing contrast between the printed and nonprinted regions. LFM images showed good contrast between the printed (dark grey) and non printed (light grey) (Figure 3.3e) regions. For these studies, PDMS stamps with a target protein coverage area of 85% were used for printing. The actual printed coverage area was quantified for each

LFM sample (n=10) and found to be 85.5% +/- 0.9%, suggesting an accurate protein transfer efficiency.

3.3.2 Effect of Priming Platelets with Fibrinogen Immobilized to SMCC Modified Surfaces on Downstream Adhesion, Activation, and Aggregation

Surface adsorbed proteins, such as fibrinogen, are capable of activating quiescent circulating platelets independent of other activation agonists [193]. Here, a fibrinogen priming region was covalently immobilized to SMCC reactive substrates using μCP and the effect on downstream adhesion was quantified. Average adhesion was calculated in a 25 mm^2 area at a distance of 5mm-9mm downstream from the priming region (Figure 3.4). These adhesion values were compared with samples that contained covalently immobilized albumin and no priming regions. All values were normalized against background adhesion that occurred on bare sulfo-SMCC modified surfaces upstream of the priming region. Error bars represent the standard error of the mean with a confidence interval of 95% (n = 30). A significant increase ($p < 0.001$) in downstream adhesion on fibrinogen samples was observed suggesting that immobilized fibrinogen is capable of transiently interacting with platelets, promoting downstream adhesion. No significant increase in downstream adhesion occurred on samples without a printed priming region. Interestingly, a significant increase in downstream adhesion was also observed on albumin samples although this increase was not as substantial as the increase on fibrinogen printed samples. This was surprising since albumin is believed to be relatively inert to platelet adhesion and activation [104] thus no stimulatory effect was expected. Also interesting to note

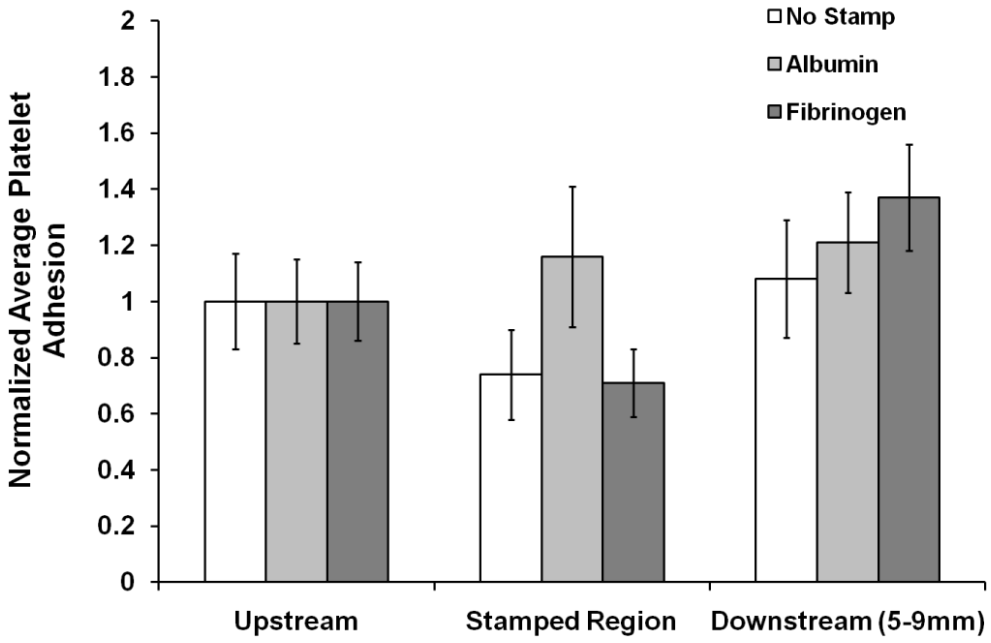

Figure 3.4 The effect of "priming" platelets with immobilized fibrinogen on sulfo-SMCC substrates. Downstream adhesion was quantified by covalently immobilizing fibrinogen and albumin to the reactive samples using μCP. These values were compared with samples that did not contain a priming region (n = 30). Error bars represent the standard error of the mean with a 95% confidence interval.

is that adhesion in the stamped region was highest on albumin printed samples which again is counterintuitive since fibrinogen is a known platelet adhesive ligand and albumin is not.

Recently Sivaraman *et al*. discovered that immobilized albumin is capable of supporting platelet adhesion and that this is dependent on the exposure of a binding epitope upon surface-induced unfolding. [35]. Therefore it is possible that platelet interactions with albumin may induce some amount of surface activation. However, it is still unlikely that adhesion would be drastically larger on albumin vs. fibrinogen stamped regions.

A substantial amount of platelet adhesion was observed on bare sulfo-SMCC surfaces with no immobilized protein ligands present (data not shown). Priming regions were printed with 85% relative coverage areas leaving 15% of the area of the background sulfo-SMCC surface exposed. It is therefore more likely that results are representative of platelet interactions with the background substrate. It was concluded that experiments should be redesigned with a substrate background that could be passivated, providing a more accurate representation of the downstream adhesion effect of immobilized upstream fibrinogen.

3.3.3 Effect of Priming Platelets with Fibrinogen Immobilized to PEG Hydrogel Substrate on Downstream Adhesion, Activation, and Aggregation

In order to reduce the background effect described in 3.3.2, experiments were redesigned with commercially purchased Nexterion-H glass slides. These substrates are coated with a PEG based hydrogel matrix functionalized with

reactive NHS ester groups providing a mechanism for protein covalent immobilization [194]. PEG based surface coatings have been shown to drastically reduce nonspecific protein adsorption and cell adhesion [18,100,106,191,194] making Nexterion-H slides better model substrates for the subsequent experiments.

Here, samples were prepared with a covalently immobilized fibrinogen priming and capture region as described above (3.2.3) with 85% coverage area stamps. The background was passivated with covalently immobilized albumin. The effect of fibrinogen priming on the downstream platelet response was quantified by comparing overall average adhesion, spreading area, and aggregate formation in the downstream capture region with controls that did not contain a priming region (Figure 3.5). Aggregates were defined as 3 or more platelets in a single cluster. In all three cases, adhesion, spreading area, and aggregation were significantly higher on samples with the fibrinogen priming region ($p < 0.001$), suggesting that upstream platelet-protein interactions are capable of eliciting a downstream response.

To explicitly confirm that the presence of the upstream immobilized priming region is amplifying the downstream platelet response, a test sample was prepared with the upstream priming region blocked by a polyclonal antibody for fibrinogen. Average adhesion in the downstream capture region was compared with adhesion values on samples with and without an upstream fibrinogen priming region (Figure 3.6). Platelet adhesion on samples primed with upstream fibrinogen was again significantly higher than samples that did not possess an

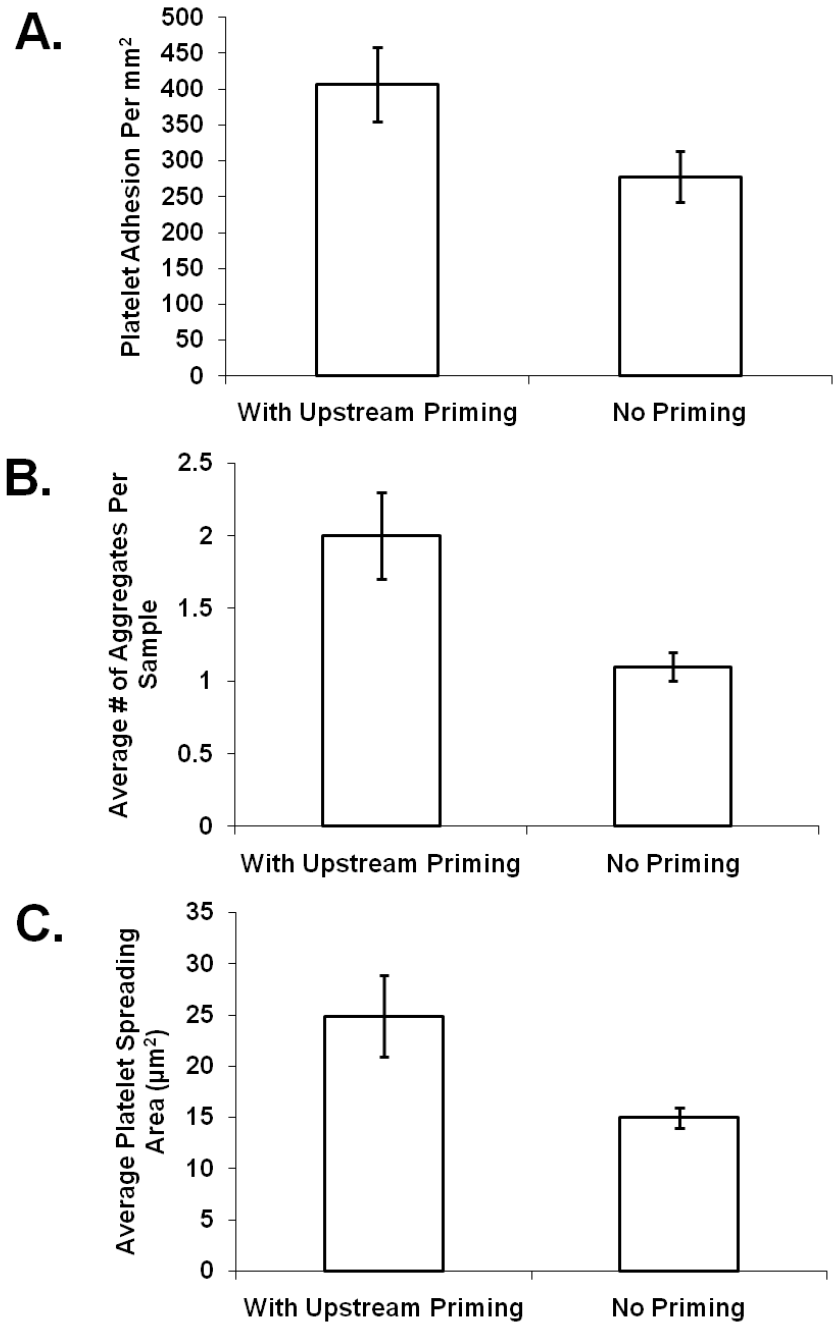

Figure 3.5 Effect of an upstream immobilized fibrinogen priming region on downstream (A) adhesion, (B) aggregation, and (C) spreading area on Nexterion-H substrates. Samples (n = 30) were acquired 10-15mm downstream of the priming region. The error bars represent the standard error of the mean with a 95% confidence interval.

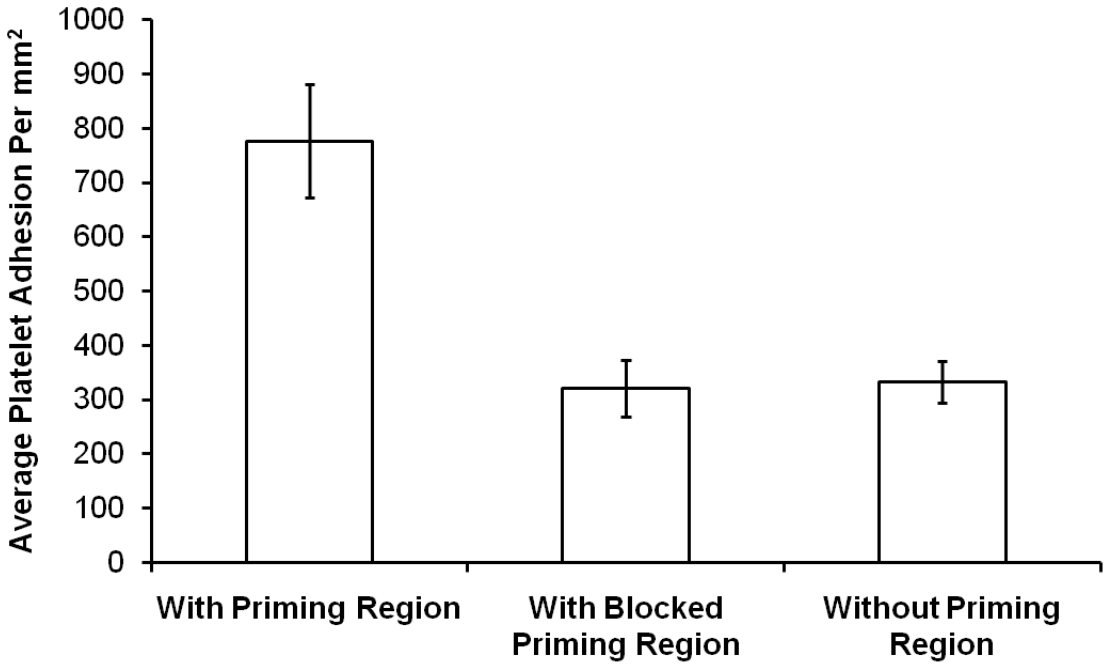

Figure 3.6 Blocking fibrinogen priming region with an anti-fibrinogen polyclonal antibody attenuates the downstream adhesion response. The effect of priming platelets with immobilized upstream fibrinogen on downstream adhesion was compared with samples containing no priming region and a priming region blocked with an anti-fibrinogen polyclonal antibody. Samples (n = 30) in the downstream capture region were averaged and error bars represent the standard error of the mean with a 95% confidence interval.

upstream priming region. Also, when the upstream priming region was blocked with an antihuman fibrinogen polyclonal antibody the downstream platelet adhesive response was attenuated and there was no significant difference with unprimed samples ($p < 0.001$). These results further confirm that the presence of upstream immobilized protein agonists can in fact prime platelets for downstream adhesion. Traditionally, blood compatibility studies focus on establishing the local platelet response to the biomaterial. However, since platelet surface interactions are often transient [163], these studies may not be sufficient to understand the whole picture. Platelet membrane receptor interactions with surface immobilized proteins, such as vWf-GPIb-IX-V and fibrinogen-$\alpha_{IIb}\beta_3$, are capable of activating platelets [40,42,81,84,184]. It is unlikely that these transient contacts leave the phenotype unchanged. For example, upstream platelet activation on devices such as prosthetic heart valves and stents has been shown to cause downstream thromboembolic complications [5,195]. Also, it has been hypothesized that transient platelet-surface interactions trigger platelet microparticle formation at the site of contact [187]. Platelet microparticles have procoagulant surface properties and may have serious blood compatibility implications in the absence of stable platelet adhesion [196,197]. It is evident that the “history” of transient platelet-substrate contacts is an important consideration in the design of *in vitro* blood compatibility studies.

Characterizing the effect of transient interactions on the downstream platelet response is also an important aspect in the development of cardiovascular devices. When a device such as a vascular graft or heart valve is

implanted there exists a region in which the native vessel is joined with the synthetic material. This region, also known as the anastomotic region, is characterized by high rates of stenosis (narrowing) and subsequently, higher fluid shear rates [100]. The anastomosis is also characterized by adsorption of pro-coagulant proteins such as fibrinogen due to damage of the vessel endothelium at this location [198]. This presents an ideal environment for platelet activation to occur and may have serious consequences for the blood compatibility of the downstream biomaterial. Another implication is in the use of grafts or shunts in hemodialysis patients. Traditionally, the most common cause of arteriovenous graft failure is neointimal hyperplasia at the graft-venous anastomoses [164,165]. The exact mechanism is not yet understood. However, it has been suggested that the physiology of the venous endothelial layer may play a role [165]. It is possible however, that the upstream artery-graft anastomoses may be preactivating platelets for downstream adhesion since this region is characterized by both high shear forces as well as a damaged endothelial layer. In order to better understand the role of platelet activation in device failure we must take into account the transient nature of adhesion and activation. This will, in turn, help us develop more hemocompatible biomaterials.

Here, we established that immobilized fibrinogen is capable of priming platelets for downstream adhesion, activation and aggregation which has implications for both the design of in vitro blood compatibility studies as well as the development of blood compatible medical devices. However, as discussed

above, platelet contacts are mostly transient therefore it is also important to characterize the effect of fibrinogen priming on the bulk platelet response.

3.3.5 Evaluation of PAC-1 and P-Selectin Expression on Platelets Primed by Upstream Protein Agonists

Platelet interactions with immobilized protein agonists may be transient [163]. However, even in the absence of an adhesion event these transient interactions may be capable of activating platelets. In section 3.3.4 we found that upstream immobilized fibrinogen was capable of increasing the platelet response downstream. To further investigate this phenomenon our goal was to characterize the bulk platelet response to surface immobilized fibrinogen.

PAC-1 recognizes an epitope on the integrin $\alpha_{IIb}\beta_3$ complex of activated platelets near the fibrinogen receptor. Platelet activation induces a calcium-dependent conformational change in integrin $\alpha_{IIb}\beta_3$ that exposes a ligand binding site thus PAC-1 binds only to activated platelets [52]. P-Selectin is stored in the α-granules of platelets and is rapidly transported to the platelet membrane upon activation [199]. Here, platelets were fluorescently labeled for PAC-1 and P-selectin following perfusion over samples containing immobilized fibrinogen and albumin. Unstimulated platelets and thrombin activated platelets were collected prior to perfusion and served as negative and positive controls, respectively. Expression of each receptor was quantified by detecting 10,000 events using flow cytometry.

Slight increases in P-selectin and PAC-1 were observed on samples perfused over fibrinogen coated versus albumin coated substrates and negative

controls (Figure 3.7). It should be noted that the negative control had a relatively high level of PAC-1 expression at 62.52%, which suggests that some amount of platelet activation occurred prior to this study. To confirm that this observation is conserved, the study could be expanded to test platelets from more than one donor. Furthermore, the increase in expression for both markers was appreciably low when compared to thrombin activated positive controls, making the observed results less convincing. However, if one considers the number of platelets capable of interacting with the surface compared to the total bulk platelet concentration, the slight differences can be explained.

According to the Von Smoluchowski-Levich approximation, the platelet flux to the surface in a parallel plate flow cell can be modeled by the following equation [200-202]:

$$j^* = \frac{D_{plt}c}{0.89}\left(\frac{6V_m}{18Dbx}\right)^{1/3}$$

where j^* = the instantaneous platelet flux [platelets/cm^2-sec] to the interface, D_{plt} = diffusion coefficient, c = bulk platelet concentration (~2.5·10^7 platelets/ml), a = platelet radius (~ 1 μm), b = ½ the height of the flow cell, Pe = Peclet number (ratio of convective to diffusive transport, see Appendix B) and x = position in the flow cell. This assumes the flow is laminar and fully developed (for full derivation see Appendix B). According to this model, the deposition rate changes with the position x (distance from the flow inlet) due to the presence of a hydrodynamic boundary later. Thus if this function is integrated with respect to the time it takes

	Before Perfusion (Unstimulated)	Before Perfusion (Thrombin Activated)	After Perfusion (Albumin Substrate)	After Perfusion (Fibrinogen Substrate)
P-Selectin	1.81%	63.50%	7.88%	12.39%
PAC-1	62.52%	91.77%	63.78%	66.70%

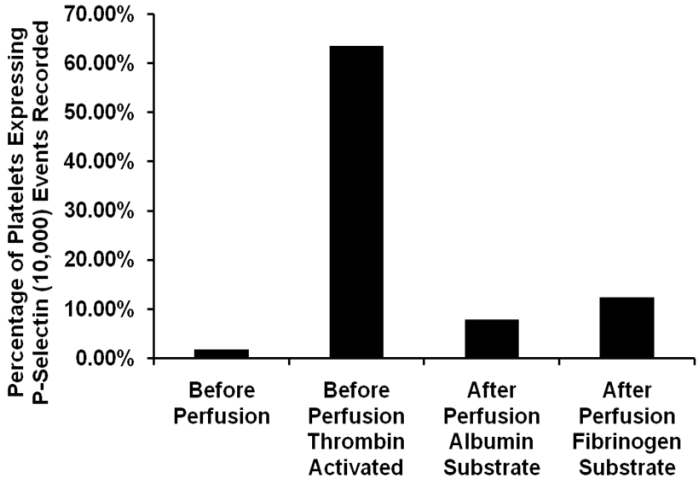

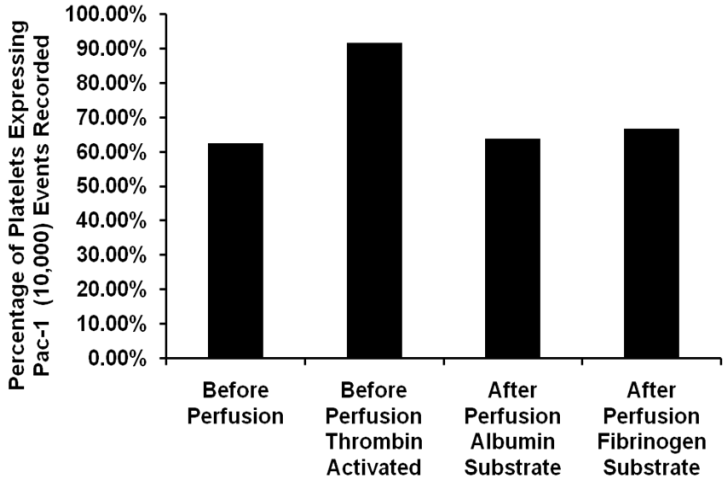

Figure 3.7 Flow cytometry analysis of bulk platelet activation for one human donor. Pac-1 and P-selectin expression on platelets were quantified after perfusion over albumin and fibrinogen substrates. These samples were also compared with an unstimulated and thrombin activated sample collected prior to perfusion. Values are recorded as a percent of positive events that occurred out of 10,000 events recorded.

for the sample volume of platelets to travel through the flow cell you obtain the overall deposition rate as a function of distance from the flow inlet per area (Figure 3.8). If platelets are assumed to be spheres, D_{plt} can be estimated using the Stokes-Einstein relationship:

$$D_{plt} = \frac{k_b T}{6\pi\mu a}$$

where k_b = the Boltzman constant ($1.3806503 \times 10^{-23}$ m^2 kg s^{-2} K^{-1}), T = absolute temperature (310.15K = 37° C) and μ = absolute viscosity, making $D_{plt} \approx 10^{-13}$ m^2/sec (For complete set of calculations see Appendix B).

The average platelet deposition rate in the center of the substrate (between 2cm ≤ x ≤ 5cm) where fibrinogen was immobilized was calculated to be ~36 platelets/cm^2-sec. If you multiply this by the time it takes for one sample volume (0.1 ml) to travel over the area of printed fibrinogen (t = 18 sec, A = 1.5 cm^2) the total number of platelet contacts per sample is ~964 platelets. This only represents approximately 0.04% of the total platelets present in the bulk solution (~2,500,000). Consequently, it is not surprising that increases in activation due to platelet surface-interactions are small when compared to the total number of platelets in the bulk sample. It is also important to note that platelet and coagulation mechanisms are inherently designed to be amplified in the physiological environment so even a small amount of activation can be significant. It should be noted that this approximation does not take into account external forces on platelets including gravity, buoyancy, van der Walls forces and

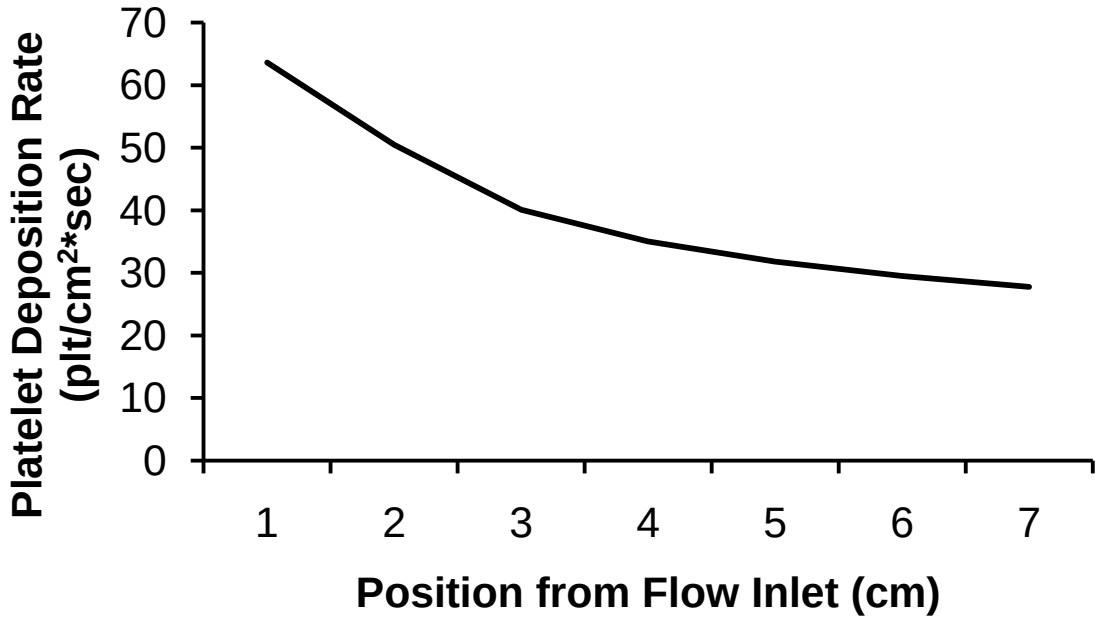

Figure 3.8 Platelet deposition rate in a parallel plate flow cell as predicted by the Smoluchowski-Levich approximation (see Appendix B).

electrostatic interactions. It is impossible to obtain analytical solutions including these variables although some numerical solutions do exist [200, 203]. One way to further confirm that the slight increases in bulk platelet activation are in fact due to platelet interactions with fibrinogen at the surface is to try and amplify the response. This can be done by changing parameters such as the surface area of immobilized fibrinogen available to platelets and the flow rate of the washed platelet suspension , both resulting in an increase in the potential platelet interactions with immobilized fibrinogen.

3.4 Conclusions

In this study, the effect of priming platelets with covalently immobilized fibrinogen on the downstream platelet response was investigated. Priming regions were prepared using μCP on surfaces capable of protein covalent immobilization. Initially, test samples were prepared by modifying silanized quartz slides with the heterobifunctional crosslinker, sulfo-SMCC. Unfortunately, these samples also resulted in high background platelet adhesion which made the results difficult to decipher. The use of commercially available Nexterion-H slides with a PEG based surface chemistry eliminated this background response and therefore was used as the model substrate. The difference in the platelet response to these two substrates was believed to be primarily due to the presence of the PEG hydrogel on the surface. However, it is also possible the protein immobilization scheme may affect the conformation of fibrinogen (See Appendix C) which has also been shown to affect the platelet response [34, 36, 204-209].

The downstream platelet response on PEG based model substrates was quantified by comparing adhesion, spreading area, and aggregation values with control samples that did not contain an upstream priming region. The results presented suggest that immobilized fibrinogen is capable of priming platelets and their response may be transient. The effect on immobilized fibrinogen on the bulk platelet activation was also quantified by measuring expression levels of P-selectin and PAC-1 expression. Although slight, there was an increase in expression after perfusion over fibrinogen substrates. This has both clinical significance and will be an important consideration in the design of future *in vitro* studies.

The work described in this chapter used μCP to prepare surface immobilized fibrinogen regions in well defined positions on the sample. The use of μCP to design well-defined protein patterns has many other potential applications for in vitro platelet studies. In the next chapter, we developed random fibrinogen micropatterns with three different relative coverage areas (20%, 50%, and 85%). The ability of these patterns to control platelet adhesion and spreading morphologies was explored. If good morphological control could be achieved, these well-defined patterns could be applied to study fundamental platelet adhesion and activation using similar methods that have been applied to other cells on μCP substrates [120, 134-136, 145].

CHAPTER 4

WELL DEFINED FIBRINOGEN MICROPATTERNS FOR ADHESION AND ACTIVATION STUDIES PREPARED BY MICROCONTACT PROTEIN PRINTING

4.1 Introduction

As discussed in section 1.2.2, platelet adhesion is supported by interactions between GPIb-V-IX and integrin $\alpha_{IIb}\beta_3$ with vWf and fibrinogen respectively [53,61,66,181]. Specifically, GPIb-V-IX binds to surface immobilized vWf to arrest platelets in flowing conditions. Although this interaction is weak and reversible, it is crucial in facilitating stable integrin $\alpha_{IIb}\beta_3$ fibrinogen binding, thus both proteins work synergistically to promote stable platelet adhesion [45,212,213].

Following adhesion, platelet activation is characterized by morphological changes including the extension of filopods, lamelipod formation, and spreading as more specific adhesive contacts with adsorbed protein ligands are established. Activation also leads to the up-regulation of high affinity binding sites for adhesion proteins involved in further platelet adhesion, activation and aggregation [166,214,215]. Platelet spreading also facilitates the centralization of

granules that secrete procoagulant factors involved in further platelet recruitment and activation [166]. An extensive amount of effort has been devoted to understanding both adhesion and activation; however, many of the mechanisms are still not well understood. Although *in vivo* models provide the most accurate conditions to study these mechanisms, it is often difficult elucidate cause and effect relationships because the biochemical events are complex and highly interdependent. The ability to develop well controlled studies *in vitro,* where specific platelet interactions with the surface are promoted or inhibited, is crucial in developing an improved understanding of basic activation mechanisms.

Microcontact printing (μCP) has demonstrated to be a powerful technique in many fundamental cell biology studies [135]. This tool is capable of generating well-defined patterns of immobilized protein ligands in which the type, size, shape and spacing are precisely controlled [145]. As discussed in section 1.3, μCP of proteins has been used to study many different cell phenomena including adhesion, migration, apoptosis and proliferation [118,120,135,136]. This technique has also been used to pattern 2-D protein arrays for high-throughput drug screening and disease diagnosis [216].

Microcontact printing has shown potential value in many platelet adhesion and activation studies. As discussed in section 1.3.3, Basabe-Desmonts *et al.* demonstrated platelets could be isolated from whole blood using micro contact printed dots of platelet specific protein ligands demonstrating a potential application of μCP in the development of platelet functionality assays and fundamental adhesion and activation studies [152]. Kastrup *et al*. used protein

patterning to control a coagulation stimuli patch size discovered that there exists a threshold initiation response [217]. However, despite these efforts, the application of μCP to fundamental platelet adhesion studies is still relatively new.

In this work, well-defined fibrinogen patterns were covalently immobilized to reactive substrates using μCP. Stamps with three randomly patterned coverage areas (20%, 50%, and 85%) were generated and used for printing. Increasing the surface coverage area also increased the size of the fibrinogen features due to the merging of randomly placed islands. Nonprinted regions of the substrate were passivated with covalently immobilized albumin. The effect of varying the average fibrinogen feature size on platelet adhesion activation was observed and quantified using combined differential interference contrast (DIC), fluorescence, and scanning electron microscopy (SEM). Our aim was to investigate the extent in which the underlying fibrinogen pattern was able to control platelet spreading morphology. We found that both overall adhesion and activation could be controlled by varying the immobilized fibrinogen island size. Platelet morphology was also observed to be controlled by the underlying fibrinogen pattern. These studies have the potential to serve as a basis for future work in which the adhesion response morphological parameters can be correlated with physiological processes.

4.2 Methods

4.2.1 Preparation of PDMS Stamps and Printing Immobilized Fibrinogen Patterns

The protocol described in 3.2.1 was used to produce PDMS stamps with 85%, 50%, and 20% relative surface coverage areas. Stamps were "inked" with fibrinogen in PBS (c = 1 mg/ml, pH 8.5) for 15 minutes, rinsed in Milli-Q water and dried with N_2 gas. The fibrinogen covered stamps were placed in contact with Nexterion-H (Schott) reactive slides for 45 minutes with 490 Pa of pressure applied evenly using 5g of weight (See Figure 3.3). These slides are coated PEG hydrogels functionalized with terminal reactive NHS groups and are capable of protein covalent immobilization [187]. After fibrinogen was printed, the non-reacted regions were passivated by incubating the samples in an albumin solution in PBS (c = 1 mg/ml, pH 8.5) for 30 minutes. Following protein immobilization, samples were vigorously rinsed in a 1% Tween solution to remove any protein not covalently immobilized on the surface. Samples were then rinsed thoroughly with Milli-Q water, dried with N_2 gas and stored under vacuum until use.

4.2.2 Surface Characterization

Lateral force microscopy (LFM) was used to characterize the printed fibrinogen samples for each relative surface coverage area (20%, 50%, and 85%). Measurements were obtained in air on an Explorer AFM (TopoMetrix, Santa Clara, CA) with silicon cantilevers (Mikromasch, San Jose CA) having a force constant of 0.03 N/m and a radius of curvature < 10nm. Lateral force on

the cantilever tip was recorded (A = 50 µm x 50 µm) for each fibrinogen pattern (n=10) and ImageJ (Rasband, NH) was used to quantify the area of the fibrinogen features. The integrity of the fibrinogen patterns was also confirmed using fluorescence microscopy. First, fibrinogen was labeled with Alexa Fluor-488 ® (Invitrogen) following the protocol described in section 3.2.5 and then printed onto Nexterion reactive slides following the stamping protocol described in section 3.2.3.

4.2.3 Platelet Adhesion Studies

Fresh whole blood was collected from healthy human donors in a 1:7 ACD solution and washed platelets were prepared as described in section 2.24. Briefly, the blood was centrifuged for 15 minutes at 1500 rpm to separate platelet rich plasma (PRP). The PRP supernatant was transferred to a clean polypropylene test tube using a transfer pipette. Prostaglandin E_1 (PGE1, 300 nM) was added to the PRP to inhibit aggregation during preparation [174]. PRP was centrifuged for another 15 minutes at 2800 rpm to isolate the platelet pellet. The platelet poor plasma (PPP) supernatant was carefully discarded and the platelet pellet was gently resuspended in prewarmed Tyrodes-HEPES buffer (37 ^{0}C, pH 7.4) [175]. Platelets were counted using a hemocytometer and the concentration was adjusted to $1 \cdot 10^7$ platelets/ml (~10% of physiological concentration). The washed platelet suspension was maintained at 37^{0}C prior to each experiment. Patterned samples were incubated in the washed platelet suspension for 5 minutes and rinsed twice with PBS to remove unbound platelets. Samples were fixed with 3.2 % glutaraldehyde (t = 30 min) and rinsed

a final 3 times with PBS. In order to characterize the platelet response to each fibrinogen coverage area, adhesion, spreading area, and circularity were calculated. First platelets were visualized using a DIC microscope. Overall adhesion was quantified by calculating the average adhesion (n = 30) for each surface coverage. Spreading area and circularity were calculated by measuring the average area and perimeter for platelets (n = 100) on 5 different samples for each relative fibrinogen coverage. Circularity (*C*) is a ratio between the area, *A,* and the perimeter, *P*, that can be used to describe cell morphology ($C = 4\pi A/P^2$). When *C* = 1 the shape is a perfect circle corresponding to a fully spread platelet. For each data set, standard error of the mean was calculated using a 95% confidence interval and statistical significance was calculated using an unpaired t-test.

4.2.4 SEM Morphological Analysis

Fixed platelet samples were first dehydrated by incubating in ascending ethanol (50%, 75%, 100%) solutions for 15 minutes each. Samples were then dried and sputter coated with a 10 nm layer of gold with a Cressington 108 Auto sputter coater. SEM images were obtained using a Hitachi S-3000N SEM at 20 kV.

4.3 Results and Discussion

4.3.1 Immobilized Fibrinogen Pattern Characterization

Microcontact protein printing was used to covalently immobilize µm-sized human fibrinogen islands to Nexterion-H slides at a relative surface coverage of

20%, 50%, or 85%. Printing protein ligands was chosen due to its ability to reproducibly generate well-defined patterns [218]. Covalent immobilization on reactive substrates maintained the integrity and stability of the patterns, ensuring no desorption or leaching of immobilized protein over time. Furthermore, Nexterion-H slides are coated with a thin PEG-based hydrogel modified with terminal NHS ester groups and show minimal tendency for nonspecific protein adsorption and low platelet adhesion [194]. In addition, after fibrinogen immobilization, samples were backfilled by covalently immobilized albumin to further passivate the nonprinted regions since albumin is known as being inert to platelets [158]. The integrity of the surface, the size of the fibrinogen islands and the printing efficiency were characterized using both fluorescence and LFM. Samples were vigorously rinsed in a 1% Tween surfactant solution to remove nonspecifically immobilized protein. Alexa Fluor-488 labeled fibrinogen surface patterns were visualized after surfactant treatment suggesting the protein was covalently immobilized (Figure 4.1b). Examining fibrinogen surface patterns by fluorescence microscopy was used to assess the integrity of the fibrinogen patterns and ensure no defects were present prior to conducting experiments.

LFM was used to characterize the average protein feature size and the printing efficiency of the PDMS stamps at each fibrinogen coverage area (Figure 4.1c). LFM images showed good contrast between the printed fibrinogen and nonprinted albumin regions. The actual coverage of printed fibrinogen was quantified for each sample (n=10) and compared with target values (Table 4.1). No significant difference between actual and target values was found confirming

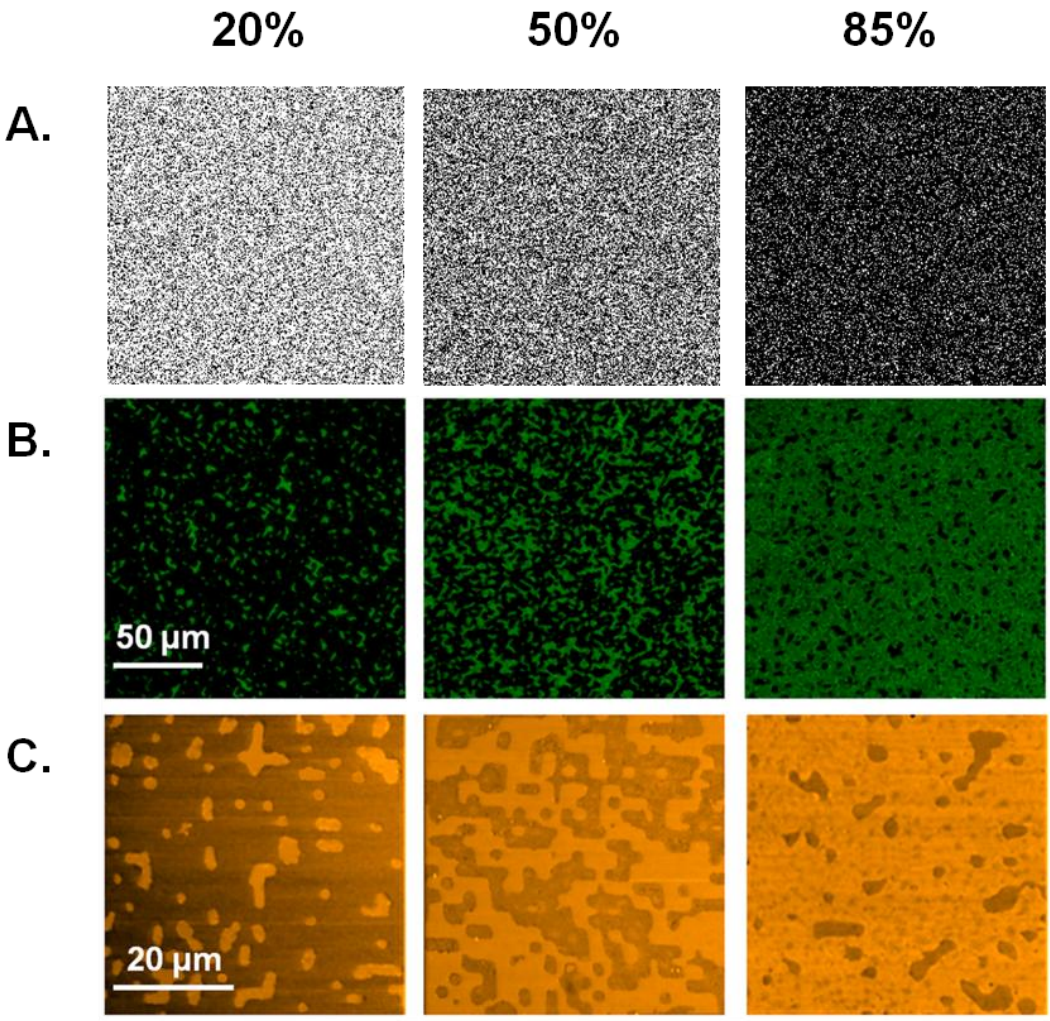

Figure 4.1 Fluorescence and LFM surface characterization of protein micropatterns: (A) Patterns used to generate photomasks, (B) Representative fluorescence (green = Alexa Fluor 488 labeled fibrinogen) and (C) lateral force AFM images (orange = fibrinogen islands) of 20%, 50% and 85% relative surface coverage of printed fibrinogen.

Table 4.1 The printing efficiency and average protein feature size for printed fibrinogen patterns.

Target Area Fraction	Actual Area Fraction	Area of Fibrinogen Features (μm^2)	Area of Background Features (μm^2)
20%	21.1% +/- 1.1%	5.3 +/- 0.4	N/A
50%	51.6% +/- 2.0%	84.1 +/- 31.4	68.2 +/- 34.0
85%	85.5% +/- 0.9%	N/A	4.8 +/- 0.6

the fidelity of protein transfer. The mean fibrinogen island size on 20% coverage samples was 5.3 +/- 0.4 μm^2. The background albumin pattern was completely interconnected thus calculating an average size was not possible. At 50%, the average fibrinogen and albumin feature sizes were 84.1 +/- 31.4 μm^2 and 68.2 +/- 34.0 μm^2, respectively. Large standard deviation was observed suggesting heterogeneous distribution of island sizes on these samples. At 85% the printed fibrinogen features were completely interconnected. The mean albumin island size was 4.8 +/- 0.6 μm^2.

4.3.2 Adhesion and Spreading on Surfaces with Varied Fibrinogen Coverage

The effect of the underlying fibrinogen pattern on platelet adhesion and spreading was studied by printing randomly placed μm-sized fibrinogen islands at different relative surface coverage areas (20%, 50%, or 85%). Due to the random nature of island placement, each coverage area corresponded to a different population of printed islands thus correlations could be made based on the size and shape of the stimuli presented to platelets. Fibrinogen was selected due to its multiple roles in platelet adhesion, activation and aggregation [72,40]. Covalent protein immobilization and the use of diluted washed platelet suspensions were chosen to control the surface protein content and ensured the phenomena observed was solely due to platelet-fibrinogen interactions. The washed platelet concentration was optimized at 10^7 platelets/ml to minimize platelet-platelet recruitment and aggregation. On each substrate AlexaFluor-488 labeled fibrinogen patterns were observed using fluorescence microscopy

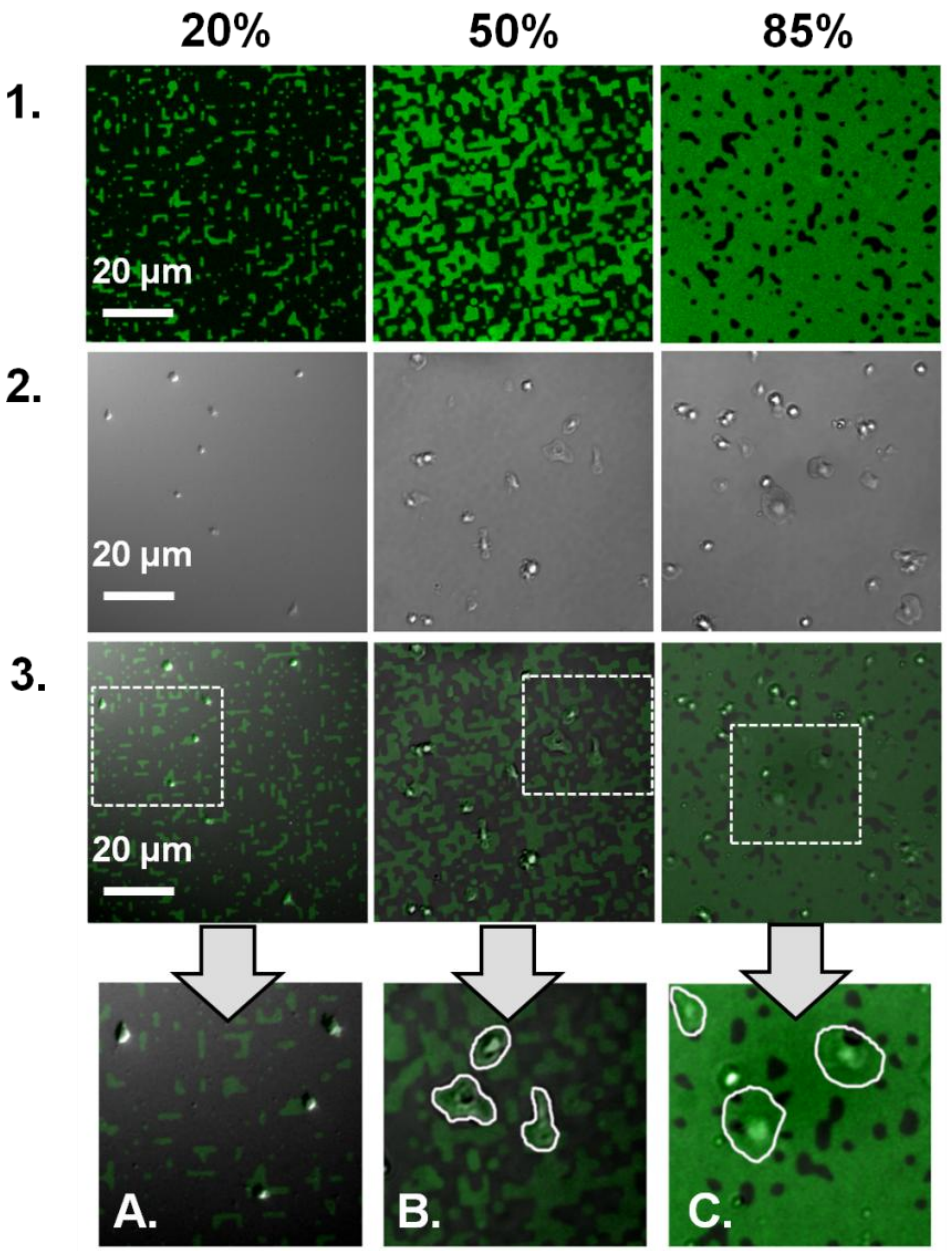

Figure 4.2 Platelet adhesion to covalently immobilized fibrinogen micropatterns at coverage areas of 20%, 50% and 85%. Nonprinted regions were blocked with covalently immobilized albumin. The top and middle rows contain fluorescence images of fibrinogen patterns and DIC images of platelet adhesion and spreading respectively. The bottom row includes superimposed images where at 20% (A) platelets rarely spread and when they do their size was strictly limited by the size of the underlying fibrinogen pattern. At 50% (B) platelets are able to spread but their morphology almost strictly depends on the shape of the underlying fibrinogen pattern. At 85% (C) platelets are able to spread over inert albumin regions and the morphology isn't necessarily dependent on the underlying fibrinogen pattern.

(Figure 4.2, row 1) while the adhered platelets were observed using DIC microscopy (Figure 4.2, row 2). Corresponding images were superimposed to study the spatial registration between the platelets and the underlying protein features (Figure 4.2, row 3). At 20% fibrinogen coverage almost no spreading was observed (Figure 4.2a). The size of the platelets was small, their shape rounded. When platelets did spread, their morphology was strictly limited by the size of the underlying fibrinogen islands. At 50% fibrinogen coverage, more extensive platelet spreading was observed; however, morphology was still dependent on the shape of the underlying pattern (Figure 4.b). At 85% fibrinogen coverage, fibrinogen islands coalesced into a continuous interconnected pattern and extensive spreading was observed. In most cases, platelets spread over the blocked albumin islands as well (Figure 4.3c). This may be due to the full interconnectivity of fibrinogen patterns at this level of surface coverage. Once platelets adhered, a path around the small inert albumin islands was available to facilitate spreading. Interactions between fibrinogen and integrin $\alpha_{IIb}\beta_3$ receptors on the platelet membrane are critical in signaling cytoskeletal reorganizational events [167]. Therefore spreading may also be dependent critical number of ligand-protein interactions being achieved.

Platelet shape change facilitates activation mechanisms crucial in ensuring the proper hemostatic response. Spreading induces $\alpha_{IIb}\beta_3$ activation and cytoskeletal reorganization events that lead to platelet degranulation and amplification of the coagulation response [167,79,168]. Filipod formation facilitates platelet-fibrin interactions and aggregation while lamellipod formation is

crucial in arresting vascular leakage upon vessel injury [168,219]. In vitro vascular injury models are commonly used to understand fundamental coagulation mechanisms. Specifically, the platelet response and thrombus formation has been investigated on surfaces preadsorbed with agonists such as collagen, fibrinogen and vWf [58,220,221]. It has been demonstrated that both fibrinogen and vWf are capable of mediating platelet adhesion and aggregate formation through synergistic interactions between integrin $\alpha_{IIb}\beta_3$ and GPIb-X-IV [43,46].

The ability to control the type and size of platelet activating ligand patches can be used to correlate morphological parameters with physiological events such as exposure of a small lesion in the vascular endothelial layer to circulating blood. The lesion size determines the number of ligands available for platelet activation and subsequently the stimuli requirements for receptor expression/distribution, intracellular calcium changes, and secretion of platelet recruiting agents. Thus, the techniques described here could be applied to physiologically relevant binary protein models, for example collagen-vWf, or fibrinogen-vWf, and used to study the mechanisms involved in these processes. Immobilized protein patterns have been used to capture platelets in whole blood for other applications [152,153]. Thus these methods could be applied to whole blood as well.

4.3.3 Quantifying the Effect of Relative Fibrinogen Coverage on the Platelet Response

In order to quantify the platelet response, adhesion, spreading area and circularity were measured for each fibrinogen surface coverage (20%, 50%, and 85%). Average adhesion was calculated for each sample (Figure 4.3a, n=30). Values were compared with a 100% fibrinogen substrate prepared using by printing flat PDMS stamp. Platelet adhesion to the albumin background was also measured but found to be negligible (data not shown). Overall adhesion increased with increasing fibrinogen surface coverage demonstrating that the random island printing can be used as a means to titrate the adhesion response.

Average platelet spreading area is shown in Figure 4.3b. Average spreading area increased with increasing fibrinogen surface coverage (i.e., with increased size of the underlying fibrinogen islands). At 20% relative fibrinogen coverage, almost no spreading was observed and the average area per platelet was 9.1 +/- 0.7 μm^2. Compared with the average fibrinogen feature size of 5.3 +/- 0.4μm^2 (Table 4.1) it appeared that the platelets formed stable adhesion only on larger fibrinogen islands. Platelet spreading area increased with increasing fibrinogen surface coverage to 50% equaling 38.9 +/- 3.6 μm^2; an area which was less than half of the average size of the coalesced fibrinogen island (Table 4.1). For this fibrinogen surface coverage, the shape of the platelets was strongly affected by the shape of fibrinogen islands (Figure 4.3b). At 85% fibrinogen coverage, spreading area was 48.2 +/- 5.0 μm^2. The increase in platelet spreading area between 20% and 50% was much more drastic than

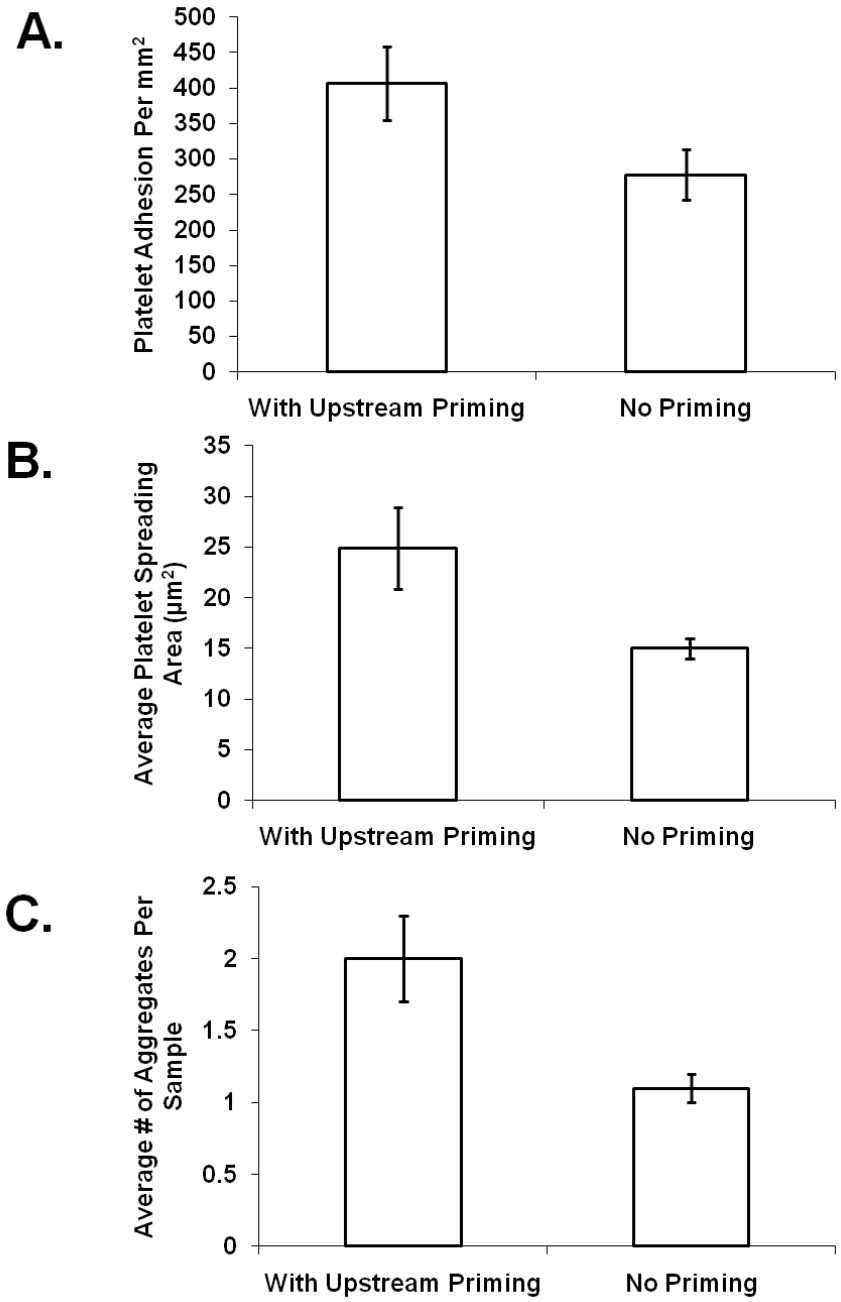

Figure 4.3 Quantification of the platelet response to fibrinogen micropatterns: (A) Platelet adhesion to printed fibrinogen substrates at 20%, 50% 85% and 100% relative surface coverage (n=30). Nexterion-H slide covered with albumin showed negligible platelet adhesion (data not shown). (B) Average platelet spreading area on samples with each relative fibrinogen coverage (n = 100). (C) Average platelet circularity for each relative fibrinogen coverage (n = 100). All error bars represent the standard error of the mean with a 95% confidence interval.

than between 50% and 85% though all were significantly different ($p < 0.001$).

Circularity has been recognized as a way to quantify the platelet morphological response [222,223]. Upon activation, the circularity will approach one as platelets reach their fully spread morphology [223]. In order to determine the extent in which spreading was affected by the underlying fibrinogen pattern, circularity was calculated (n=100) for each sample. If circularity is less than one the platelet shape was irregular with lower values corresponding to shapes that were less circular. At 20% and 85% relative fibrinogen coverage, there was no significant difference in circularity (Figure 4.3c). This is not surprising because although there was a significant difference in spreading area, both adhered and fully spread platelets display circular morphologies. At 50% relative fibrinogen coverage a significant ($p<0.001$) decrease in circularity was observed. This was due to the shape of the underlying fibrinogen pattern supporting only irregular morphologies, not allowing the platelets to spread fully (also seen in Figure 4.3b).

4.3.4 Assessment of Platelet Morphological Parameters

Following platelet activation, intracellular signals induce platelet spreading. This is also accompanied by an increase in intracellular Ca^{2+} levels, thrombin activation and platelet granule secretion [166,79,224]. As a result, platelet morphology is often used as a method to qualitatively assess the level of surface induced platelet activation. In order to further investigate the effect of varying fibrinogen feature sizes on platelet morphology, high resolution SEM images were taken for each sample. At 20% fibrinogen coverage (Figure 4.4a), almost

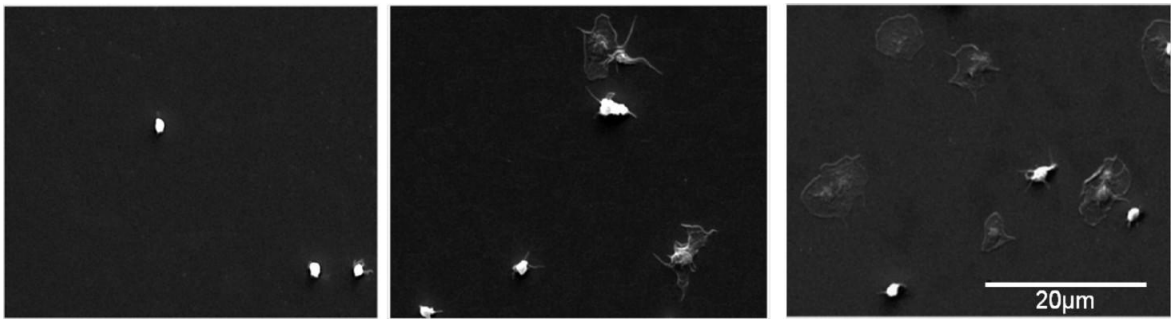

Figure 4.4 Scanning electron micrograph images of platelets spreading on surfaces printed at (A) 20%, (B) 50% and (C) 85% relative fibrinogen coverage (dotted size bar = 25 µm).

no spreading occurred and platelets displayed small spherical morphology. In some cases, however, platelet filopods were observed suggesting that these adhesion events still resulted in activation and may support platelet recruitment and aggregation over time. Samples with 50% fibrinogen coverage (Figure 4.4b), exhibited more extensive spreading and filipod formation but morphologies were irregular in shape. As discussed above this is the result of the underlying pattern restricting platelet spreading to regions in which immobilized fibrinogen is present (Figure 4.3b). At 85% coverage (Figure 4.4c) extensive spreading occurred and more platelets were observed to be in a fully spread circular shape.

Platelet activation and morphology are interrelated; as a result, shape change was qualitatively assessed by examining the extent of fillipod formation and spreading for each sample (Table 4.2). Activation levels were divided into four stages: 1) adherent but no apparent morphological changes, 2) initial formation of filopods, 3) extensive filipod formation and beginning of spreading, and 4) filopod retraction and flat rounded morphologies. SEM images (n=10) for each relative fibrinogen coverage were examined. The number of platelets in each category was calculated and normalized by the total number of adhered platelets. These values were then averaged to give an overall mean percent and standard error for each sample. The number of platelets that adhered but showed no apparent morphological changes and the number of platelets that showed initial stages of filipod formation decreased with increasing fibrinogen feature size. The number of platelets that showed extensive filipod formation or

Table 4.2 Qualitative assessment of platelet activation based on the morphology of adherent platelets (n = 10).

	Stage 1	**Stage 2**	**Stage 3**	**Stage 4**
Relative Fibrinogen Coverage	Platelets adhere and maintain a small spherical morphology	Initiation of filipod formation and extension	Extensive filipod formation and the beginning of spreading	Filipod retraction, platelet displays a round flat morphology
20%	37.0% +/- 8%	63.0% +/- 8%	0%	0%
50%	2.5% +/- 2.1%	21.7% +/- 4.9%	63.1% +/- 4.5%	12.7% +/- 2.4%
85%	0.4% +/- 0.7%	17.6% +/- 3.6%	59.0% +/- 4.3%	23.0% +/- 3.5%

rounded flat morphologies increased at higher fibrinogen area fractions. In fact, at 20% coverage, no platelets in the third or fourth stages of activation were observed. These results all suggest that overall platelet activation can be controlled by varying the size of the fibrinogen islands.

Morphology has been demonstrated as an important variable in controlling many different cellular events [118,120,136]. For example, Chen *et al*. used μCP of extracellular matrix ligands to restrict endothelial cell spreading that resulted in an increase in apoptosis [47]. Cytoskeletal reorganization events have also been implicated in many platelet activation mechanisms [166-168]; however, the use of micropatterned substrates to control platelet morphology is relatively unexplored. Given that platelet spreading is mediated by integrin-protein interactions, Grunkemeier *et al*. explored the role of different protein ligands in spreading mechanisms. Specifically, they investigated possible synergistic platelet shape change mechanisms by comparing spreading on polystyrene surfaces preadsorbed with a binary vWf-fibrinogen mixture, with homogeneous controls. More spreading was observed on the binary protein surface suggesting a synergistic role in platelet spreading; however, because the proteins were adsorbed, specific local protein-platelet effects could not be visualized [225]. The techniques presented here will facilitate future studies investigating these mechanisms with precise control of type, size and position of the immobilized protein features.

4.4 Conclusions

This study demonstrated that the surface induced platelet response could be controlled by the size and shape of immobilized protein ligands. Specifically, μCP was used to produce randomly placed, covalently immobilized, μm-sized fibrinogen islands at three different surface coverage areas as characterized by fluorescence and lateral force microscopy. It was found that the fibrinogen island number, size and shape affected both platelet adhesion and morphology. Also, these effects could be titrated by varying overall fibrinogen coverage. The ubiquitous nature of the immobilization procedure allows the same technique to be applied to any protein of interest and may serve to study additional local platelet-ligand interactions involved in adhesion and activation mechanisms.

CHAPTER 5

SUMMARY, PERSPECTIVES AND FUTURE DIRECTIONS

5.1 Summary and Perspectives

The search for a hemocompatible material has been a primary research endeavor in the field of biomaterials for over 50 years. Despite this incredible effort, no truly blood compatible material has been developed and the conflicts on how to approach the issue only seem to magnify. Platelet-material interactions have been a central focus in hemocompatibility due to their multifaceted roles in thrombus formation, inflammation, neointimal hyperplasia formation and immune responses. As a result, a principal research goal has been to tailor biomaterial surface properties to be inert to platelet adhesion and activation. Countless techniques have been employed to achieve this goal. In fact, if “biomaterial” and “reduced platelet adhesion” are entered into a Google Scholar search, approximately 1000 results are returned since 1995. In the majority of these publications, the researchers were capable of reducing platelet adhesion and/or activation on a novel surface of some variety. With this apparently large success rate, it is not unreasonable to ask, why is there a still lack of suitable materials for blood-contacting medical applications?

The physiological platelet response to a site of vascular injury or abnormality is inherently designed to be amplified. Thus, even the slightest

amount of material induced platelet activation can lead to aggregation and thrombus formation. Although the ability of novel materials to reduce the platelet response is an exciting outcome in fundamental research studies, these materials will not attain long term *in vivo* success unless the platelet response is completely attenuated. The sensitivity of platelets to varying stimuli and the complexity of the governing physiological processes make this a challenging task.

One crucial dilemma is that our basic understanding of fundamental platelet adhesion and activation mechanisms is still quite incomplete. This has led us to potentially false conclusions. For example, for many years, the ability of surfaces to minimize or eliminate fibrinogen adsorption was viewed as a key criterion to improve blood compatibility. However, more recently, it has been found that the adsorbed conformation of fibrinogen rather than the amount is a more critical determinant in the platelet response [34,36,204,206]. Also, albumin has been believed to be inert to platelet adhesion and has been extensively studied as potential blood-compatible surface coating [37,38,104,105,226]. However, Sivaraman *et al*. recently discovered that albumin is, in fact, capable of supporting platelet adhesion *in vitro* and that this may be due to the conformational dependent exposure of a binding epitope for platelets [35]. It is important we focus on decoding these fundamental cause and effect relationships that both drive and inhibit material induced platelet activation before we hastily screen and implant potential blood compatible materials into *in vivo* models. The development and use of these models is not only expensive but the

mechanism of failure/success is difficult to elucidate; this is because the physiological response is complex and highly interwoven.

The goal of the work described in this dissertation was to develop tools that allow for the study of fundamental platelet adhesion and activation mechanisms and well-defined control over the surrounding environment in which platelets were exposed was of paramount importance. In Chapter 2, a versatile negative charge density chemical gradient was developed to rapidly screen protein and platelet-surface interactions over a well defined variety of surface chemistries. These gradients not only provide a well-defined surface microenvironment but also provide a combinatorial advantage over homogeneous testing methods. Gradients were prepared by selective oxidation of a thiol monolayer to negatively charged sulfonate groups. The gradient surfaces were preadsorbed with three different protein solutions (plasma, albumin and fibrinogen) and the platelet response in flow conditions was assessed. Platelet adhesion patterns were found to be dependent on both the type and concentration of the adsorbed protein layer as well as the surface charge. However, when the orientation of the gradient was reversed, the adhesion patterns were not conserved. This indicated the response may not only be due to local effects, but instead, may be a result of upstream platelet-surface interactions. This observation was further confirmed by a significant increase in platelet adhesion seen over the length of homogeneous fibrinogen preadsorbed samples as a function of distance from the flow inlet. In order to effectively use these gradients as a screening tool, the effect of upstream platelet-surface

interactions on the downstream response needs to be addressed. Potential solutions to this problem are outlined in the future directions section of this dissertation (section 5.2).

As outlined in Chapter 3, the potential of upstream agonists to “prime” platelets for downstream adhesion and activation has both clinical implications and can affect the design of *in vitro* blood compatibility studies. Here we hypothesized that agonists, such as immobilized fibrinogen, were capable of priming platelets for downstream adhesion and activation. This hypothesis was tested by immobilizing fibrinogen in well-defined “priming” and “capture” regions using µCP on reactive PEG based substrates. The presence of the priming region on downstream platelet adhesion, spreading area, and aggregation was quantified. It was found that each variable - adhesion, spreading area, and aggregation - was significantly higher on samples that contained a fibrinogen priming region compared to control samples. The effect of fibrinogen priming on bulk platelet activation was also assessed using flow cytometry.

In Chapter 4, the ability of well defined protein micropatterns to control variables such as platelet adhesion and spreading was explored. Random fibrinogen micropatterns were covalently immobilized to reactive substrates at three different coverage areas using µCP. The background region was passivated with covalently immobilized albumin. Changing the relative coverage area resulted in a change in the size distribution of the features of the fibrinogen patterns. We found that the immobilized fibrinogen coverage area was directly related to the platelet adhesion response. Platelet morphology was controlled by

the size and shape of the fibrinogen microfeatures up to a certain point. At high coverage areas, the fibrinogen features were completely interconnected and platelets were capable of spreading over the passivated albumin background regions. The ability to control the ligands presented to platelets as well as its morphology will facilitate future fundamental studies focused on deciphering the mechanisms responsible for surface induced platelet activation.

5.2 Future Directions

In Chapter 2, the use of chemical gradients was explored as a high throughput method to screen protein and platelet-surface interactions. Specifically, negative charge density gradients were prepared by selective oxidation of a thiol monolayer to negatively charged sulfonate groups. The platelet response with different preadsorbed protein substrates was assessed. Platelet adhesion patterns were found to be dependent on both the type and concentration of the adsorbed protein layer as well as the surface charge. However, when the orientation of the same gradient sample was reversed, the adhesion patterns changed. This indicated the response may not be due to local effects only but instead may be a result of upstream platelet-surface interactions.

The initial goal of this study was to use gradients to rapidly screen both the protein and platelet response to various molecular environments. The discovery that upstream platelet interactions with the surface affect downstream adhesion patterns presents a challenge that needs to be addressed. If upstream interactions elicit a downstream response, there is no way to decipher if the local

platelet response is a direct result of the surface properties of that region, or an artifact of upstream platelet-surface interactions.

One potential solution is to redesign the patterning chamber to produce gradients in a perpendicular orientation to the flow direction. This will ensure that platelets encounter the same conditions throughout the perfusion. There still does exist possibility that platelet activity will increase along the length of the sample. Therefore results should always be compared and/or normalized to a homogeneous control.

After ensuring upstream effects are accounted for, these surface gradients provide a useful means to rapidly identify cause and effect relationships between properties of the surface microenvironment and the protein/platelet response. Detectable changes observed in the platelet or protein behavior can be exploited and studied in greater detail on homogeneous test samples.

One unique advantage of the described molecular surface gradients is their versatility. The negatively charged sulfonate groups are relatively inert to further modification; however, thiol moieties can be utilized for a variety secondary reactions making these gradients foundation for a variety of screening studies. For example, zwitterionic surface properties have shown improved hemocompatibility [111,161,227,228]; however, the exact reason for this is not completely understood. Variables such as the relative positive/negative surface charge density can be explored using positive to negatively charged gradients. These can be prepared using idoacetamides, such as Aminoethyl8™ (Thermo Scientific), which convert the neutral thiol surface to a positively charged

amine surface. The iodoalkyl group on Aminoethyl8™ specifically reacts with thiol groups via a covalent thioether bond [229]. The thiol groups can also be modified with compounds such as idoacetate which contain a terminal hydroxyl group and subsequently will create different surface dipoles on the gradient surface [230]. Heterobifunctional crosslinkers, such as sulfo-SMCC, can be conjugated to thiols [189, 190] forming protein reactive terminal NHS ester groups and can be used to develop a variety of protein/enzyme gradients. PEG is a versatile polymer that can be reacted with surfaces, proteins, and other biomolecules, and has been specifically immobilized to surfaces using silane conjugation techniques [231, 232]. PEG based substrates are not only highly resistant to nonspecific protein adsorption [230] and cell adhesion but the use of PEG spacers in the immobilization of biomolecules, such as heparin, has been shown to improve its thromboresistant activity [116, 112, 113]. This is likely because the long brush like PEG chains allow the 3-dimensional structure and mobility of biomolecules to be maintained [112, 116]. Gradients of PEG based biomolecule immobilization schemes can be used to optimize variables contributing to its blood compatibility such as surface distribution/density.

In Chapter 3, we discovered that upstream fibrinogen was capable of priming platelets for downstream adhesion and activation. In the future, it will be important to characterize if other agonists are also capable of eliciting such a response. For example, collagen is exposed at the suture site of implanted vascular devices and is known to locally promote platelet adhesion and activation [65,234] and therefore may also be capable of priming platelets for downstream

activation. It would also be interesting to explore potential synergistic interactions in these mechanisms by introducing soluble agonists such as vWf into the system.

In Chapter 4, fibrinogen micropatterns at varying surface coverage areas were prepared and found to exhibit control over platelet morphological parameters. As discussed in section 1.2.3, platelet morphological changes are a key characteristic of platelet activation. Platelet contacts with surface adsorbed proteins induce cytoskeletal rearrangements that facilitate spreading [79,166-168]. Also, the resulting geometry allows for the centralization of secretion granules and more secretion events have been observed when platelets are in their fully spread state [79]. Consequently, platelet morphological assessments are commonly used to qualitatively assess biomaterial induced platelet activation. One future study currently being designed is to establish a quantitative relationship between key platelet morphological parameters and degranulation, a central event in platelet activation. Logically, platelet spreading area may be directly related to secreted activation markers. This will be accomplished by printing random fibrinogen micropatterns at three relative surface coverage areas and measuring the release of β-thromboglobulin from the α-granules of the spreading platelets using a commercially available ELISA kit. These values will be correlated with platelet spreading area and circularity using SEM analysis, two variables often used to qualitatively assess biomaterial induced platelet activation. The goal is to develop a quantitative relationship between these parameters and degranulation.

To date, binary patterns of fibrinogen and albumin have been used by our group. The procedures used in Chapter 4, however, could be applied to any binary system of proteins leaving open the possibility for platelet spreading studies with a variety of protein substrates. For example, vWf/fibrinogen, collagen/vWf, or collagen/fibrinogen, patterns could be used to study synergistic interactions between these proteins during activation. Also, the relative amount of each protein could be titrated and used to quantify if a threshold is associated with a given response. The ubiquitous nature of this protein immobilization scheme allows for the described techniques to be applied to a wide variety of protein-platelet interactions implicated in biomaterial induced platelet adhesion and activation.

APPENDIX A

XPS ANALYSIS OF MODIFICATION OF MTS WITH SULFO-SMCC[1]

In Chapter 2, sulfo-SMCC modified MTS monolayers were used to prepare covalently immobilized fibrinogen test samples. Procedures used in this study were adapted from previous protocols developed in our lab in which RGD peptides were successfully immobilized using this chemistry. Here, XPS analysis of the modification of MTS monolayers with sulfo-SMCC is presented. Elemental composition (C, O, N, S, and Si) for an MTS thiol monolayer was compared before and after sulfo-SMCC incubation. These samples were also compared with oxidized MTS samples treated sulfo-SMCC as a negative control. Three spots for each sample were analyzed using a Surface Science Instruments x-probe spectrometer.

There was a slight amount of nitrogen observed on both nonoxidized and oxidized samples prior to sulfo-SMCC treatment possibly due to outside contamination. However, the elemental nitrogen and carbon atomic percentage both increased after sulfo-SMCC incubation on nonoxidized samples while the nitrogen content on oxidized samples actually decreased. The Si and O

[1] Mishra and Hlady, Unpublished Data

percentage (most likely due to the substrate signal) decreased which is consistent with addition of the molecule to the surface.

The ability to immobilize RGDs to reactive sulfo-SMCC modified samples was also investigated. No change in the relative atomic composition was observed prior and after RGD immobilization. This is not surprising since no new atoms were introduced into the samples after RGD treatment thus XPS alone, insufficient in characterizing RGD surface modification.

To further investigate RGD immobilization to sulfo-SMCC activated MTS monolayers, ToF-SIMS was used to detect amino acid fragments from the amino acids arginine, aspartic acid, and serine (Figures A.1 and A.2). A significant increase in these fragments was observed on sulfo-SMCC activated non-oxidized thiol monolayers versus oxidized control surfaces suggesting RGD immobilization was successful.

Table A.1 Atomic percentage (composition) as determined by XPS. Three spots per sample were taken. The average composition for each sample is reported along with the standard deviation.

		Atomic Percentage				
Sample		**C**	**O**	**N**	**S**	**Si**
MTS Unoxidized	AVG	32.2	39.5	0.6	3.3	24.5
	STDV	0.9	0.6	0.1	0.1	0.8
MTS Fully Oxidized	AVG	27.8	45.5	1.5	1.7	23.6
	STDV	2.3	1.8	0.2	0.3	0.8
MTS + sSMCC Unoxidized	AVG	43.6	33.3	2.8	2.9	17.5
	STDV	0.7	0.5	0.1	0.5	0.5
MTS + sSMCC Oxidized	AVG	22.2	48.6	0.7	1.1	27.4
	STDV	0.8	1	0	0.3	0.6
with RGD Unoxidized	AVG	43	33.4	2.6	3.2	17.8
	STDV	1.3	1	0.1	0.2	0.5
With RGD Oxidized	AVG	24	48.1	0.9	0.9	26.6
	STDV	0.4	0.4	0.1	0.2	0.3

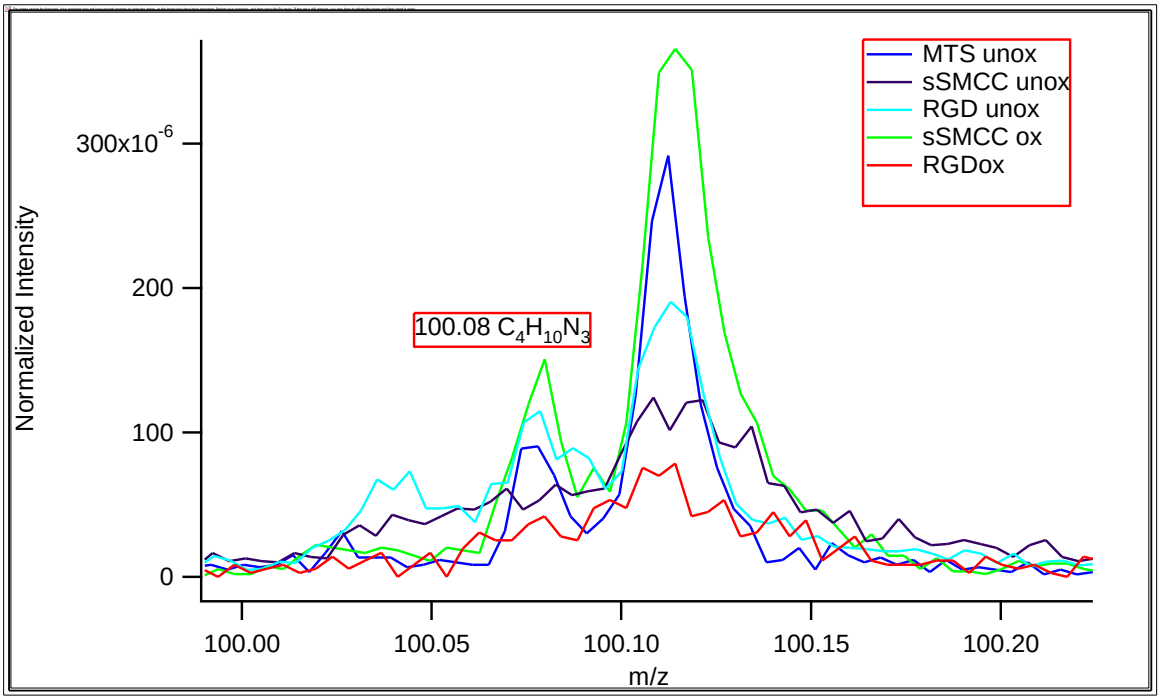

Figure A.1 Positive ToF-SIMS spectra of m/z 100.1 $C_4H_{10}N_3$ fragment (shown to be indicative of the amino acid arginine [239]. Spectra have been normalized to the overall spectral intensity.

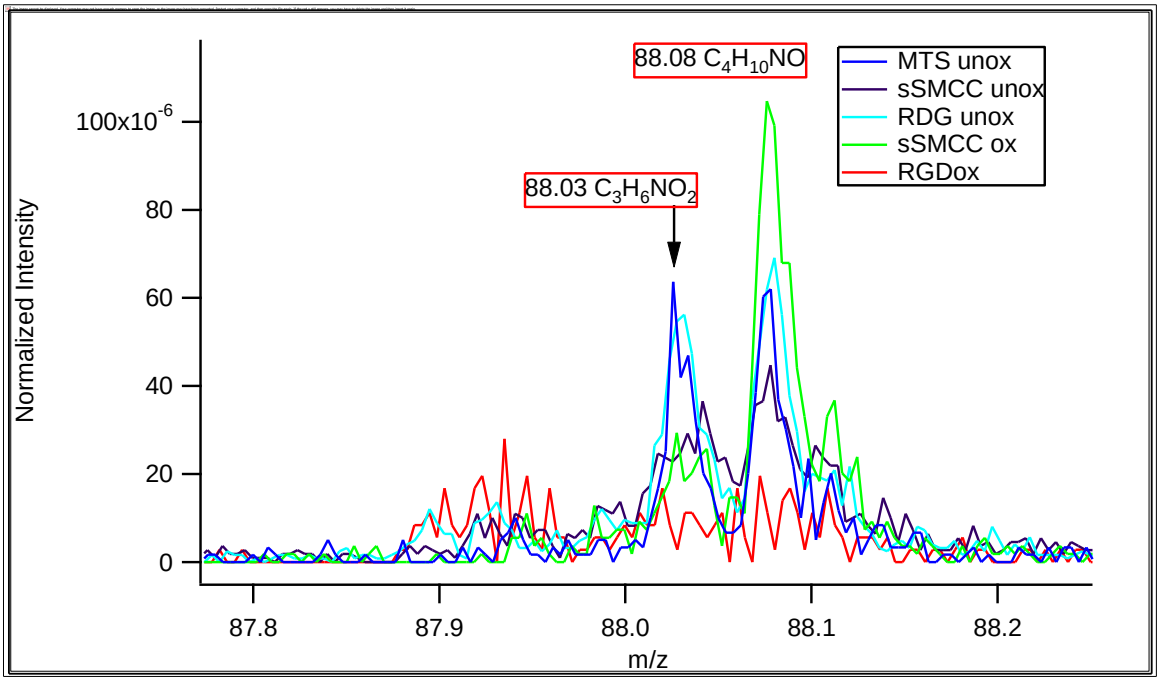

Figure A.2 Positive ToF-SIMS spectra of m/z 88.0 region. The $C_3H_6NO_2$ fragment has been reported to be indicative ot the amino acid aspartic acid [239]. Spectra have been normalized to the overall spectral intensity.

APPENDIX B

DERIVATION OF LEVICH APPROXIMATION

In order to determine the number of platelets that are capable of interacting with the surface we estimated the convective/diffusive driven flux of the platelets to the surface using the Smoluchowski-Levich approximation. Here, the flow –induced transport of colloidal particles to an interface can be described by a convective-diffusion equation. Assuming an absence of interaction forces this equation becomes [200]:

$$\frac{\partial c}{\partial t} + v_x \frac{\partial c}{\partial x} + v_y \frac{\partial c}{\partial y} = D\left[\frac{d^2 c}{\partial y^2} + \frac{d^2 c}{\partial x^2}\right]$$

The solution for velocity in the *x* direction of a parallel plate flow cell [200, 202]:

$$v_x = \frac{3}{2} V_m \frac{y}{b}\left(2 - \frac{y}{b}\right)$$

where
V_m = the mean velocity
b = ½ the depth of the flow cell

In our system, the platelets are constantly being supplied to the flow chamber at a concentration of $2.5*10^7$ platelets/ml (~25% of physiological concentration). Thus no decrease in concentration over time is observed in the bulk. In this case we can assume our system is at steady state and:

$$\frac{\partial c}{\partial t} = 0$$

The dimensionless form of this equation is given by the Peclet (*Pe*) number which represents the ratio between diffusion and convective mass transport:

$$Pe = \frac{u_0 L}{D}$$

where:
L = characteristic length of the system
u_0 = characteristic velocity

Thus the dimensionless steady state convective- diffusive equation is:

$$v_x \frac{\partial C}{\partial X} + v_y \frac{\partial C}{\partial Y} = \frac{1}{Pe}\left[\frac{d^2 C}{\partial Y^2} + \frac{d^2 C}{\partial X^2}\right]$$

where:
$X = x/L$
$Y = y/L$
$V_i = v_i/u0$
$C = c/c_{bulk}$

After substitution of v_x in the equation we get:

$$0 = \left[\frac{d^2 c}{\partial y^2} - \frac{3}{2}\frac{V_m}{D}\frac{y}{b}\left(2 - \frac{y}{b}\right)\frac{\partial c}{\partial x}\right]$$

For simplicity during integration we substitute:

$$\varphi = y\left(\frac{6V_m}{18Dbx}\right)^{1/3} \rightarrow 0 = \frac{d^2 c}{d\varphi^2} + 3\varphi^2 \frac{dc}{d\varphi}$$

After double integration with respect to the bulk concentration we get

$$c_{bulk} = \int_0^{\infty} Ae^{-\varphi^3} d\varphi$$

Substituting $\varphi^3 = u$:

$$c_{bulk} = \frac{A}{3}\int_0^{\infty} Ae^{-u}\, u^{\frac{1}{3}-1} du = \frac{A}{3}\Gamma\left(\frac{1}{3}\right) = \mathrm{A}\Gamma\left(\frac{4}{3}\right)$$

By applying Ficks law for diffusion we get

$$j_0 = D\frac{\partial c}{\partial y}\Big| y = 0 = D\left(\frac{6V_m}{18Dbx}\right)^{\frac{1}{3}} \frac{\partial c}{\partial \varphi}\Big| \varphi = 0$$

$$= \frac{D}{\Gamma\left(\frac{4}{3}\right)}\left(\frac{6V_m}{18Dbx}\right)^{1/3} * C_{bulk}$$

The deposition rate is often represented as a dimensionless quantity called the Sherwood number, *Sh, where:*

$$Sh = \frac{k_1}{D} = \frac{j_0}{Dc}$$

:

$$Sh_o = \frac{1}{0.89} * \left(\frac{2}{9} * \frac{Pe}{X}\right)^{1/3}$$

This gives:

$$j_0 = \frac{D_{plt}c}{0.89}\left(\frac{6V_m}{18Dbx}\right)^{1/3}$$

where:
j_0 = initial deposition rate
D = Diffusion coefficient
c = bulk concentration
Pe = the dimensionless Peclet number (Adamczyk and van de Ven) for flow deposition of colloidal particles in a parallel plate flow cell [202, 203].

$$Pe = \frac{3V_m a^3}{2b^2 D}$$

where:

a = the platelet radius
X = *x/b* where *x* is the distance from the flow inlet and *b* is ½ the height of the flow cell.

For the system described in Chapter 3:

$c = 2.5*10^7$ plt/cm^3	$V_m = 0.44$ cm/sec	$\mu = 1$ kg/m*sec
$T = 310.15$ K	$a = 10^{-6}$ m	$b = 0.025$ cm

The platelet diffusion coefficient can be estimated using the Stokes-Einstein

relationship:

$$D_{Plt} = \frac{k_b T}{6\pi\mu a}$$

$$= \frac{1.38 * 10^{-23}\ \frac{m^2 kg}{s^2 K} * (310.15\ K)}{6\pi\left(1\frac{kg}{m * sec}\right)(10^{-6} m)} = 10^{-13}\frac{m^2}{sec}$$

$$D_{plt} = \ 10^{-9}\frac{cm^2}{sec}$$

The Peclet for the system is:

$$Pe = \frac{3V_m a^3}{2b^2 D_{plt}}$$

$$= \frac{3\left(0.44\frac{cm}{sec}\right)(10^{-4}cm)^3}{2(0.025\ cm)^2\left(10^{-9}\frac{cm^2}{sec}\right)}$$

$$Pe = 1.05$$

The flux as a function of distance from the flow inlet is (See Figure 3.8):

$$j_0 = \frac{D_{plt}c}{0.89}\left(\frac{6V_m}{18Dbx}\right)^{1/3}$$

$$= 0.112 * \left(\frac{2.64}{(4.5 * 10^{-10})X}\right)^{\frac{1}{3}}$$

APPENDIX C

EFFECT OF PROTEIN IMMOBILIZATION SCHEME ON PLATELET ADHESION PATTERNS

C.1 Introduction

Fibrinogen has been implicated in being essential for stable platelet adhesion to biomaterials [41,72]. Subsequently, platelet-fibrinogen interactions have been studied extensively. When fibrinogen adsorbs to the surface, epitopes within the molecule are exposed that bind to the integrin αIIbβ3 on the platelet membrane. This interaction converts platelets to an active state in which they begin to spread and recruit more platelets. It has been shown that surface distribution, concentration, and conformation can all affect the platelet response [36,176,204,205,207,222,235]. In fact, conformation is believed to be of critical importance since in its soluble form, fibrinogen is relatively inert to platelets when no agonists are present [34,42].

Surface patterning is a technique used to study protein-cell and protein-platelet interactions. There many different approaches to patterning protein on a surface including direct methods such as inkjet deposition [236] and micro-contact printing [135, 145,150,237,238], as well as indirect methods involving site specific adsorption using custom designed microfluidic chambers [135,145,153].

The value in surface patterning lies in the ability to precisely control the type, concentration and distribution of the protein on the surface. Surface patterning has also been coupled with the use of reactive surface chemistry capable of covalently immobilizing the protein to the surface. This not only increases the stability of the surface but also allows for patterning of surfaces that are resistant to protein adsorption.

Although patterned surfaces show great promise in studies relating to platelet adhesion, activation and spreading as well as promise in being used as tools for platelet screening assays. The effects of the patterning technique on fibrinogen conformation and platelet adhesion have not been well documented. In this work we examined how different methods of protein immobilization affected the platelet response. Two protein reactive substrates were compared; sulfo-SMCC activated quartz, and NHS ester activated Nexterion-H slides (preparation methods discussed in section 3.2). Fibrinogen was immobilized on each sample by passive adsorption as well as μCP. We found that the platelet response and the relative amount of protein immobilized on each sample were significantly different depending on the immobilization technique. The platelet response, however, did not directly correlate with the amount of adsorbed fibrinogen suggesting other factors such as protein conformation may be contributing to the varied response.

C.2 Methods

C.2.1 Preparation and Characterization of Fibrinogen Immobilized Surfaces

Preparation of sulfo-SMCC reactive surfaces followed protocols outlined in section 3.2.1. Passive immobilization was carried out by incubating both sulfo-SMCC and Nexterion-H (Schott) reactive substrates with human fibrinogen (Calbiochem) in 0.1 M PBS (c = 0.1 mg/ml, 1 mg/ml or 10 mg/ml) for 45 minutes. Printed fibrinogen substrates were prepared following protocols outlined in section 3.2.2 using μCP at a 100% relative coverage area. Following immobilization, samples were vigorously rinsed in a 1% Tween surfactant solution to remove protein not covalently bound to the surface. Samples were dried with N2 gas and then stored under vacuum until use.

C.2.2 Washed Platelet Preparation and Adhesion Studies

Washed platelets were prepared as described in section 3.2.6 in a Tyrodes-HEPES buffer (c = 10^7 platelets/ml). Platelets were perfused over each sample for 5 minutes in a parallel plate flow cell as described in section 2.2.5. DIC microscopy was used to visualize platelet adhesion on each sample. Average adhesion was quantified (n=30) and significance was calculated using unpaired t-tests.

C.2.3 Quantifying Relative Amount of Surface Immobilized Fibrinogen

The relative amount of surface immobilized fibrinogen was calculated by measuring the mean fluorescence intensity (n = 30) of Alexafluor-488 labeled fibrinogen after protein immobilization (see section 3.2.4 for labeling protocol).

The mean fluorescence was normalized against background fluorescence for each sample.

C.3 Results

C.3.1 Effect of Surface Chemistry and Protein Immobilization Scheme on Platelet Adhesion

Overall average platelet adhesion was compared on fibrinogen surfaces prepared using two different patterning techniques (passive immobilization, direct printing) on substrates with two different protein immobilization chemistries (sulfo-SMCC modified quartz, NHS activated PEG based hydrogel). It was found that the platelet adhesion response was different depending on both the patterning technique and the immobilization chemistry for three different concentrations of fibrinogen in solution (Figures C.1 and C.2).

Although the fibrinogen solutions used at the beginning of the patterning process were all at equal concentrations, the efficiency of the protein transfer may not be the same for each technique or immobilization chemistry. Thus, the relative amount of fibrinogen was measured by quantifying fluorescence intensity of Alexa Fluor-488 labeled fibrinogen for each sample (Figure C.3). All values were normalized against background fluorescence for each sample. It was found that the amount of relative fibrinogen on the surface for each sample was, in fact, different. However, when the relative amount of fibrinogen was plotted against average platelet adhesion, no direct correlation could be established (Figure C.4). This suggests that other factors may contribute to the variation in platelet response to fibrinogen surfaces prepared using different immobilization schemes.

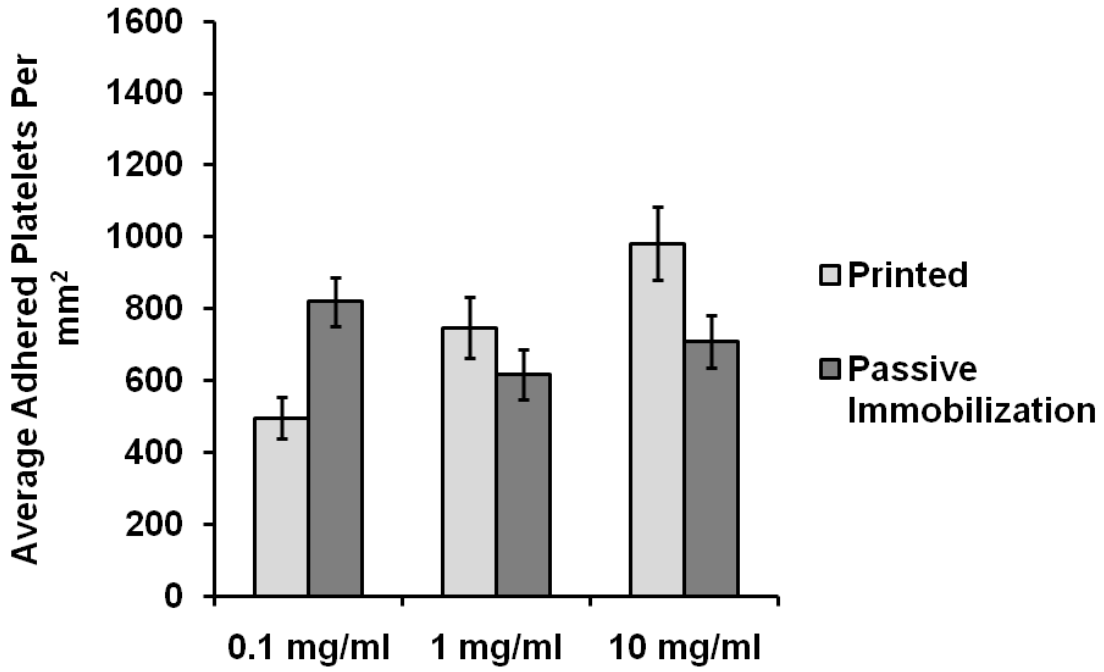

Figure C.1 The effect of the protein immobilization technique on platelet adhesion to Nexterion-H substrates. Fibrinogen was either printed on or adsorbed to the reactive substrates at three concentrations. Overall platelet adhesion was significantly different ($n = 30$, $p < 0.001$) on printed versus passively immobilized fibrinogen substrates at all concentrations.

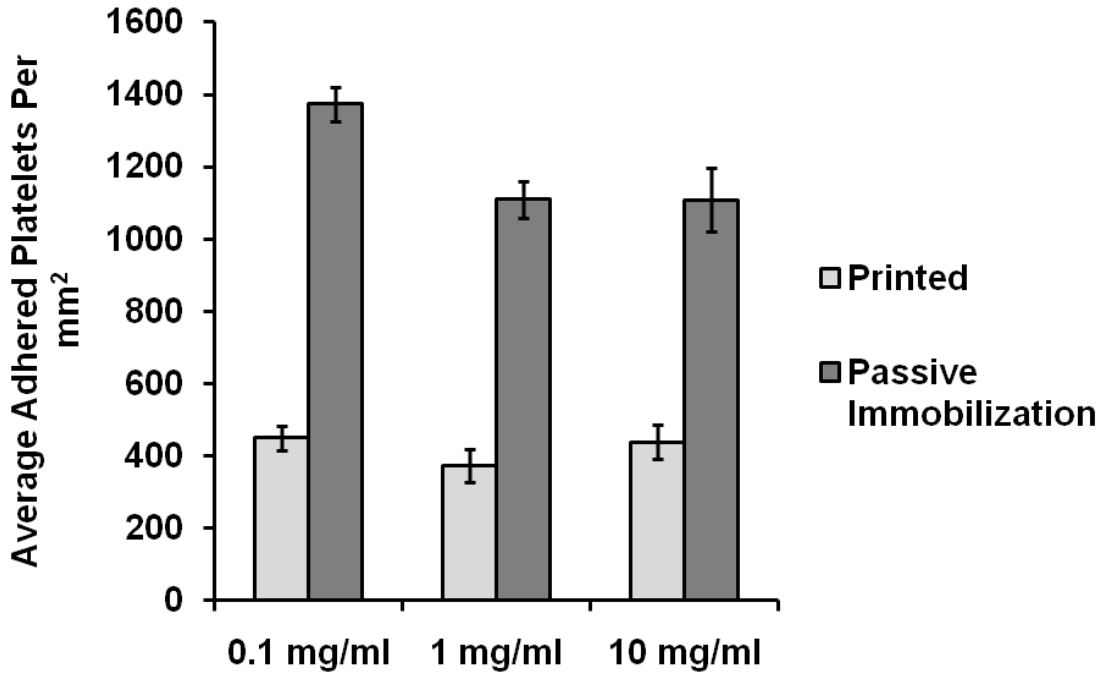

Figure C.2 The effect of the protein immobilization technique on platelet adhesion to sulfo-SMCC activated quartz slides. Fibrinogen was either printed on or adsorbed to the reactive substrates at three concentrations. Overall platelet adhesion was significantly higher ($n = 30$, $p < 0.001$) on passively immobilized versus printed fibrinogen substrates at all concentrations.

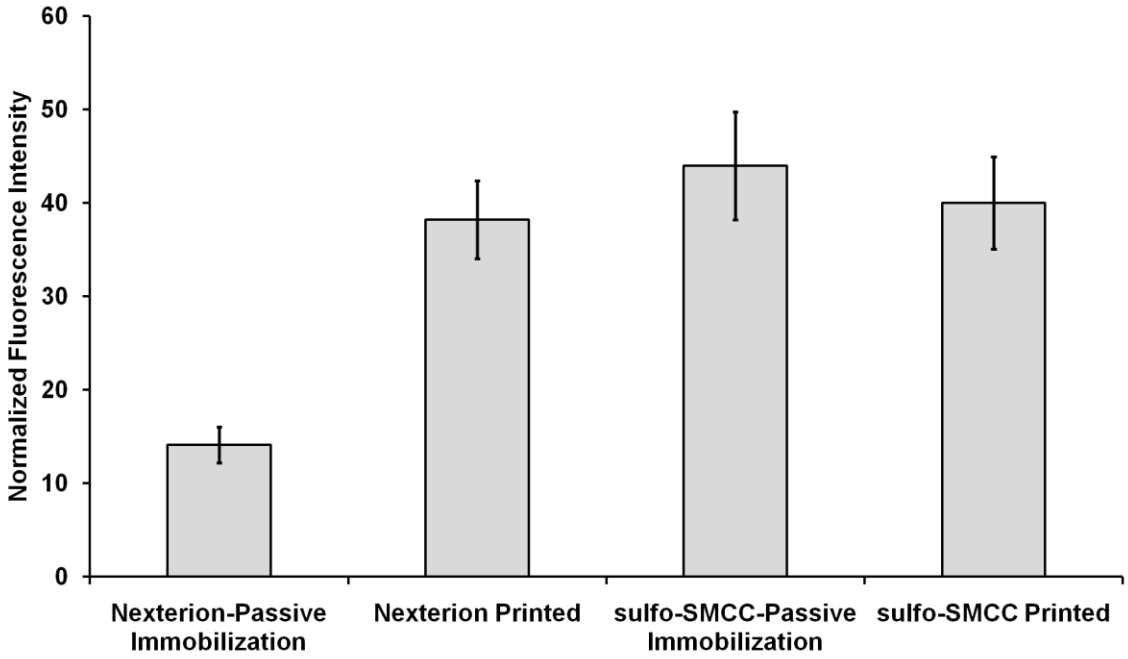

Figure C.3 The relative amount of fibrinogen immobilized to each sample measured by fluorescence intensity. For each immobilization scheme 30 samples were averaged and normalized against the background fluorescence. Error bars represent +/- the standard error of the mean.

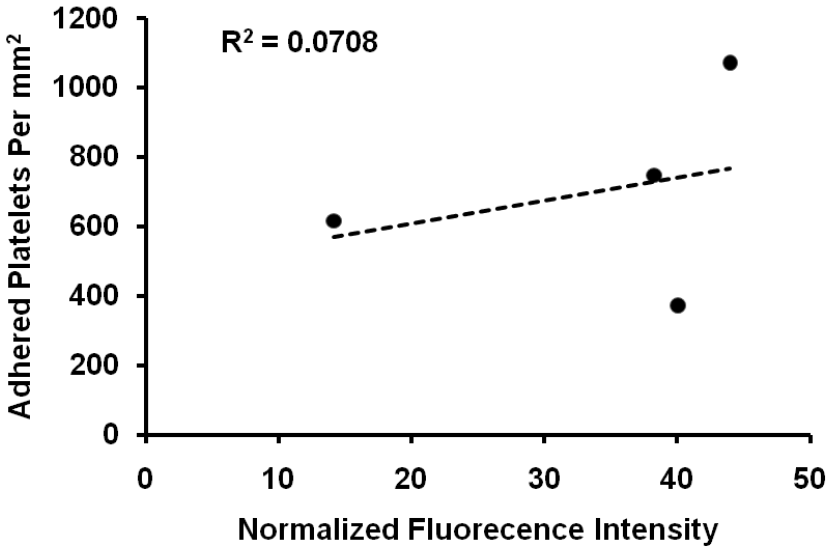

Figure C.4 The relationship between overall platelet adhesion and relative amount of immobilized fibrinogen for sulfo-SMCC and Nexterion-H samples Fibrinogen was immobilized using passive adsorption and direct printing techniques."

C.4 Conclusions

Here, we observed significant changes in platelet adhesion patterns on immobilized fibrinogen surfaces. The immobilization process (passive or printing) as well as the underlying surface chemistry both was observed to play a role. When we investigated the relative amount of fibrinogen immobilized to the surface using fluorescence microscopy we found that there in fact was different surface protein concentrations depending on the immobilization procedure. However, when the relative fibrinogen concentration was plotted against platelet adhesion, no direct relationship was observed. This suggests other factors may be affecting the platelet response including the immobilized fibrinogen conformation or distribution.

REFERENCES

[1] P.A. Heidenreich, J.G. Trogdon, O.A. Khavjou, J. Butler, K. Dracup, M.D. Ezekowitz, E.A. Finkelstein, Y. Hong, S.C. Johnston, A. Khera, D.M. Lloyd-Jones, S.A. Nelson, G. Nichol, D. Orenstein, P.W.F. Wilson, Y.J. Woo, and S.C., "Forecasting the future of cardiovascular disease in the United States: A policy statement from the American Heart Association," Circulation, 2011.

[2] J.S. Hanker and B.L. Giammara, "Biomaterials and biomedical devices," Science, vol. 242, 1988, pp. 885-892.

[3] B.D. Ratner, "The catastrophe revisited: Blood compatibility in the 21st century," Biomaterials, vol. 28, 2007, pp. 5144-5147.

[4] J. Hu, J.W. Eaton, T.P. Ugarova, and L. Tang, "Molecular basis of biomaterial-mediated foreign body reactions," Blood, vol. 98, 2001, pp. 1231-1238.

[5] S.C. Cannegieter, F.R. Rosendaal, and E. Briet, "Thromboembolic and bleeding complications in patients with mechanical heart valve prostheses," Circulation, vol. 89, 1994, pp. 635-641.

[6] M.B. Gorbet and M.V. Sefton, "Biomaterial-associated thrombosis: Roles of coagulation factors, complemennt, platelets, and leukocytes," Biomaterials, vol. 25, 2004, pp. 5681-5703.

[7] K.M. Giacomini, R.M. Krauss, D.M. Roden, M. Eichelbaum, M.R. Hayden, and Y. Nakamura, "When good drugs go bad," Nature, vol. 446, Apr. 2007, pp. 975-977.

[8] J.D. Andrade and V. Hlady, "Protein adsorption and materials biocompatibility: A tutorial review and suggested hypotheses," in *Biopolymers/Non-Exclusion HPLC,* Berlin/Heidelberg, Germany: Springer, 1986, pp. 1-63.

[9] L. Vroman, *Blood*, New York: Natural History Press, Doubleday and Co, 1967.

[10] J.K. Yun, K. DeFife, E. Colton, S. Stack, A. Azeez, L. Cahalan, M. Verhoeven, P. Cahalan, and J.M. Anderson, "Human monocyte/macrophage adhesion and cytokine production on surface-modified poly(tetrafluoroethylene/hexafluoropropylene) polymers

with and without protein preadsorption," Journal of Biomedical Materials Research, vol. 29, 1995, pp. 257-268.

[11] K. Dee, D. Puleo, and R. Bizios, "Protein-surface interactions," in *An introduction to tissue-biomaterial interactions*, Hoboken, NJ, John Wiley and Sons, 2002.

[12] T.G. Drummond, M.G. Hill, and J.K. Barton, "Electrochemical DNA sensors," Nat Biotech, vol. 21, Oct. 2003, pp. 1192-1199.

[13] J. Nam, C.S. Thaxton, and C.A. Mirkin, "Nanoparticle-based bio-bar codes for the ultrasensitive detection of proteins," Science, vol. 301, 2003, pp. 1884-1886.

[14] Y. Lee and M. Mrksich, "Protein chips from concept to practice," Trends in Biotechnology, vol. 20, 2002, pp. 14-18.

[15] Z. Zhang, M. Zhang, S. Chen, T. Horbett, B. Ratner, and S. Jiang, "Blood compatibility of surfaces with superlow protein adsorption," Biomaterials, vol. 32, 2008, pp. 4285-4291.

[16] P. Roach, D. Farrar, and C.C. Perry, "Surface tailoring for controlled protein adsorption: Effect of topography at the nanometer scale and chemistry," Journal of the American Chemical Society, vol. 128, Mar. 2006, pp. 3939-3945.

[17] K. Ishihara, N.P. Ziats, B.P. Tierney, N. Nakabayashi, and J.M. Anderson, "Protein adsorption from human plasma is reduced on phospholipid polymers," Journal of Biomedical Materials Research, vol. 25, 1991, pp. 1397-1407.

[18] K. Bergström, K. Holmberg, A. Safranj, A.S. Hoffman, M.J. Edgell, A. Kozlowski, B.A. Hovanes, and J.M. Harris, "Reduction of fibrinogen adsorption on PEG-coated polystyrene surfaces," Journal of Biomedical Materials Research, vol. 26, 1992, pp. 779-790.

[19] D. Beyer, W. Knoll, H. Ringsdorf, J. Wang, R.B. Timmons, and P. Sluka, "Reduced protein adsorption on plastics via direct plasma deposition of triethylene glycol monoallyl ether," Journal of Biomedical Materials Research, vol. 36, 1997, pp. 181-189.

[20] D.R. Schmidt, H. Waldeck, and W.J. Kao, "Protein adsorption to biomaterials," in *Biological interactions on materials surfaces*, New York, Springer, 2009, pp. 1-18.

[21] M. Malmsten, "Formation of adsorbed protein layers," J Colloid Interface Sci, vol. 207, 1998, pp. 186-199.

[22] C.F. Wertz and M.M. Santore, “Effect of surface hydrophobicity on adsorption and relaxation kinetics of albumin and fibrinogen: Single-species and competitive behavior,” Langmuir, vol. 17, May. 2001, pp. 3006-3016.

[23] W. Norde, F. Macritchie, G. Nowicka, and J. Lyklema, “Protein adsorption at solid-liquid interfaces: Reversibility and conformation aspects,” J Colloid Interface Sci, vol. 112, 1986, pp. 447-456.

[24] Y. Ding, S. Streitmatter, B.E. Wright, and V. Hlady, “Spatial variation of the charge and sulfur oxidation state in a surface gradient affects plasma protein adsorption,” Langmuir, vol. 26, Jul. 2010, pp. 12140-12146.

[25] T.E. Creighton, “Protein folding,” Biochem. J., vol. 270, 1990, pp. 1-16.

[26] K. Dill, S. Bromberg, K. Yue, K.M. Fiebig, D.P. Yee, P.D. Thomas, and H.S. Chan, “Principles of protein folding--a perspective from simple exact models,” Protein Sci, vol. 4, 1995, pp. 561-602.

[27] C. Haynes and W. Norde, “Globular proteins at solid/liquid interfaces,” Colloids Surfaces [B], vol. 2, 1994, pp. 517-566.

[28] D. Asthagiri and A.M. Lenhoff, “Influence of structural details in modeling electrostatically driven protein adsorption,” Langmuir, vol. 13, Dec. 1997, pp. 6761-6768.

[29] J.D. Andrade and V. Hlady, “Plasma protein adsorption: The big twelve,” Annals of the New York Academy of Sciences, vol. 516, 1987, pp. 158-172.

[30] L. Vroman and A. Adams, “Findings with the recording ellipsometer suggesting rapid exchange of specific plasma proteins at liquid/solid interfaces,” Surface Science, vol. 16, 1969, pp. 438-446.

[31] C.F. Wertz and M.M. Santore, “Fibrinogen adsorption on hydrophilic and hydrophobic surfaces: Geometrical and energetic aspects of interfacial relaxations,” Langmuir, vol. 18, Feb. 2002, pp. 706-715.

[32] F. Caruso and C. Schüler, “Enzyme multilayers on colloid particles: Assembly, stability, and enzymatic activity,” Langmuir, vol. 16, Nov. 2000, pp. 9595-9603.

[33] Y. Wu, F.I. Simonovsky, B.D. Ratner, and T.A. Horbett, “The role of adsorbed fibrinogen in platelet adhesion to polyurethane surfaces: A comparison of surface hydrophobicity, protein adsorption, monoclonal antibody binding, and platelet adhesion,” Journal of Biomedical Materials Research Part A, vol. 74A, 2005, pp. 722-738.

[34] B. Sivaraman and R.A. Latour, “The relationship between platelet adhesion on surfaces and the structure versus the amount of adsorbed fibrinogen,” Biomaterials, vol. 31, 2009, pp. 832-839.

[35] B. Sivaraman and R.A. Latour, “The adherence of platelets to adsorbed albumin by receptor-mediated recognition of binding sites exposed by adsorption induced unfolding,” Biomaterials, vol. 31, 2009, pp. 1036-1044.

[36] A. Chiumiento, S. Lamponi, and R. Barbucci, “Role of fibrinogen conformation in platelet activation,” Biomacromolecules, vol. 8, Feb. 2007, pp. 523-531.

[37] C. Tsai, H. Huo, P. Kulkarni, and R. Eberhart, “Biocompatible coatings with high albumin affinity,” ASAIO Trans, vol. 36, pp. M307-M310.

[38] Y. Ishikawa, S. Sasakawa, M. Takase, and Y. Osada, “Effect of albumin immobilization by plasma polymerization on platelet reactivity,” Thrombosis Research, vol. 35, 1984, pp. 193-202.

[39] M. Amiji and K. Park, “Surface modification of polymeric biomaterials with poly(ethylene oxide), albumin, and heparin for reduced thrombogenicity,” Journal of Biomaterials Science, Polymer Edition, vol. 4, 1993, pp. 217-234.

[40] J.M. Grunkemeier, W.B. Tsai, C.D McFarland, and T.A Horbett, “The effect of adsorbed fibrinogen, fibronectin, von Willebrand factor and vitronectin on the procoagulant state of adherent platelets,” Biomaterials, vol. 21, 2000, pp. 2243-2252.

[41] W. Tsai, J.M. Grunkemeier, and T.A. Horbett, “Human plasma fibrinogen adsorption and platelet adhesion to polystyrene,” Journal of Biomedical Materials Research, vol. 44, 1999, pp. 130-139.

[42] E.W. Salzman, J. Lindon, G. McManama, and J.A. Ware, “Role of fibrinogen in activation of platelets by artificial surfaces,” Annals of the New York Academy of Sciences, vol. 516, 1987, pp. 184-195.

[43] B. Savage, E. Saldvar, and Z.M. Ruggeri, “Initiation of platelet adhesion by arrest onto fibrinogen or translocation on von Willebrand factor,” Cell, vol. 84, Jan. 1996, pp. 289-297.

[44] S. Goto, D.R. Salomon, Y. Ikeda, and Z.M. Ruggeri, “Characterization of the unique mechanism mediating the shear-dependent binding of soluble von Willebrand factor to platelets,” Journal of Biological Chemistry, vol. 270, 1995, pp. 23352-23361.

[45] W.S. Nesbitt, S. Kulkarni, S. Giuliano, I. Goncalves, S.M. Dopheide, C.L. Yap, I.S. Harper, H.H. Salem, and S.P. Jackson, “Distinct glycoprotein Ib/V/IX and integrin $\alpha_{IIb}\beta_3$-dependent calcium signals cooperatively regulate platelet adhesion under flow,” Journal of Biological Chemistry, vol. 277, Jan. 2002, pp. 2965 -2972.

[46] B. Savage, S.J. Shattil, and Z.M. Ruggeri, “Modulation of platelet function through adhesion receptors. A dual role for glycoprotein IIb-IIIa (integrin alpha IIb beta 3) mediated by fibrinogen and glycoprotein Ib-von Willebrand factor,” Journal of Biological Chemistry, vol. 267, Jun. 1992, pp. 11300 -11306.

[47] J.M. Grunkemeier, W.B. Tsai, C.D. McFarland, and T.A. Horbett, “The effect of adsorbed fibrinogen, fibronectin, von Willebrand factor and vitronectin on the procoagulant state of adherent platelets,” Biomaterials, vol. 21, Nov. 2000, pp. 2243-2252.

[48] W. Tsai and T. Horbett, “The role of fibronectin in platelet adhesion to plasma preadsorbed polystyrene,” Journal of Biomaterials Science, Polymer Edition, vol. 10, 1999, pp. 163-181.

[49] H.J. Weiss, V.T. Turitto, H.R. Baumgartner, Y. Nemerson, and T. Hoffmann, “Evidence for the presence of tissue factor activity on subendothelium,” Blood, vol. 73, 1989, pp. 968-975.

[50] J.H. Lawson, M. Kalafatis, S. Stram, and K.G. Mann, “A model for the tissue factor pathway to thrombin. I. An empirical study,” Journal of Biological Chemistry, vol. 269, 1994, pp. 23357-23366.

[51] C.L. Wagner, M.A. Mascelli, D.S. Neblock, H.F. Weisman, B.S. Coller, and R.E. Jordan, “Analysis of GPIIb/IIIa receptor number by quantification of 7E3 binding to human platelets,” Blood, vol. 88, 1996, pp. 907-914.

[52] B. Coller, E. Peerschke, L. Scudder, and C. Sullivan, “A murine monoclonal antibody that completely blocks the binding of fibrinogen to platelets produces a thrombasthenic-like state in normal platelets and binds to glycoproteins IIb and/or IIIz,” J Clin Invest, vol. 72, 1983, pp. 325-338.

[53] G. Marguerie, E. Plow, and T. Edgington, “Human platelets possess an inducible and saturable receptor specific for fibrinogen,” J Biol Chem, vol. 254, Jun. 1979, pp. 5357-63.

[54] D.H. Farrell, P. Thiagarajan, D.W. Chung, and E.W. Davie, “Role of fibrinogen alpha and gamma chain sites in platelet aggregation,” Proceedings of the National Academy of Sciences of the United States of America, vol. 89, 1992, pp. 10729-10732.

[55] T.K. Gartner and J.S. Bennett, “The tetrapeptide analogue of the cell attachment site of fibronectin inhibits platelet aggregation and fibrinogen binding to activated platelets,” Journal of Biological Chemistry, vol. 260, 1985, pp. 11891-11894.

[56] R.R. Hantgan, S.C. Endenburg, J.J. Sixma, and P.G. de Groot, “Evidence that fibrin alpha-chain RGDX sequences are not required for platelet adhesion in flowing whole blood,” Blood, vol. 86, 1995, pp. 1001-1009.

[57] M.M. Rooney, D.H. Farrell, B.M. van Hemel, P.G. de Groot, and S.T. Lord, “The contribution of the three hypothesized integrin-binding sites in fibrinogen to platelet-mediated clot retraction,” Blood, vol. 92, 1998, pp. 2374-2381.

[58] T.N. Zaidi, L.V. McIntire, D.H. Farrell, and P. Thiagarajan, “Adhesion of platelets to surface-bound fibrinogen under flow,” Blood, vol. 88, 1996, pp. 2967-2972.

[59] A. Kasirer-Friede, B. Moran, J. Nagrampa-Orje, K. Swanson, Z.M. Ruggeri, B. Schraven, B.G. Neel, G. Koretzky, and S.J. Shattil, “ADAP is required for normal {alpha}IIb{beta}3 activation by VWF/GP Ib-IX-V and other agonists,” Blood, vol. 109, 2007, pp. 1018-1025.

[60] B. Savage and Z.M. Ruggeri, “Selective recognition of adhesive sites in surface-bound fibrinogen by glycoprotein IIb-IIIa on nonactivated platelets,” J. Biol Chem, vol. 266, 1991, pp. 11227-11233.

[61] Z.M. Ruggeri and G.L. Mendolicchio, “Adhesion mechanisms in platelet function,” Circ Res, vol. 100, 2007, pp. 1673-1685.

[62] E. Asch and E. Podack, “Vitronectin binds to activated human platelets and plays a role in platelet aggregation,” J Clinical Investigation, vol. 85, 1990, pp. 1372-1378.

[63] C.R. Ill, E. Engvall, and E. Ruoslahti, “Adhesion of platelets to laminin in the absence of activation,” The Journal of Cell Biology, vol. 99, Dec. 1984, pp. 2140 -2145.

[64] R.S. Piotrowicz, R.P. Orchekowski, D.J. Nugent, K.Y. Yamada, and T.J. Kunicki, “Glycoprotein Ic-IIa functions as an activation-independent fibronectin receptor on human platelets,” The Journal of Cell Biology, vol. 106, Apr. 1988, pp. 1359 -1364.

[65] W.D. Staatz, S.M. Rajpara, E.A. Wayner, W.G. Carter, and S.A. Santoro, “The membrane glycoprotein Ia-IIa (VLA-2) complex mediates the Mg++-dependent adhesion of platelets to collagen,” The Journal of Cell Biology, vol. 108, May. 1989, pp. 1917 -1924.

[66] R. Andrews, E. Gardiner, Y. Shen, J. Whisstock, and M. Berndt, “Glycoprotein Ib-IX-V,” The International Journal of Biochemistry and Cell Biology, vol. 35, 2003, pp. 1170-1174.

[67] A. Kasirer-Friede, M.R. Cozzi, M. Mazzucato, L. De Marco, Z.M. Ruggeri, and S.J. Shattil, “Signaling through GP Ib-IX-V activates {alpha}IIb{beta}3 independently of other receptors,” Blood, vol. 103, 2004, pp. 3403-3411.

[68] R. Andrews, Y. Shen, E. Gardiner, J.F. Dong, J. Lopez, and M. Berndt, “The glycoprotein Ib-IX_V complex in platelet adhesion and signaling,” Thromb Hameost, vol. 82, 1999, pp. 357-364.

[69] G.M. Romo, J. Dong, A.J. Schade, E.E. Gardiner, G.S. Kansas, C.Q. Li, L.V. McIntire, M.C. Berndt, and J.A. López, “The Glycoprotein Ib-IX-V complex is a platelet counterreceptor for P-selectin,” The Journal of Experimental Medicine, vol. 190, 1999, pp. 803-814.

[70] D.I. Simon, Z. Chen, H. Xu, C.Q. Li, J. Dong, L.V. McIntire, C.M. Ballantyne, L. Zhang, M.I. Furman, M.C. Berndt, and J.A. López, “Platelet glycoprotein Ibα Is a counterreceptor for the leukocyte integrin Mac-1 (Cd11b/Cd18),” The Journal of Experimental Medicine, vol. 192, 2000, pp. 193-204.

[71] Y. Wu, M. Zhang, K.D. Hauch, and T.A. Horbett, “Effect of adsorbed von Willebrand factor and fibrinogen on platelet interactions with synthetic materials under flow conditions,” Journal of Biomedical Materials Research Part A, vol. 85A, 2008, pp. 829-839.

[72] W.B. Tsai, J.M. Grunkemeier, C.D. McFarland, and T.A. Horbett, “Platelet adhesion to polystyrene-based surfaces preadsorbed with plasmas selectively depleted in fibrinogen, fibronectin, vitronectin, or von Willebrand's factor,” Journal of Biomedical Materials Research, vol. 60, 2002, pp. 348-359.

[73] M. Broberg, C. Eriksson, and H. Nygren, “GpIIb/IIIa is the main receptor for initial platelet adhesion to glass and titanium surfaces in contact with whole blood,” J Lab Clin Med, vol. 139, 2002, pp. 163-172.

[74] M. Davey and E. Luscher, “Actions of thrombin and other coagulant proteolytic enzymes on blood platelets,” Nature, vol. 216, 1967, pp. 857-858.

[75] P. Comfurius, P. Williamson, E.F. Smeets, R.A. Schlegel, E.M. Bevers, and R.F.A. Zwaal, “Reconstitution of phospholipid scramblase activity from human blood platelets,” Biochemistry, vol. 35, Jan. 1996, pp. 7631-7634.

[76] D. Phillips, L. Nannizzi-Alaimo, and K. Prasad, “Beta 3 tyrosine phosphorylation in alpha II Beta 3 (GP IIb-IIIa) outside-in integrin signalling,” Thromb Haemost, vol. 86, 2001, pp. 246-258.

[77]S. Shattil, H. Kashiwagi, and N. Pampori, “Integrin signaling: the platelet paradigm,” Blood, vol. 91, 1998, pp. 2645-2657.

[78] J. Ware and B. Coller, “Platelet morphology, biochemistry and function,” in *Williams hematology*, New York: McGraw-Hill, 1995, pp. 1161-1201.

[79] R. Flaumenhaft, J.R. Dilks, N. Rozenvayn, R.A. Monahan-Earley, D. Feng, and A.M. Dvorak, “The actin cytoskeleton differentially regulates platelet {alpha}-granule and dense-granule secretion,” Blood, vol. 105, 2005, pp. 3879-3887.

[80] R. Allen, L. Zacharski, S. Widirstky, R. Rosenstein, L. Zaitlin, and D. Burgess, “Transformation and motility of human platelets: details of the shape change and release reaction observed by optical and electron microscopy,” Journal of Cell Biology, vol. 83, 1979, pp. 126-142.

[81] K. Niiya, E. Hodson, R. Bader, V. Byers-Ward, J.A. Koziol, E.F. Plow, and Z.M. Ruggeri, “Increased surface expression of the membrane glycoprotein IIb/IIIa complex induced by platelet activation. Relationship to the binding of fibrinogen and platelet aggregation,” Blood, vol. 70, 1987, pp. 475-483.

[82] W.S. Nesbitt, S. Giuliano, S. Kulkarni, S.M. Dopheide, I.S. Harper, and S.P. Jackson, “Intercellular calcium communication regulates platelet aggregation and thrombus growth,” The Journal of Cell Biology, vol. 160, 2003, pp. 1151-1161.

[83] Y. Yuan, S. Kulkarni, P. Ulsemer, S.L. Cranmer, C.L. Yap, W.S. Nesbitt, I. Harper, N. Mistry, S.M. Dopheide, S.C. Hughan, D. Williamson, C. de la Salle, H.H. Salem, F. Lanza, and S.P. Jackson, “The von Willebrand factor-glycoprotein Ib/V/IX interaction induces actin polymerization and cytoskeletal reorganization in rolling platelets and glycoprotein Ib/V/IX-transfected cells,” Journal of Biological Chemistry, vol. 274, Dec. 1999, pp. 36241 -36251.

[84] S.P. Jackson, S.M. Schoenwaelder, Y. Yuan, I. Rabinowitz, H.H. Salem, and C.A. Mitchell, “Adhesion receptor activation of phosphatidylinositol 3-kinase. von Willebrand factor stimulates the cytoskeletal association and activation of phosphatidylinositol 3-kinase and pp60c-src in human platelets,” Journal of Biological Chemistry, vol. 269, Oct. 1994, pp. 27093 -27099.

[85] V. Leytin, D. Allen, S. Mykhaylov, L. Mis, E. Lyubimov, B. Garvey, and J. Freedman, “Pathologic high shear stress induces apoptosis events in human platelets,” Biochem Biophys Res Commun, vol. 320, 2004, pp. 303-310.

[86] G. Anderson, J. Hellums, J. Moake, and C.J. Alfrey, “Platelet lysis and aggregation in shear fields,” Blood Cells, vol. 4, 1978, pp. 499-511.

[87] G.P. Clagett, W.E. Burkel, J.B. Sharefkin, J.W. Ford, H. Hufnagel, D.W. Vinter, R.H. Kahn, L.M. Graham, J.C. Stanley, and P.W. Ramwell, “Platelet reactivity in vivo in dogs with arterial prostheses seeded with endothelial cells,” Circulation, vol. 69, 1984, pp. 632-639.

[88] F. Hess, S. Steeghs, R. Jerusalem, O. Reijnders, C. Jerusalem, B. Braun, and P. Grande, “Patency and morphology of fibrous polyurethane vascular prostheses implanted in the femoral artery of dogs after seeding with subcultivated endothelial cells,” Eur J Vasc Surg, vol. 7, 1993, pp. 402-408.

[89] R. Lith and G.A. Ameer, “Biohybrid strategies for vascular grafts,” in *Tissue Engineering*, Berlin/Heidelberg, Germany: Springer, 2011, pp. 279-316.

[90] J. Heyligers, C. Arts, H. Verhagen, P. de Groot, and F. Moll, “Improving small-diameter vascular grafts: From the application of an endothelial cell lining to the construction of a tissue-engineered blood vessel,” Annals of Vascular Surgery, vol. 19, May. 2005, pp. 448-456.

[91] F. Fauvel-Lafeve and W. Kwang, “Microfibrils from the arterial subendothelium,” International Review of Cytology, vol. 188, 1999, pp. 1-40.

[92] M.W. Radomski, R.M. Palmer, and S. Moncada, “The role of nitric oxide and cGMP in platelet adhesion to vascular endothelium,” Biochemical and Biophysical Research Communications, vol. 148, Nov. 1987, pp. 1482-1489.

[93] K.A. Mowery, M. H. Schoenfisch, J.E. Saavedra, L.K. Keefer, and M.E. Meyerhoff, “Preparation and characterization of hydrophobic polymeric films that are thromboresistant via nitric oxide release,” Biomaterials, vol. 21, Jan. 2000, pp. 9-21.

[94] D.J. Smith, D. Chakravarthy, S. Pulfer, M.L. Simmons, J.A. Hrabie, M.L. Citro, J.E. Saavedra, K.M. Davies, T.C. Hutsell, D.L. Mooradian, S.R. Hanson, and L.K. Keefer, “Nitric oxide-releasing polymers containing the [N(O)NO]-group,” Journal of Medicinal Chemistry, vol. 39, Jan. 1996, pp. 1148-1156.

[95] M.C. Frost, M.M. Reynolds, and M.E. Meyerhoff, “Polymers incorporating nitric oxide releasing/generating substances for improved biocompatibility of blood-contacting medical devices,” Biomaterials, vol. 26, May. 2005, pp. 1685-1693.

[96] H. Fan, P. Chen, R. Qi, J. Zhai, J. Wang, L. Chen, L. Chen, Q. Sun, Y. Song, D. Han, and L. Jiang, “Greatly improved blood compatibility by microscopic multiscale design of surface architectures,” Small, vol. 5, 2009, pp. 2144-2148.

[97] T. Tsuruta, “Contemporary topics in polymeric materials for biomedical applications,” in *Biopolymers liquid crystalline polymers phase emulsion*, Berlin/Heidelberg, Germany: Springer, 1996, pp. 1-51.

[98] A. Lewis, L. Tolhurst, and P. Stratford, “Analysis of a phosphorylcholine – based polymer coating on a coronary stent pre- and post-implantation,” Biomaterials, vol. 23, 2002, pp. 1697-1706.

[99] K.A.R. Karel K. J. Kuiper, “Phosphorylcholine-coated metallic stents in rabbit iliac and porcine coronary arteries,” Scand Cardiovasc J, vol. 32, Feb. 2011, pp. 261-268.

[100] H. Shin, K. Park, Ji Heung Kim, J. Kim, Dong Keun Han, M. Moon, K. Lee, and Ji Hoon Shin, “Biocompatible PEG grafting on DLC-coated nitinol alloy for vascular stents,” Journal of Bioactive and Compatible Polymers, vol. 24, 2009, pp. 316-328.

[101] G. Dearnaley and J. Arps, “Biomedical applications of diamond-like carbon (DLC) coatings: A review,” Surface & Coatings Technology, vol. 200, 2005, pp. 2518-2524.

[102] S.L. Goodman, K.S. Tweden, and R.M. Albrecht, “Platelet interaction with pyrolytic carbon heart-valve leaflets,” Journal of Biomedical Materials Research, vol. 32, 1996, pp. 249-258.

[103] X. Kapfer, W. Meichelboeck, and F. Groegler, “Comparison of carbon-impregnated and standard ePTFE prostheses in extra-anotomical anterior tibial artery bypass: A prospective randomized multicenter study,” Eur J Vasc Endovasc Surg, vol. 32, 2006, pp. 155-168.

[104] K. Kottke-Marchant, J. Anderson, Y. Umemura, and R. Marchant, “Effect of albumin coating on the in vitro blood compatibility of dacron arterial prostheses,” Biomaterials, vol. 10, 1989, pp. 147-155.

[105] F. Kudo, T. Nishibe, K. Miyazaki, J. Flores, and K. Yasuda, “Albumin-coated knitted dacron aortic prosthses. Study of postoperative inflammatory reactions,” Int Angiol, vol. 21, 2002, pp. 214-217.

[106] D. Li, H. Chen, W. Glenn McClung, and J. Brash, “Lysine-PEG modified polyurethane as a fibrinolytic surface: Effect of PEG chain length on protein interactions, platelet interactions and clot lysis,” Acta Biomater, vol. 5, 2009, pp. 1864-1871.

[107] H. Lee, J. Lee, and J. Andrade, “Blood compatibility of polyethylene oxide surfaces,” *Prog in Polym Sci*, vol. 20, 1995, pp. 1043-1079.

[108] J. Lee, B. Jeong, and H.B Lee, “Plasma protein adsorption and platelet adhesion onto comb-like PEO gradient surfaces,” J Biomed Mat Res, vol. 34, 1997, pp. 105-114.

[109] A. Roosjen, J. de Vries, H.C. van der Mei, W. Norde, and H.J. Busscher, “Stability and effectiveness against bacterial adhesion of poly(ethylene oxide) coatings in biological fluids,” Journal of Biomedical Materials Research Part B: Applied Biomaterials, vol. 73B, 2005, pp. 347-354.

[110] H.B Lee, J. Lee, and J.D Andrade, “Blood compatibility of polyethylene oxide surfaces,” Prog in Polym Sci, vol. 20, 1995, pp. 1043-1079.

[111] M.C. Tanzi, “Bioactive technologies for hemocompatibility,” Expert Review of Medical Devices, vol. 2, 2005, pp. 473-492.

[112] P. Joshi, K.F. Schilke, A. Fry, J. McGuire, and K. Bird, “Synthesis and evaluation of heparin immobilized ‘side-on’ to polystyrene microspheres coated with end-group activated polyethylene oxide,” International Journal of Biological Macromolecules, vol. 47, Aug. 2010, pp. 98-103.

[113] M.L. Kirkwood, G.J. Wang, B.M Jackson, M.A. Golden, R.M. Fairman and E.Y. Woo, “Lower limb revascularization for PAD using a heparin-coated PTFE conduit,” Vascular and Endovascular Surgery, [Epub ahead of print], Mar. 2011.

[114] G. Jain, M. Allon, S. Saddekni, J.F. Barker, I.D. Maya, “Does heparin coating improve patency or reduce infection of tunneled dialysis catheters,” Clinical Journal of the American Society of Nephrology, vol. 4, Sep. 2009, pp. 1787-1790.

[115] A. Kishida, Y. Ueno, I. Maruyama, and M. Akashi, “Immobilization of human thrombomodulin on biomaterials: Evaluation of the activity of immobilized human thrombomodulin,” Biomaterials, vol. 15, 1994, pp. 1170-1174.

[116] Y. Byun, H.A. Jacobs, and S. Wan Kim, “Mechanism of thrombin inactivation by immobilized heparin,” Journal of Biomedical Materials Research, vol. 30, 1996, pp. 423-427.

[117] E. Cavalcanti-Adam, T. Volberg, A. Micoulet, B. Kessler, B. Geiger, and J. Spatz, “Cell spreading and focal adhesion dynamics are regulated by spacing of integrin ligands,” Biophys J, vol. 92, 2007, pp. 2964-2974.

[118] L. Dike, C. Chen, M. Mrksich, J. Tien, G. Whitesides, and D. Ingber, “Geometric control of switching between growth, apoptosis, and differentiation during angiogenesis using micropatterned substrates,” In Vitro Cellular & Developmental Biology - Animal, vol. 35, Sep. 1999, pp. 441-448.

[119] J. Lahiri, E. Ostuni, and G.M. Whitesides, “Patterning ligands on reactive SAMs by microcontact printing,” Langmuir, vol. 15, Mar. 1999, pp. 2055-2060.

[120] R. Singhvi, A. Kumar, G.P. Lopez, G.N. Stephanopoulos, D.I. Wang, G.M. Whitesides, and D.E. Ingber, “Engineering cell shape and function,” Science, vol. 264, 1994, pp. 696-698.

[121] J.H. Lee and H.B. Lee, “Platelet adhesion onto wettability gradient surfaces in the absence and presence of plasma proteins,” Journal of Biomedical Materials Research, vol. 41, 1998, pp. 304-311.

[122] S.K. Bhatia, J.L. Teixeira, M. Anderson, L.C. Shriverlake, J.M. Calvert, J.H. Georger, J.J. Hickman, C.S. Dulcey, P.E. Schoen, and F.S. Ligler, “Fabrication of surfaces resistant to protein adsorption and application to two-dimensional protein patterning,” Analytical Biochemistry, vol. 208, Jan. 1993, pp. 197-205.

[123] Y. Ito, M. Hayashi, and Y. Imanishi, “Gradient micropattern immobilization of heparin and its interaction with cells,” Journal of Biomaterials Science, Polymer Edition, vol. 12, 2001, pp. 367-378.

[124] J. Lee, H. Kim, G. Khang, and H. Lee, “Characterization of wettability gradient surfaces prepared by corona discharge treatment,” J Colloid Interface Sci, vol. 151, 1992, pp. 563-570.

[125] H. Spijker, R. Bos, H. Busscher, T. van Kooten, and W. van Oeveren, “Platelet adhesion and activation on a shielded plasma gradient prepared on polyethylene,” Biomaterials, vol. 23, 2002, pp. 757-766.

[126] M. Kim, G. Khang, and H.B Lee, “Gradient polymer surfaces for biomedical applications,” Prog. in Polym. Sci., vol. 33, 2008, pp. 138-164.

[127] H. Elwing, A. Askendal, and I. Lundström, “Protein exchange reactions on solid surfaces studied with a wettability gradient method,” Surface Forces and Surfactant Systems, Springer Berlin / Heidelberg, 1987, pp. 103-107.

[128] C.G Golander, Y.S. Lin, V. Hlady, and J.D Andrade, “Wetting and plasma-protein adsorption studies on surfaces with a hydrophobicity gradient,” Colloids Surf., vol. 49, 1990, pp. 289-302.

[129] M. Zelzer, R. Majani, J. Bradley, F. Rose, M. Davies, and M. Alexander, “Investigation of cell-surface interactions using chemical gradients formed from plasma polymers,” Biomaterials, vol. 29, 2007, pp. 172-184.

[130] Y. Iwasaki, K. Ishihara, N. Nakabayashi, G. Khang, J. Jeon, J. Lee, and H.B. Lee, “Platelet adhesion on the gradient surfaces grafted with phospholipid polymer,” J. Biomater. Sci. Polym. Ed., vol. 9, 1998, pp. 801-816.

[131] L.E. Corum and V. Hlady, “Screening platelet-surface interactions using negative surface charge gradients,” Biomaterials, vol. 31, 2010, pp. 3148-3155.

[132] J.A. Hubbell, “Biomaterials science and high-throughput screening,” Nat Biotech, vol. 22, Jul. 2004, pp. 828-829.

[133] S. Huang, C.S. Chen, and D.E. Ingber, “Control of cyclin D1, p27Kip1, and cell cycle progression in human capillary endothelial cells by cell shape and cytoskeletal tension,” Mol. Biol. Cell, vol. 9, 1998, pp. 3179-3193.

[134] C.S. Chen, M. Mrksich, S. Huang, G.M. Whitesides, and D.E. Ingber, “Geometric control of cell life and death,” Science, vol. 276, 1997, pp. 1425-1428.

[135] R.S. Kane, S. Takayama, E. Ostuni, D.E. Ingber, and G.M. Whitesides, “Patterning proteins and cells using soft lithography,” Biomaterials, vol. 20, Dec. 1999, pp. 2363-2376.

[136] C.S. Chen, M. Mrksich, S. Huang, G.M. Whitesides, and D.E. Ingber, “Micropatterned surfaces for control of cell shape, position, and function,” Biotechnology Progress, vol. 14, 1998, pp. 356-363.

[137] J.A. Finlay, S. Krishnan, M.E. Callow, J.A. Callow, R. Dong, N. Asgill, K. Wong, E.J. Kramer, and C.K. Ober, “Settlement of ulva zoospores on patterned fluorinated and PEGylated monolayer surfaces,” Langmuir, vol. 24, Jan. 2008, pp. 503-510.

[138] L. Wanli, J.O. Tegenfeldt, L. Chen, R.H. Austin, S.Y. Chou, P.A. Kohl, J. Krotine and J.C. Sturm, “Sacrificial polymers for nanofluidic channels in biological applications,” Nanotechnology, vol. 14, April 2003, pp.578-583.

[139] T. Bohanon, G. Elender, W. Knoll, P. Koberle, J. Lee, A. Offenhausser, H. Ringsdorf, E. Sackmann, J. Simon, G. Tovar, and F. Winnik, “Neural cell pattern formation on glass and oxidized silicon surfaces modified with poly(N-isopropylacrylamide),” Journal of Biomaterials Science, Polymer Edition, vol. 8, 1997, pp. 19-39.

[140] T. Takezawa, Y. Mori, and K. Yoshizato, “Cell culture on a thermo-responsive polymer surface,” Nat Biotech, vol. 8, print. 1990, pp. 854-856.

[141] G. Chen, Y. Ito, Y. Imanishi, A. Magnani, S. Lamponi, and R. Barbucci, “Photoimmobilization of sulfated hyaluronic acid for antithrombogenicity,” Bioconjugate Chemistry, vol. 8, 1997, pp. 730-734.

[142] C.S. Dulcey, J.H. Georger, V. Krauthamer, D.A. Stenger, T.L. Fare, and J.M. Calvert, “Deep UV photochemistry of chemisorbed monolayers: Patterned coplanar molecular assemblies,” Science, vol. 252, 1991, pp. 551-554.

[143] S.K. Bhatia, J.J. Hickman, and F.S. Ligler, “New approach to producing patterned biomolecular assemblies,” Journal of the American Chemical Society, vol. 114, 1992, pp. 4432-4433.

[144] D. Brambley, B. Martin, and P.D. Prewett, “Microlithography: An overview,” Advanced Materials for Optics and Electronics, vol. 4, 1994, pp. 55-74.

[145] Y.X. Xia and G.M. Whitesides, “Soft lithography,” Ann Rev Mater Sci, vol. 28, 1998, pp. 153-184.

[146] Y.X. Xia, J.J. McClelland, R. Gupta, D. Qin, X. Zhao, L.L. Sohn, R.J. Celotta, and G.M. Whitesides, “Replica molding using polymeric materials: A practical step toward nanomanufacturing,” Advanced Materials, vol. 9, 1997, pp. 147-149.

[147] E. Kim, Y. Xia, and G.M. Whitesides, “Micromolding in capillaries: Applications in materials science,” Journal of the American Chemical Society, vol. 118, Jan. 1996, pp. 5722-5731.

[148] S. Kobel, M. Limacher, S. Gobaa, T. Laroche, and M.P. Lutolf, “Micropatterning of hydrogels by soft embossing,” Langmuir, vol. 25, 2009, pp. 8774-8779.

[149] A. Kumar, N.L. Abbott, H.A. Biebuyck, E. Kim, and G.M. Whitesides, “Patterned self-assembled monolayers and meso-scale phenomena,” Accounts of Chemical Research, vol. 28, 1995, pp. 219-226.

[150] C.D. James, R.C. Davis, L. Kam, H.G. Craighead, M. Isaacson, J.N. Turner, and W. Shain, “Patterned protein layers on solid substrates by thin stamp microcontact printing,” Langmuir, vol. 14, Feb. 1998, pp. 741-744.

[151] C. Lee, P. Huie, T. Leng, M. Peterman, M. Marmor, M. Blumenkranz, S. Bent, and H. Fishman, “Microcontact printing on human tissue for retinal cell transplantation,” Arch Ophthalmol., vol. 120, 2002, pp. 1714-1718.

[152] L. Basabe-Desmonts, S. Ramstrom, G. Meade, S. O’Neill, A. Riaz, L.P. Lee, A.J. Ricco, and D. Kenny, “Single-step separation of platelets from whole

blood coupled with digital quantification by interfacial platelet cytometry (iPC)," Langmuir, vol. 26, 2010, pp. 14700-14706.

[153] T. Ekblad, L. Faxälv, O. Andersson, N. Wallmark, A. Larsson, T.L. Lindahl, and B. Liedberg, "Patterned hydrogels for controlled platelet adhesion from whole blood and plasma," Advanced Functional Materials, vol. 20, 2010, pp. 2396-2403.

[154] C.J. Kastrup, M.K. Runyon, F. Shen, and R.F. Ismagilov, "Modular chemical mechanism predicts spatiotemporal dynamics of initiation in the complex network of hemostasis," Proceedings of the National Academy of Sciences, vol. 103, Oct. 2006, pp. 15747 -15752.

[155] C. Selhuber-Unkel, T. Erdmann, M. Lopez-Garcia, H. Kessler, U. Schwarz, and J. Spatz, "Cell adhesion strength is controlled by intermolecular spacing of adhesion receptors," Byophis J., vol. 98, 2010, pp. 543-551.

[156] M. Zhang and T.A. Horbett, "Tetraglyme coatings reduce fibrinogen and von Willebrand factor adsorption and platelet adhesion under both static and flow conditions," Journal of Biomedical Materials Research Part A, vol. 89A, 2009, pp. 791-803.

[157] E.K.F. Yim and M.V. Sefton, "Amidine surface modification of poly(acrylonitrile-co-vinyl chloride) reduces platelet adhesion," Journal of Biomedical Materials Research Part A, vol. 89A, 2009, pp. 780-790.

[158] M. Amiji and K. Park, "Prevention of protein adsorption and platelet adhesion on surfaces by PEO/PPO/PEO triblock copolymers," Biomaterials, vol. 13, 1992, pp. 682-692.

[159] G. Annich, J. Meinhardt, K. Mowery, B. Ashton, S. Merz, R. Hirschl, M. Meyerhoff, and R. Bartlett, "Reduced platelet activation and thrombosis in extracorporeal circuits coated with nitric oxide release polymers," Critical Care Medicine, vol. 28, 2000, pp. 915-920.

[160] L. Cao, S. Sukavaneshvar, B.D. Ratner, and T.A. Horbett, "Glow discharge plasma treatment of polyethylene tubing with tetraglyme results in ultralow fibrinogen adsorption and greatly reduced platelet adhesion," Journal of Biomedical Materials Research Part A, vol. 79A, 2006, pp. 788-803.

[161] Y. Iwasaki, A. Mikami, K. Kurita, N. Yui, K. Ishihara, and N. Nakabayashi, "Reduction of surface-induced platelet activation on phospholipid polymer," Journal of Biomedical Materials Research, vol. 36, 1997, pp. 508-515.

[162] J.H. Lee, G. Khang, J.W. Lee, and H.B. Lee, "Platelet adhesion onto chargeable functional group gradient surfaces," Journal of Biomedical Materials Research, vol. 40, 1998, pp. 180-186.

[163] M.N. Godo and M.V. Sefton, “Characterization of transient platelet contacts on a polyvinyl alcohol hydrogel by video microscopy,” Biomaterials, vol. 20, Jun. 1999, pp. 1117-1126.

[164] A. Asif, F.N. Gadalean, D. Merrill, G. Cherla, C.D. Cipleu, D.L. Epstein, and D. Roth, “Inflow stenosis in arteriovenous fistulas and grafts: A multicenter, prospective study,” Kidney Int, vol. 67, May. 2005, pp. 1986-1992.

[165] B. Kelly, S. Heffelfinger, and J. Whiting, “Agressive venous neointimal hyperplasia in a pig model of arteriovenous graft stenosis,” Kidney Int, vol. 62, 2002, pp. 2272-2280.

[166] J.H. Hartwig, “Mechanisms of actin rearrangements mediating platelet activation,” The Journal of Cell Biology, vol. 118, 1992, pp. 1421-1442.

[167] B. Haimovich, L. Lipfert, J. Brugge, and S. Shattil, “Tyrosine phosphorylation and cytoskeletal reorganization in platelets are triggered by interaction of integrin receptors with their immobilized ligands,” J. Biol. Chem., vol. 268, 1993, pp. 15868-15877.

[168] J.E. Fox and D.R. Phillips, “Role of phosphorylation in mediating the association of myosin with the cytoskeletal structures of human platelets,” Journal of Biological Chemistry, vol. 257, Apr. 1982, pp. 4120 -4126.

[169] Z. Bai, M.J. Filiaggi, R.J. Sanderson, L.B. Lohstreter, M.A. McArthur, and J.R. Dahn, “Surface characteristics and protein adsorption on combinatorial binary Ti-M (Cr, Al, Ni) and Al-M (Ta, Zr) library films,” Journal of Biomedical Materials Research Part A, vol. 92A, 2010, pp. 521-532.

[170] T. Ruardy, J. Schakenraad, H. vanderMei, and H. Busscher, “Preparation and characterization of chemical gradient surfaces and their application for the study of cellular interaction phenomena,” Surf. Sci. Rep., vol. 27, 1997, pp. 3-30.

[171] S. Bhatia, J. Teixeira, M. Anderson, L. Shriver-Lake, J. Calvert, J. Georger, J. Hickman, C. Dulcey, and F. Ligler, “Fabrication of surfaces resistant to protein adsorption and application to two-dimensional protein patterning,” Anal Biochem, vol. 208, 1993, pp. 197-205.

[172] J. Liu and V. Hlady, “Chemical pattern on silica surface prepared by UV irradiation of 3-mercaptopropyltriethoxy silane layer: surface characterization and fribrinogen adsorption,” Colloids Surf B Biointerfaces, vol. 8, 1996, pp. 25-37.

[173] J.F. Mustard and M.A. Packham, “Factors influencing platelet function: Adhesion, release and aggregation,” Pharmacological Reviews, vol. 22, 1970, pp. 97-187.

[174] A. McNicol, “Platelet preparation and estimation of functional responses,” in *Platelets: A practical approach*, New York: Oxford University Press, 2002, p. 5.

[175] J. Brash and P. ten Hove, “Effect of plasma dillution on adsorption of fibrinogen to solid surfaces,” Thromb Haemost, vol. 51, 1984, pp. 326-330.

[176] J. Chinn, T. Horbett, and B. Ratner, “Baboon fibrinogen adsorption and platelet adhesion to polymeric materials,” Thromb Hameost, vol. 65, 1991, pp. 608-617.

[177] J.M. Grunkemeier, W.B. Tsai, C.D. McFarland, and T.A. Horbett, “The effect of adsorbed fibrinogen, fibronectin, von Willebrand factor and vitronectin on the procoagulant state of adherent platelets,” Biomaterials, vol. 21, Nov. 2000, pp. 2243-2252.

[178] D.K. Han, K. Park, K.D. Park, K. Ahn, and Y.H. Kim, “In vivo biocompatibility of sulfonated PEO-grafted polyurethanes for polymer heart valve and vascular graft,” Artificial Organs, vol. 30, 2006, pp. 955-959.

[179] H. Yeh and J. Lin, “Surface characterization and in vitro platelet compatibility study of surface sulfonated chitosan membrane with amino group protection-deprotection strategy,” Journal of Biomaterials Science, Polymer Edition, vol. 19, 2008, pp. 291-310.

[180] D. Phillips, I. Charo, L. Parise, and L. Fitzgerald, “The platelet membrane glycoprotein IIb-IIIa complex,” Blood, vol. 71, 1988, pp. 831-843.

[181] V.T. Turitto and H.J. Weiss, “Red blood cells: Their dual role in thrombus formation,” Science, vol. 207, 1980, pp. 541-543.

[182] S. Slack and T. Horbett, “The Vroman effect: A critical review,” in *Proteins at interfaces II: Fundamentals and applications*, Washington DC: American Chemical Society, 1995, pp. 112-128.

[183] S.P. Jackson, N. Mistry, and Y. Yuan, “Platelets and the injured vessel wall-- "rolling into action": Focus on glycoprotein Ib/V/IX and the platelet cytoskeleton,” Trends in Cardiovascular Medicine, vol. 10, Jul. 2000, pp. 192-197.

[184] A. Kasirer-Friede, M.R. Cozzi, M. Mazzucato, L. De Marco, Z.M. Ruggeri, and S.J. Shattil, “Signaling through GP Ib-IX-V activates {alpha}IIb{beta}3 independently of other receptors,” Blood, vol. 103, 2004, pp. 3403-3411.

[185] M.T. Khorasani and H. Mirzadeh, “In vitro blood compatibility of modified PDMS surfaces as superhydrophobic and superhydrophilic materials,” Journal of Applied Polymer Science, vol. 91, 2004, pp. 2042-2047.

[186] R. Roy, H. Choi, J. Yi, M. Moon, K. Lee, D. Han, J. Shin, A. Kamijo, and T. Hasabe, “Hemocompatibiility of surface-modified, silicon-incorporated, diamond-like carbon films,” Acta Biomater, vol. 5, 2008, pp. 249-256.

[187] N. Ferraz, J. Carlsson, J. Hong, and M. Ott, “Influence of nanoporesize on platelet adhesion and activation,” Journal of Materials Science: Materials in Medicine, vol. 19, Sep. 2008, pp. 3115-3121.

[188] N. Rhodes, D. Wilson, and R. Williams, “The effect of gas plasma modification on platelet and contact phase activation processes,” Biomaterials, vol. 28, 2007, pp. 4561-4570.

[189] J. Raj, G. Herzog, M. Manning, C. Volcke, B.D. MacCraith, S. Ballantyne, M. Thompson, and D.W. Arrigan, “Surface immobilisation of antibody on cyclic olefin copolymer for sandwich immunoassay,” Biosensors and Bioelectronics, vol. 24, Apr. 2009, pp. 2654-2658.

[190] M. Beyer, T. Felgenhauer, F. Ralf Bischoff, F. Breitling, and V. Stadler, “A novel glass slide-based peptide array support with high functionality resisting non-specific protein adsorption,” Biomaterials, vol. 27, Jun. 2006, pp. 3505-3514.

[191] H. Takahashi, K. Emoto, M. Dubey, D.G. Castner, and D.W. Grainger, “Imaging surface immobilization chemistry: Correlation with cell patterning on non-adhesive hydrogel thin films,” Advanced Functional Materials, vol. 18, 2008, pp. 2079-2088.

[192] E.L. Schmid, T.A. Keller, Z. Dienes, and H. Vogel, “Reversible oriented surface immobilization of functional proteins on oxide surfaces,” Analytical Chemistry, vol. 69, Jun. 1997, pp. 1979-1985.

[193] Z.M. Ruggeri, J.N. Orje, R. Habermann, A.B. Federici, and A.J. Reininger, “Activation-independent platelet adhesion and aggregation under elevated shear stress,” Blood, vol. 108, 2006, pp. 1903 -1910.

[194] G.M. Harbers, K. Emoto, C. Greef, S.W. Metzger, H.N. Woodward, J.J. Mascali, D.W. Grainger, and M.J. Lochhead, “Functionalized poly(ethylene glycol)-based bioassay surface chemistry that facilitates bio-immobilization and inhibits nonspecific protein, bacterial, and mammalian cell adhesion,” Chemistry of Materials, vol. 19, 2007, pp. 4405-4414.

[195] K. Nedeltchev, L. Remonda, D. Do, C. Breckenfeld, C. Ozdoba, M. Arnold, H. Mattle, and G. Schroth, “Acute stenting and thrombaspiration in basilar artery occlusions due to embolism from the dominating vertebral artery,” Neuroradiology, vol. 46, 2004, pp. 686-691.

[196] H. Sandberg, A.P. Bode, F.A. Dombrose, M. Hoechli, and B.R. Lentz, “Expression of coagulant activity in human platelets: Release of membranous vesicles providing platelet factor 1 and platelet factor 3,” Thrombosis Research, vol. 39, Jul. 1985, pp. 63-79.

[197] P.J. Sims, E.M. Faioni, T. Wiedmer, and S.J. Shattil, “Complement proteins C5b-9 cause release of membrane vesicles from the platelet surface that are enriched in the membrane receptor for coagulation factor Va and express prothrombinase activity,” Journal of Biological Chemistry, vol. 263, Dec. 1988, pp. 18205 -18212.

[198] P. Johnson, K. Garrett, J. Brash, R. Cornelius, S. Kaplan, and V. Warty, “Deliery of pasivating proteins to sutures during passage through the vessel wall reduces subsequent platelet deposition by blocking fibrinogen adsorption,” Arterioscler Thromb Vasc Biol, vol. 12, 1992, pp. 727-735.

[199] S. Hsu-Lin, C.L. Berman, B.C. Furie, D. August, and B. Furie, “A platelet membrane protein expressed during platelet activation and secretion. Studies using a monoclonal antibody specific for thrombin-activated platelets.,” Journal of Biological Chemistry, vol. 259, Jul. 1984, pp. 9121 -9126.

[200] V. Levich, *Physicochemical hydrodynamics*, Englewood Cliffs, NJ: Prentice Hall, 1962.

[201] T. Dabroś and T.G.M. van de Ven, “A direct method for studying particle deposition onto solid surfaces,” Colloid & Polymer Science, vol. 261, Aug. 1983, pp. 694-707.

[202] Z. Adamczyk, T. Dabros, J. Czarnecki, and T. Van de Ven, “Particle transfer to solid surfaces,” Adv. Coll. Int. Sci., vol. 19, 1983, pp. 183-252.

[203] Z. Adamczyk and T.G.M. Van De Ven, “Deposition of particles under external forces in laminar flow through parallel-plate and cylindrical channels,” Journal of Colloid and Interface Science, vol. 80, Apr. 1981, pp. 340-356.

[204] K.A. Moskowitz, B. Kudryk, and B.S. Coller, “Fibrinogen coating density affects the conformation of immobilized fibrinogen: Implications for platelet adhesion and spreading,” Biomaterials, vol. 79, 1998, pp. 824-831.

[205] J.A. Chinn, S.E. Posso, T.A. Horbett, B.D. Ratner, “Postadsorptive transitions in fibrinogen adsorbed to Biomer: Changes in baboon platelet

adhesion, antibody binding , and sodium dodecyl sulfate elutability," Journal of Biomedical Materials Research, vol. 25, April. 1991, pp. 535-555.

[206] J.N. Lindon, G. McManama, L. Kushner, E.W. Merrill, and E.W. Salzman, "Does the conformation of adsorbed fibrinogen dictate platelet interactions with artificial surfaces?," Blood, vol. 68, 1986, pp. 355-362.

[207] K.A. Moskowitz, B. Kudryk, B.S. Coller, "Fibrinogen coating density affects the conformation of immobilized fibrinogen: Implications for platelet adhesion and spreading," Thromb. Haemost., vol. 79, April 1998, pp. 824-831.

[208] M. Tanaka, T. Motomura, M. Kawada, T. Anzai, Y. Kasori, T. Shiroya, K. Shimura, M. Onishi, A. Mochizuki, "Blood compatible aspects of poly(2-methoxyethylacrylate) (PEMA)—relationship between protein adsorption and platelet adhesion on PEMA surface," Biomaterials, vol. 21, Jul. 2000, pp. 1471-1481.

[209] B. Sivaraman, K.P. Fears, and R.A. Latour, "Investigation of the effects of surface chemistry and solution concentration on the conformation of adsorbed proteins using an improved circular dichroism method," Langmuir, vol. 25, Mar. 2009, pp. 3050-3056.

[210] L. Xu and C.A. Siedlecki, "Atomic force microscopy studies of the initial interactions between fibrinogen and surfaces," Langmuir, vol. 25, Mar. 2009, pp. 3675-3681.

[211] L.E. Corum and V. Hlady, "Screening platelet-surface interactions using negative surface charge gradients," Biomaterials, vol. 31, Apr. 2010, pp. 3148-3155.

[212] D. Kwak, Y. Wu, and T.A. Horbett, "Fibrinogen and von Willebrand's factor adsorption are both required for platelet adhesion from sheared suspensions to polyethylene preadsorbed with blood plasma," Journal of Biomedical Materials Research Part A, vol. 74A, 2005, pp. 69-83.

[213] B. Savage, E. Saldvar, and Z.M. Ruggeri, "Initiation of platelet adhesion by arrest onto fibrinogen or translocation on von Willebrand factor," Cell, vol. 84, Jan. 1996, pp. 289-297.

[214] S. Shattil, M. Ginsberg, and J. Brugge, "Adhesive signaling in platelets," Curr Opin Cell Biol, vol. 6, 1994, pp. 695-704.

[215] I. Goncalves, S.C. Hughan, S.M. Schoenwaelder, C.L. Yap, Y. Yuan, and S.P. Jackson, "Integrin $\alpha_{IIb}\beta_3$-dependent calcium signals regulate platelet-fibrinogen interactions under flow," Journal of Biological Chemistry, vol. 278,

2003, pp. 34812 -34822.

[216] Lin, Tseng, Huang, Huang, and Chieng, “Microsized 2D protein arrays immobilized by micro-stamps and micro-wells for disease diagnosis and drug screening,” Fresenius' Journal of Analytical Chemistry, vol. 371, Sep. 2001, pp. 202-208-208.

[217] C. Kastrup, F. Shen, M. Runyon, and R. Ismagilov, “Characterization of the threshold response of initiation of blood clotting to stimulus patch size,” Biophys. J., vol. 93, 2007, pp. 2969-2977.

[218] R.S. Kane, S. Takayama, E. Ostuni, D.E. Ingber, and G.M. Whitesides, “Patterning proteins and cells using soft lithography,” Biomaterials, vol. 20, Dec. 1999, pp. 2363-2376.

[219] E. Cramer and M. Fontenay, “Platelets: Structure related to function,” in *Hemostasis and thrombosis: Basic principles and clinical practice*, Philadelphia, PA: Lippincott Williams and Wilkins, 2006.

[220] K. Neeves, S. Maloney, K. Fong, A. Schmaier, M. Kahn, L. Brass, and S. Diamond, “Microfluidic focal thrombosis model for measuring murine platelet deposition and stability: PAR4 signaling enhances shear-resistance of platelet aggregates,” J. Thromb. Haemost., vol. 6, 2008, pp. 2193-2201.

[221] T. Colace, E. Falls, X. Zheng, and S. Diamond, “Analysis of morphology of platelet aggregates formed on collagen under laminar blood flow,” Ann. Biomed. Engr., vol. 39, 2011, pp. 922-929.

[222] T.M. Massa, M.L Yang, J.Y.C. Ho, J.L Brash, and J. Santerre, “Fibrinogen surface distribution correlates to platelet adhesion pattern on fluorinated surface-modified polyetherurethane,” Biomaterials, vol. 26, Dec. 2005, pp. 7367-7376.

[223] K. Park, F. Mao, and H. Park, “Morphological characterization of surface-induced platelet activation,” Biomaterials, vol. 11, 1990, pp. 24-31.

[224] M. Kroll and A. Schafer, “Biochemical mechanisms of platelet activation,” Blood, vol. 74, 1989, pp. 1181-1195.

[225] J. Grunkemeier, W. Tsai, and T. Horbett, “Co-adsorbed fibrinogen and von Willebrand factor augment platelet procoagulant activity and spreading,” Journal of Biomaterials Science, Polymer Edition, vol. 12, 2001, pp. 1-20.

[226] M. Amiji, H. Park, and K. Park, “Study on the prevention of surface-induced platelet activation by albumin coating,” Journal of Biomaterials Science, Polymer Edition, vol. 3, 1992, pp. 375-388.

[227] Z. Jun, Y. Youling, W. Kehua, S. Jian, and L. Sicong, “Surface modification of segmented poly(ether urethane) by grafting sulfo ammonium zwitterionic monomer to improve hemocompatibilities,” Colloids and Surfaces B: Biointerfaces, vol. 28, Apr. 2003, pp. 1-9.

[228] Q. Sun, Y. Su, X. Ma, Y. Wang, and Z. Jiang, “Improved antifouling property of zwitterionic ultrafiltration membrane composed of acrylonitrile and sulfobetaine copolymer,” Journal of Membrane Science, vol. 285, Nov. 2006, pp. 299-305.

[229] M. Thevis, R.R. Ogorzalek Loo, and J.A. Loo, “In-Gel derivatization of proteins for cysteine-specific cleavages and their analysis by mass spectrometry,” Journal of Proteome Research, vol. 2, Apr. 2003, pp. 163-172.

[230] J. Li, J. Carlsson, J. Lin, and K.D. Caldwell, “Chemical modification of surface active poly(ethylene oxide)−poly(propylene oxide) triblock copolymers,” Bioconjugate Chemistry, vol. 7, Jan. 1996, pp. 592-599.

[231] S. Jo and K. Park, “Surface modification using silanated poly(ethylene glycol)s,” Biomaterials, vol. 21, Mar. 2000, pp. 605-616.

[232] J. Harris, *Poly(ethylene glycol) chemistry biotechnical and biomedical applications*, New York, NY: Plenum Press, 1992.

[233] S. VandeVondele, J. Vörös, and J.A. Hubbell, “RGD-grafted poly-l-lysine-graft-(polyethylene glycol) copolymers block non-specific protein adsorption while promoting cell adhesion,” Biotechnology and Bioengineering, vol. 82, 2003, pp. 784-790.

[234] D. Varga-Szabo, I. Pleines, and B. Nieswandt, “Cell adhesion mechanisms in platelets,” Arterioscler Thromb Vasc Biol, vol. 28, 2008, pp. 403-412.

[235] W. Tsai, J.M. Grunkemeier, and T.A. Horbett, “Variations in the ability of adsorbed fibrinogen to mediate platelet adhesion to polystyrene-based materials: A multivariate statistical analysis of antibody binding to the platelet binding sites of fibrinogen,” Journal of Biomedical Materials Research Part A, vol. 67A, 2003, pp. 1255-1268.

[236] L. Pardo, W.C. Wilson, and T. Boland, “Characterization of patterned self-assembled monolayers and protein arrays generated by the ink-jet method,” Langmuir, vol. 19, Mar. 2003, pp. 1462-1466.

[237] A.P. Quist, E. Pavlovic, and S. Oscarsson, “Recent advances in microcontact printing,” Analytical and Bioanalytical Chemistry, vol. 381, Feb. 2005, pp. 591-600.

[238] D.J. Graber, T.J. Zieziulewicz, D.A. Lawrence, W. Shain, and J.N. Turner, “Antigen binding specificity of antibodies patterned by microcontact printing,” Langmuir, vol. 19, Jun. 2003, pp. 5431-5434.

[239] M. Henry, C. Dupont-Gillain, P. Bertand, “Conformation change of albumin adsorbed on polycarbonate membranes as revealed by ToF-SIMS,” Langmuir, vol.19, Jun. 2003, pp6271-6276.